# Optimal Allocation of Distributed Generation for Power Loss Reduction and Voltage Profile Improvement




BY

**Osaloni Oluwafunso Oluwole**

Supervisors: **Mrs K. O. Awodele**
**Prof K. A. Folly**

**Dissertation submitted in fulfilment of the requirements for the degree of Master of Science in Electrical Engineering**

MARCH 2016

**Department of Electrical Engineering**
**University of Cape Town**
**South Africa**

## Declaration

This MSc research work is my original work and has not been presented for a degree award in this or any other university. I know the meaning of plagiarism and declare that all of the work in the dissertation, save for that which is properly acknowledged, is my own.

Signed by candidate 22/03/2016

O. O. Osaloni

# Dedication

I dedicate this work to the loving memory of my grandparents, Pa James Kowe Osaloni and Madam Abigail Dolapo Osaloni.

## Acknowledgements

First and foremost, I give glory, honour, thanks and adoration to Almighty God for His infinite mercy and unmerited favour and blessing He gave me before, during and after the completion of this programme. May His name be praised for evermore.

My sincere gratitude goes to Mrs K.O. Awodele, my research supervisor, for her support, guidance, helpful suggestions and continued monitoring of my progress during the research work. Her motherly understanding, compassion and encouragement were in no small measure a great prime mover to the outcome of the work. Thank you for believing in me. Also to Prof. K. Folly, for his guidance, support, encouragement throughout the course of this research work

To my parents, Chief and Mrs Osaloni, I say a big thank you for your financial support, prayers, encouragement and counsel throughout this programme. Also, to my big brother Engr. Afolabi Oluwadare Osaloni for the brotherly stand he took throughout the program, I say thank you sir.

I would like to thank all my friends and my fellow students especially Priye Ainah. Thank you for sharing with me your excitement and thirst for knowledge and for always being willing to assist me in working through the occasional tough problems.

Lastly, to my best friend, my confidant, my love, my jewel of inestimable value and my wife Rebecca Aanuoluwa Omotola Osaloni, I say thank you so much.

God bless us all.

# Abstract

Distributed generation (DG) integration in a distribution system has increased to high penetration levels. There is a need to improve technical benefits of DG integration by optimal allocation in a power system network. These benefits include electrical power losses reduction and voltage profile improvement. Optimal DG location and sizing in a power system distribution network with the aim of reducing system power losses and improving the voltage profile still remain a major problem.

Though much research has been done on optimal DG location and sizing in a power system distribution network with the aim of reducing system power losses and improving the voltage profile, most of the existing works in the literature use several techniques such as computation, artificial intelligence and an analytical approach, but they still suffer from several drawbacks.

As a result, much can still be done in coming up with new algorithms to improve the already existing ones so as to address this important issue more efficiently and effectively. The majority of the proposed algorithms emphasize real power losses only in their formulations. They ignore the reactive power losses which are the key to the operation of the power systems. Hence, there is an urgent need for an approach that will incorporate reactive power and voltage profile in the optimization process, such that the effect of high power losses and poor voltage profile can be mitigated.

This research used Genetic Algorithm and Improved Particle Swarm Optimization (GA-IPSO) for optimal placement and sizing of DG for power loss reduction and improvement of voltage profile. GA-IPSO is used to optimize DG location and size while considering both real and reactive power losses. The real and reactive power as well as power loss sensitivity factors were utilized in identifying the candidate buses for DG allocation. The GA-IPSO algorithm was programmed in Matlab.

This algorithm reduces the search space for the search process, increases its rate of convergence and also eliminates the possibility of being trapped in local minima. Also, the new approach will help in reducing power loss and improve the voltage profile via placement and sizing.

Two different scenarios were investigated using GA-IPSO algorithm and Genetic Algorithm (GA). The first uses Photovoltaic (type one) and Wind (type two) DG under peak and base loading conditions on IEEE 33-bus test system. The second scenario used the two types of DG under peak and base loading conditions on a modified Western Cape real network. The result

from the GA-IPSO approach and GA were compared to justify the effectiveness of the algorithm. Better voltage improvement was obtained and reduced loss in both scenarios for the IEEE 33-bus test system as well as the real network. The penetration of DG required for minimum loss and improved voltage profile is reduced in the proposed approach.

# Table of Contents

# List of Figures

# List of Tables

# Acronyms

| | |
|---|---|
| ANSI | America National Standard Institute |
| BIPV | Building-integrated photovoltaic |
| CHP | Combine Heat and power |
| CNG | Combustion Natural Gas |
| DFIG | Double Feed Induction Generator |
| DG | Distributed Generation |
| DISCO | Distribution Company |
| DPSO | Discrete Particle Swamp Optimization |
| EPSO | Evolutionary Particle Swamp Optimization |
| GA | Genetic Algorithm |
| GDP | Gross Domestic Product |
| GHG | Green House Gas |
| ICE | Internal combustion engine |
| IGBT | Insulated Gate Bipolar Transistor |
| IPSO | Improved Particle Swamp Optimization |
| LOC | Levelized Cost Electricity |
| LNG | Liquefied Natural Gas |
| MIP | Mixed Integer Programming |
| MOF | Multi objective Function |
| MT | Micro Turbine |
| NBPSO | Novel Binary Particle Optimization |
| NLP | Non linear Programming |
| OPF | Optimal Power Flow |
| PCC | Point of Common Connection |
| PMSG | Permanent Magnet Synchronous Generator |
| PSO | Particle Swamp optimization |
| PV | Photovoltaic |
| RES | Renewable Energy sources |
| SCIG | Squirrel Cage Induction Generation |

| | |
|---|---|
| SHP | Small Hydro Power |
| SCR | Silicon Controlled-Rectifier |
| SUMT | Sequential Unconstrained Minimization Techniques |
| THD | Total Harmonic Distortion |
| VPII | Voltage Profile Improvement Index |

# Chapter 1

# OVERVIEW OF THE RESEARCH

## 1. Introduction

Energy is vital for all living-beings on earth. Energy can neither be created nor destroyed but can be transformed from one form to another. In light of this, modern life styles have further increased its importance, since a faster life means faster communication, faster manufacturing processes and transport. One of the largest consumer markets in the world is the electric power industry. The electrical power system is in massive need of alternative generation other than conventional type since it is facing mounting demand [1] [2]. For instance, in the United States, 3% of America's Gross Domestic Product (GDP) is spent on electric energy purchases, which are increasing faster than the rate of economic growth. The cost of electricity is estimated at around 50% for fuel, 20% for generation, 5% for transmission and 25% for distribution which increases the need for alternative power source at distribution level [3]. The X/R ratio for distribution levels is low compared to transmission levels, resulting in high power losses and a dip in voltage magnitude along radial distribution lines [4]. Distribution systems must deliver electricity to each customer's service centre at an appropriate voltage rating.

In addition, research shows that roughly 13% of the total power generated is lost at the distribution level. Such non-negligible losses have a direct impact on the financial aspect and overall efficiency of distribution utilities [5]. All these lead to an increase in energy demand. The innovative power distribution network has always been confronted with an ever growing load demand, this increasing load is leading to increased burden and reduced voltage profiles. Even in certain industrial areas that have critical loading, it may lead to voltage collapse [2]. Therefore, to improve the voltage profile and reduce electrical losses, optimal placement and sizing of distributed generation is needed.

Research has indicated that demand globally is expected to grow at an annual pace of 1.4 % between now and 2020 [6]. In lieu of this, Distributed Generation (DG) or the alternate energy systems are expected to play an increasing role in the future of the power systems. The installations of Distributed Generation (DG) units is becoming more prominent in distribution systems due to their overall positive impacts on power networks. Distributed Generation (DG) technologies under the smart grid concept form the spine of our world electric distribution networks [7]. The DG can also improve the reliability of the system by functioning as a backup

generator for some clients in case of disruptions from the utility. These DG technologies are classified into two groups: (i) renewable energy sources (RES), and (ii) fossil fuel-based sources (non-renewable). Fossil fuel based DGs are the internal combustion engines (IC), combustion turbines and fuel cells. Renewable energy source (RES) based DGs are wind turbines, photovoltaic, biomass, geothermal, small hydro, etc. [8] [9]. It is important to evaluate the technical impacts of DG in power networks. Evaluation of the technical impacts of DG in the power networks is very critical and laborious. Thus, the generators are required to be connected in distributed systems in such a way that power losses and poor voltage profile are avoided. Poor allocation of DG in terms of its location and capacity may cause an increase in fault currents, voltage variations, interference in voltage-control processes, increased losses, increased system capital and operating costs, etc. [10]. Also, installing DG units is not forthright, and thus the placement and sizing of DG units to reduce losses and improve voltage should be carefully addressed [10] [11]. However, in order to maximize benefits, solution techniques for DG placement should be obtained by optimization approaches [5]. Investigating this optimization problem is the key motivation of this research.

DG allocation is a complicated combinatorial optimization problem which demands concurrent optimization of multiple objectives such as minimizations of real and reactive power losses, carbon emission, line loading, and short circuit capacity and maximization of network reliability, etc. The aim is to determine the optimal location(s) and size(s) of DG units in a distribution network. The optimization is carried out under the constraints of maximum DG sizes and the voltage limit of the nodes [12].

There are many optimization techniques used in past works for multi-objective search. In [13], an analytical approach to determine the optimal location of DG is presented. In most of the recent works, population based evolutionary algorithms are used as solution strategies. This includes evolutionary programming [14], particle swarm optimization (PSO) [15] [16] and genetic algorithm (GA) [17] etc. The advantages of population-based meta-heuristics algorithms such as GA and PSO are that a set of non-dominated solutions can be found in a single run because of their multi-point search capacity. They are also less prone to dimensionality problems [12].

## 1.1 Motivation

The electric power system consists of generation, transmission and distribution and loads. The purpose of power system is to facilitate the transport of electrical energy from the production to the consumption, while sustaining an acceptable power quality and voltage quality for all customers (producers and consumers). The traditional power systems were designed for unidirectional energy flows from a small number of generators to scattered areas of demand through long transmission and distribution networks. Such generators are at large power plants, mainly turbo (fossil fuel and nuclear) and hydro, which are placed remotely from consumption centres.

The early 1990s introduction of open electricity market in many countries, pave way for involvement of new competitors to enter the electricity market. The deregulation of the electricity market was as a result of introduction of new electricity production. With regards to environmental matters, several of the conventional types of generators emit carbon dioxide which may lead to the much-discussed global warming. Changing from conventional generation based on fossil fuels, such as coal, gas and oil, to renewable sources, such as solar and wind, would thus reduce the emission. Many countries have created incentives mechanism to improve the use of renewable energy source as an alternative source to encourage power producers.

The renewable incentives meet the targets agreed under the Kyoto Protocol. Alternatively, fossil fuel could be made more expensive by means of taxation or for example, a trading mechanism for emission rights. Some of the incentive schemes have been very successful (Germany, Denmark, and Spain), while others were less successful [6].

Since electricity generated is to be consumed at the same time due to the fact that it cannot be stored efficiently in a large amounts, it is required that power system operators must constantly balance power generation and demand. Even though, the redial design of distribution system with the integration of distributed generation at the level was not considered in the design. This is due to serious fear entertained by power system operators that reliability and quality of the network may be altered or not guaranteed [18]. This makes the coordination of the integration of DGs essential to meet the system technical and economical demand by optimally placing and sizing DGs. Optimal allocation and sizing find a major application in this regard using algorithms for decision making.

## 1.2 Distribution Systems Power Loss Minimization

As formally explained, among the many benefits of distributed generation, reduction in system line losses is one. Commonly, the real power loss attracts more interest from the utilities, as it reduces the effectiveness of transmitting energy to customers. However, reactive power loss is obviously not less significant. This is due to the fact that reactive power flow in the system needs to be maintained at a certain amount for a sufficient voltage level. Therefore, reactive power makes it possible real power flow through transmission and distribution lines to consumers. System loss reduction by optimally placed DG along the network feeder can be very useful if the decision maker is committed to minimizing losses, improving network performance, and maintaining investments to a fairly low level [19]. This feature may be applicable in case of revenue recovered by the distribution company (DISCO) which is founded not only on the asset value but also on network performance.

## 1.3 Distribution Systems Voltage Profile Improvement

In a distribution system, operators are duty-bound to maintain the voltage level of each customer in the network within the required limit. To maintain voltage profiles at a satisfactory level in distribution systems, different standards has been established. For example, the American National Standards Institute (ANSI) standard C84.1 has stipulated that voltage variations in a distribution system should be controlled within the range of -13% to 7% [20]. Actually, in practice, many electricity companies try to control voltage variations within the range of ±6%. One of the upcoming widely adopted methods for improving voltage profiles of distribution systems is by introducing distributed generation (DG). The DG units improve voltage profiles by changing power flow patterns. The locations and sizes of DGs would have a significant impact on the voltage profiles.

## 1.4 Distributed Generator Placement and Sizing

Normally there is a load growth in a distribution network and at a stage existing capacity of the network may be inadequate, whereby a new capacity must be added to the network. Requirements for new substations or expanding existing substations' capacities and their associated new feeders or both is usually involved. Even so, the flexibility, technology, technical and pecuniary benefits and concepts of DG planning are gaining credibility as a

solution to the distribution planning problems with the prohibitive high cost of power curtailment in the changing regulatory and economic scenarios. This increase DG as one of distribution planning options that avoids causing degradation of power quality, reliability and control of the utility network [21] [22].

Generally, DGs are connected with the existing distribution system and a lot of studies have been done to ascertain the best location and size of DGs to produce utmost benefits. Due to high costs, the DGs should be allocated optimally to enhance the system performance in order to reduce system loss as well as to get some improvements in the voltage profile while maintaining the stability of the system. The effect of integration of DG on network parameters usually differs with respect to its type, location and load at the point of connection [23].

Figure 1.1 presents a plot of power loss versus size of DG at each bus in a certain distribution test system [8]. From the figure, it is obvious that for a particular bus, as the size of DG is increased, the losses are reduced to a minimum value and increased beyond a size of DG (that is, the optimal DG size) at that location. Any further increase in size of DG will result in increase in loss and it is likely that it may overshoot the losses of the base case.

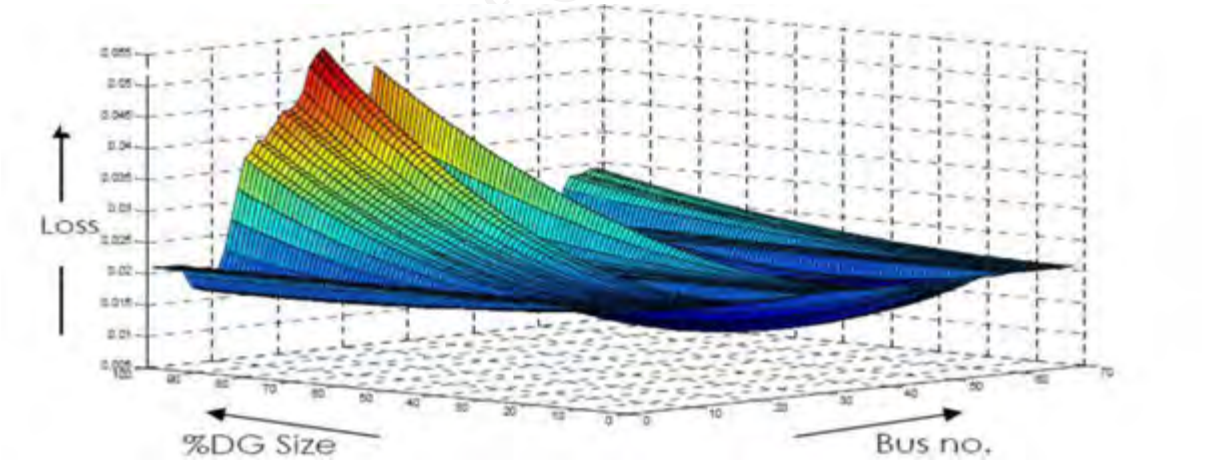


Figure 1.1: Effect of size and location of DG on system loss [8]

Also notice that the location of DG plays significant role in minimizing the losses. More often than not, most DG units are owned by the customers. The grid operators cannot decide the locations of the DG units. Normally, it is assumed that losses decrease when generation takes place closer to the load site. However, as it was mentioned, local increase in power flow in low voltage cables may have undesired consequences due to thermal characteristics [24].

## 1.5 Objectives

To achieve the objective of reducing system losses and improving voltage profile by optimal placement and sizing of distributed generation (DG), the following were addressed.

- To utilize both real and reactive power flow and power loss sensitivity factors in reducing the algorithms search space.
- To formulate a multi-objective function taking into consideration real power loss reduction index (PLRI), reactive power loss reduction index (QLRI) and voltage profile improvement index (VPII).
- To design a hybrid approach for optimizing DG location and size in a distribution system. The hybrid algorithm will combine both GA and PSO optimization techniques.
- To investigate the effect of DG penetration on system power losses and voltage profiles using wind and photovoltaic DGs, and using a real network and a test system to justify the algorithm above.
- To compare the results from the above and draw conclusion and recommendation.

## 1.6 Research Questions

The performance and deliverables of the power distribution system are important issues that many engineers and researchers have studied and have proposed various solutions. This matter is important in order to fulfil load demands, which increase significantly year by year. However, the progress in enhancing the efficiency of the system is hindered by two major factors, which are the existence of high real power losses and poor voltage profile. Several research questions that this thesis will try to answer when analyzing the effect of placemen and sizing on the distribution system are listed are:

- What is the appropriate method that can be applied to solve the of DG integration problems?
- Which types of DG combination gives minimal loss and improved voltage profile in the distribution system?
- What happens to the performance of voltage profile and power loss when allocation and sizing are performed on the system?

- What are the advantages of the GA-IPSO over classical Genetic Algorithm in placing and sizing of DG?

## 1.7 Methodology

Optimal allocation of DGs on distribution networks is carried out by a standard test system which is IEEE 33-bus test feeder and the simplified Western Cape Network, MATLAB/SIMULINK is used for the network design and simulations.

- The network voltage profile obtained from the Newton-Raphson load flow was put in graphic form (base case) to know the weakest bus when DG is not connected to the network. Some buses and the farthest bus are chosen as candidate buses for DG connection in relation to the penetration level.
- The GA- IPSO algorithm was used for decision making on placement and sizing of DG in the chosen networks
- Algorithm code written on Matlab for allocation was used to interact with Newton-Raphson load flow program and some predetermined conditions of grid code.
- The results obtained from power losses and voltage profile of both GA and GA-IPSO were compared using two types of DGs and loading conditions. From there conclusion and recommendation were made.

## 1.8 Scope of the Research

The dissertation is limited to the optimal allocation of distributed generation in a distribution network. The impact of distributed generation DG on the distribution network and the impact of DG generating only active (photovoltaic) and the one generating both active and reactive (wind) were investigated. The thesis is limited to investigating only the impact on losses and voltage profile.

## 1.9 Outline of the Dissertation

The dissertation is organized as follows:

Chapter One gives the introduction, detail of the dissertation, the objectives, methodology, contributions to a body of knowledge, the scope of work and the outline of the dissertation.

Chapter Two presents the literature review on Distributed Generation, assesses the various sources of renewable energy and non-renewable, their technology, merit and demerit of each.

Chapter Three discusses the impact of DG on a distribution system; it also provides basic concepts of DG integration and various interface technologies in use.

Chapter Four is about modelling and problem formulations. It also presents the system loss sensitivity formulation and constraints for optimal allocation.

Chapter Five gives detailed information about OPF programming and theory of optimization techniques that can be used and the advantage of using GA-IPSO compared to other methods.

Chapter Six showcases the methodology, hybridization of GA and PSO to give GA-IPSO and step implementation of the approach.

Chapter Seven presents simulation procedures and results from two different scenarios of load condition using stochastic nature of two types of DGs and two different approaches under a period of time.

Chapter Eight discusses the loss reduction and voltage profile improvement with the allocation method used above and the impact of the two types of DGs used as well as the effectiveness of the approach used.

Chapter Nine presents the conclusions and recommendations for future work.



### 1.10 Publications during the completion of the dissertation

O. O. Osaloni and K. O. Awodele, "Analytical Approach for Optimal Distributed Generation Allocation in Primary Distribution Networks," in *Proc. 2016 South African Universities Power Engineering Conference*, pp. 115-120

### 1.11 Summary

This chapter has given the introduction, details of the dissertation, the objectives, methodology, the scope of work and the outline of the dissertation. The next chapter will present the literature review of Distributed Generation and its technology, also its benefits to the distribution system.

# Chapter 2

# LITERATURE REVIEW ON DISTRIBUTED GENERATION SOURCES

## 2. Introduction

This chapter presents the definition of distributed generation. Types of distributed generation technology were given and their benefits to the Distribution Network are reviewed.

## 2.1 Distributed Generation

Distributed Generation (DG) is one of the latest trends in power systems used to support the increased demand. DG concepts involves many technology and application, in lieu of this there is no common acceptable definition. Notations such as “embedded generation”, “dispersed generation” or “decentralized generation” are used by different countries. Furthermore, several definition are given by different organizations such as (IEEE) and (CIGRE) for distributed generation.

DG was defines by as “the generation of electricity by facilities that are sufficiently smaller than central generating plants so as to allow interconnection at nearly any point in a power system.” IEEE compared the size of the DG to that of a conventional generating plant. A more precise definition is provided by the International Council on Large Electric Systems (CIGRE) [25] Chambers looks into the economic side in his definition. He defines distributed generation as “the relatively small generation units of 30 MW or less that are sited at or near customer sites to meet specific customer needs, to support the economic operation of the distribution grid, or both [26].

Don-diet defines distributed generation as “a small source of electric power generation or storage (typically ranging from less than a kW to tens of MW) that is not a part of a large central power system and is located close to the load.” He included the storage facilities in his definition [27]. Ackermann [28] defines a distributed generation source as “an electric power generation source connected directly to the distribution network or on the customer side of the meter.” Ackermann’s definition is the most generic one, because there is no limit on the DG size and capacity. The definition covers the location of the DG. In this dissertation, the Fortoul definition is used [29]. Distributed generation is considered as an electrical source connected

to the power system, in a point very close to/or at a consumer´s site, which is small enough compared with the centralized power plants.

## 2.2 Distributed Generation Technology

Different distributed generation technologies are involved in power systems. Some of these technologies have been in use for a long time while others are newly emerging. However, the features that all DG technologies have in common are to improve efficiency and cut down costs related to installation, running and maintenance. DG technologies are broadly categorized into two types: renewable technologies (for example, photovoltaic and wind turbine) and non-renewable technologies (for example, mini and micro-turbines, combustion turbines and fuel cells). DG technologies have an important impact on the choice of the appropriate size and place, to be connected to a power system or customer loads. The next sections provide details on the most popular DG technologies currently in the market [30]. They are shown in Figure 2.1 below [30].

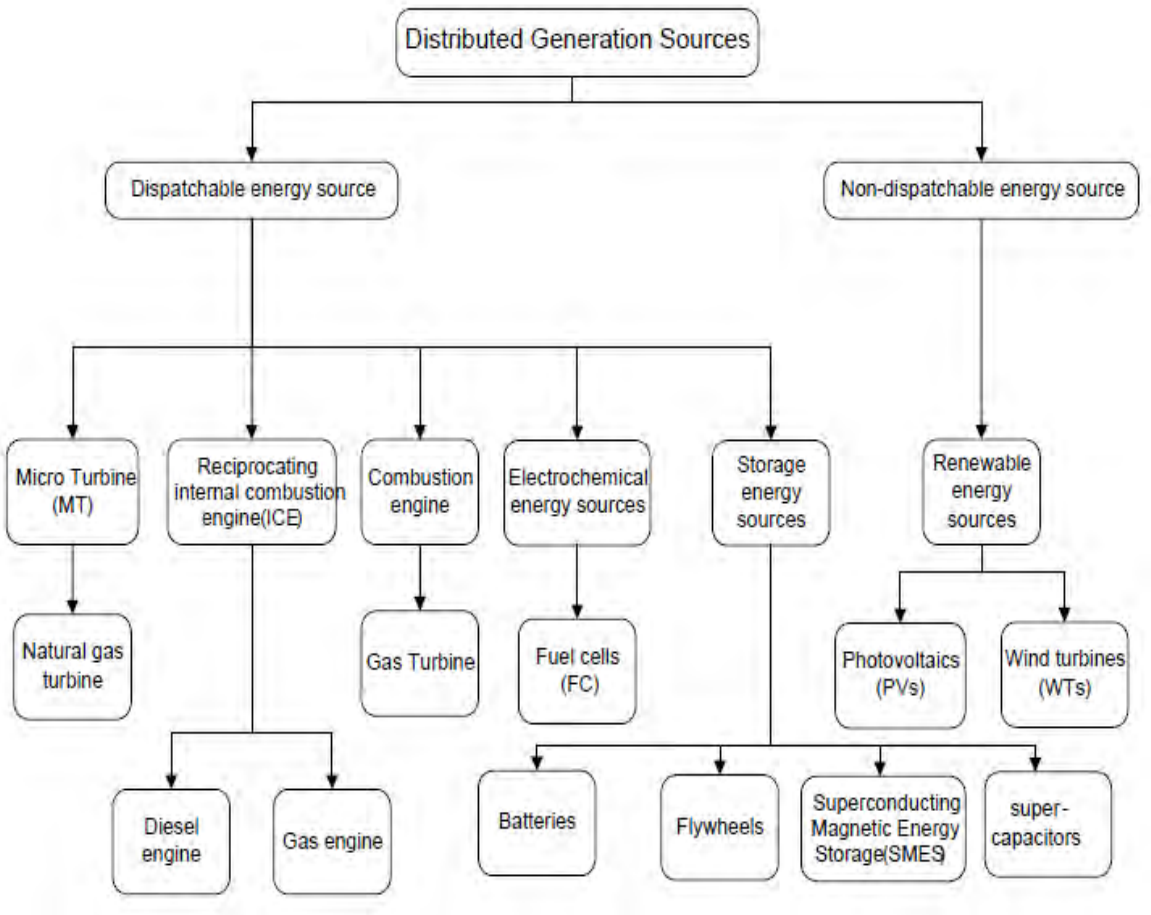


Figure 2.1: Distributed Generation sources

## 2.3 Internal Combustion Engines

Internal combustion engine (ICE) is a heat engine where the combustion of a fuel take place with an oxidizer in a combustion chamber that is an integral part of the working fluid flow circuit. In an internal combustion engine, the expansion of the high-temperature and high-pressure gases produced by combustion apply direct force to some part of the engine. The force is applied topically to pistons, turbine blades, or a nozzle. This force set the element in motion over a distance, converting chemical energy into useful mechanical energy. Typically an ICE is fed with fossil fuels like natural gas or petroleum products such as gasoline, diesel fuel or fuel oil. [31].

The application of ICE is a very familiar technology for DG. The factors such as proven technology with low capital cost, large size range, from a few kW to MW, good efficiency, and good operating reliability make it suitable for DG application. These features, combined with the engines' ability to start up automatically make them more efficient. Shows in Figure 2.2(a) below is a basic ICE and Figure 2.2(b) shows ICE with piston fuel conversion.

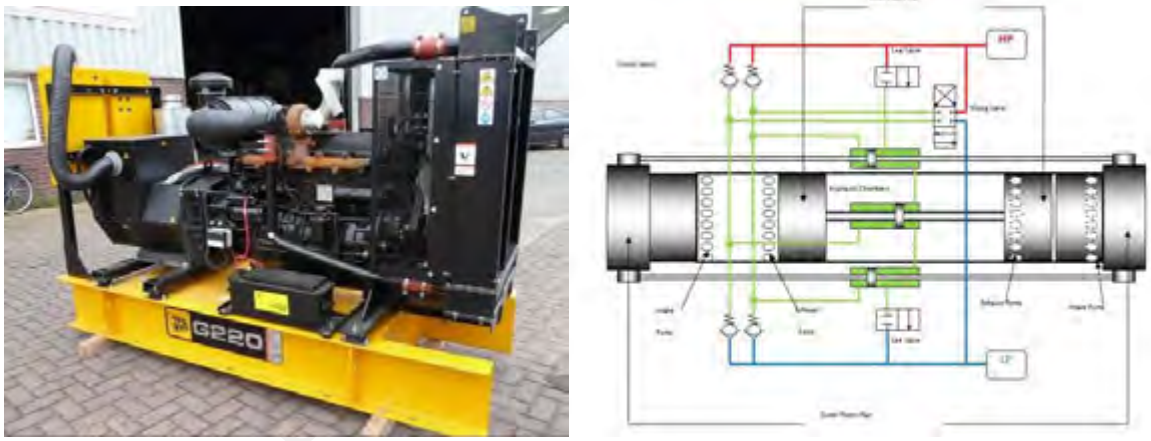


(a) (b)

Figure 2.2: (a) Basic (ICE) and (b) Piston showing fuel conversion [32]

Fast starts during a power outage and not needing much space for facility; make them the principal choice for emergency or standby power supplies. Higher maintenance and fuel cost, which is the highest among the DG technologies, high noise pollution are the key barriers to ICE usage [32]. Also in the market today we have what is called sound proofing aimed at reducing the noise produced by the ICE and to make it applicable at any location. Shown in Figure 2.3 below is a typical example of sound proofing.


Figure 2.3: Sound-proof Internal Combustion Engine (ICE) [33]

### 2.3.1 Advantages of an Internal Combustion Engine

- An internal combustion engine has higher efficiency. An internal combustion engine is about 40% efficient, which means that an internal combustion engine can convert 40 per cent of heat energy.
- An internal combustion engine is quite safe to use. Gas produces at high pressure in the cylinder at very short interval and utilized as soon as they are formed.

## 2.4 Fuel Cells

Fuel cells are relatively new and considered an emerging DG technology. Their application as distributed generation ranges from 1 kW to 3 MW capacity. Fuel cells can be used as an electrical power generation technology or in CHP applications. They are ideally good enough for laboratory or process loads. The waste heat from fuel cells can be used in low-pressure steam heating applications tied into hot water distribution systems [32].

In fuel cells, electrochemical devices convert the chemical energy of a fuel directly to electricity and heat without combustion. This is quite different from most electric generating devices (for example, steam turbines, gas turbines, and combustion engines) which first convert the chemical energy of a fuel to thermal energy, then to mechanical energy, and, finally, to electricity. Fuel cells efficiencies ranges from 40 to 60% in production of electricity, with negligible harmful emissions, and operate so quietly that they can be used in residential

environment. These are the merits of fuel cells, besides their scalability and modularity. The main disadvantage of the commercialization of fuel cells is the huge investment cost [26].

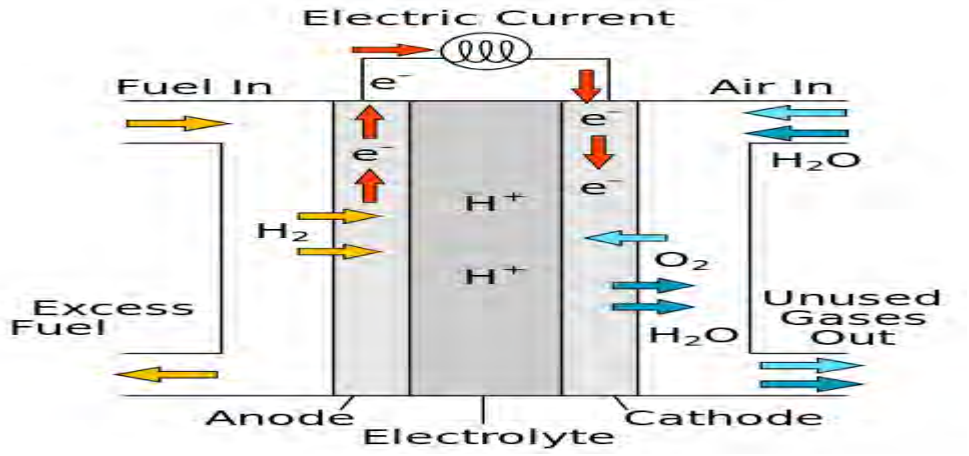


Figure 2.4: Schematic diagram of a fuel cell [34]

### 2.4.1 Technology Description

Fuel cells operate on hydrogen and typically utilize an on-board natural gas reformer to convert natural gas into hydrogen. Two electrodes a cathode and an anode pass charged ions in an electrolyte to generate electricity and heat as shown in Figure 2.4 above. The fuel reacts electrochemically and is not composted, resulting in less significantly emissions than a standard CHP plant [25].

### 2.4.2 Advantages of Fuel Cell

One main advantage of fuel cells is that they are the neatest fuel-powered Distributed Generation technology. This is because a fuel cell does not combust the fuel and the fuel subsystem processing system is the only source of emissions.

- Direct conversion of fuel to electricity without any combustion, make them more efficient than any other electrical generating technology available today.
- Unlike batteries that must be disposed off once their chemicals are used up, fuel cell reaction do not degrade over time and can theoretically provide continuous electricity.
- Economically, fuel cells represent a cautious path to provide a country electric power because their installation can be done more quickly, are fuel flexible, and can be put in place incrementally, reduce the need for more costly and sweeping charges [35].

### 2.4.3 Disadvantages of Fuel Cell

- Hydrogen is currently very expensive, not because it is rare (it is the most common element in the universe), but because it is difficult to generate, handle, and store, requiring bulky and heavy tanks like those for compressed natural gas (CNG) or complex insulating bottles if stored as a cryogenic (super-cold) liquid like liquefied natural gas (LNG).

- A tank containing metal-hydride absorber or carbon absorber can be used for its storage at moderate temperatures and pressures, though these are currently very expensive [27].

## 2.5 Biomass

Biomass resources include the following: agricultural waste, animal manure, forest waste, industrial waste, municipal waste, sewage sludge, crops, etc. Biomass as an energy source can either be used directly by combustion to produce heat, or indirectly after converting it to discrete forms of biofuel. Conversion of biomass to biofuel can be achieved by different methods which are loosely classified into: electrochemical conversion methods, thermal, chemical, and biochemical conversion. Another alternative is to convert the solid biomass into a fuel gas. Generally, piston-driven engines are found of using biofuel, high efficiency gas turbine generator as well as fuel cell also use biofuel [36].

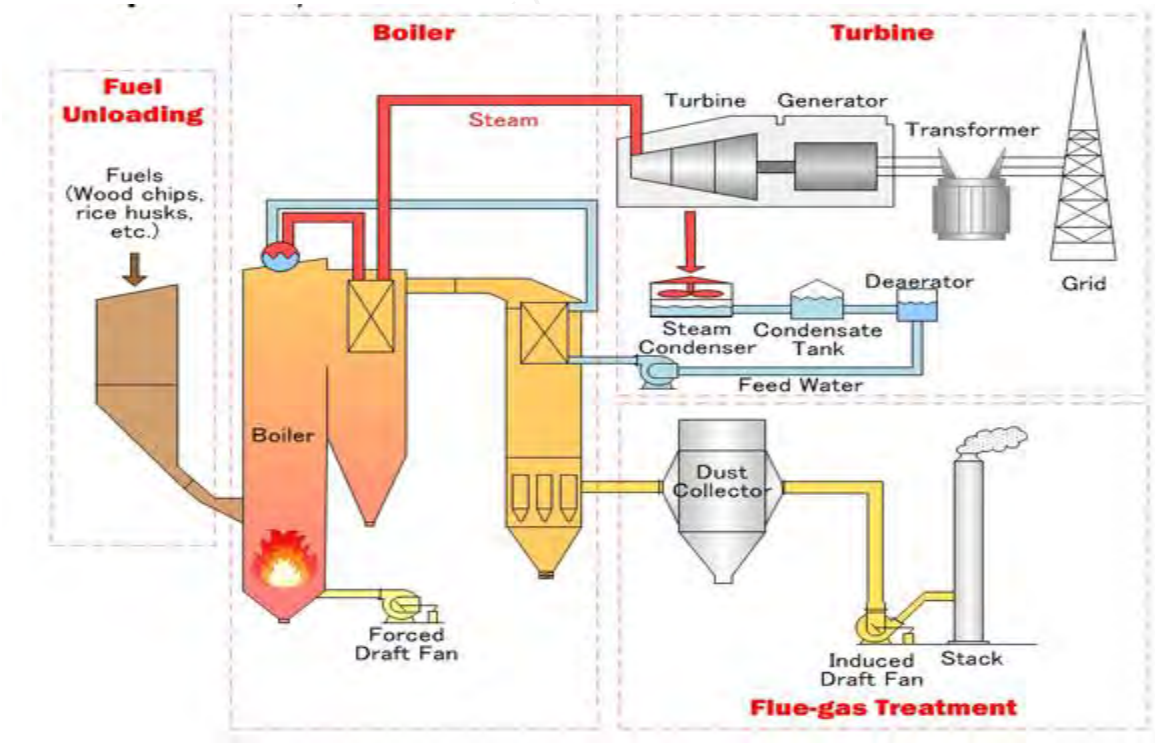


Figure 2.5: Direct/Mixed Combustion Power Generation Methods [37]

Biomass plants typically are of the direct combustion, mixed combustion, or gasification type. With the direct combustion power generation method, steam is produced from the heat generated by the burning of materials such as wood waste, agricultural waste, and livestock waste as shown in Figure 2.5 above. The steam turns a turbine, which in turn drives a generator that produces electricity. With this method, it is important to secure a stable supply of biomass materials and maintain uniform moisture content in these materials.

## 2.6 Micro Turbines

A small turbines for generating electricity using variety of fuels, including natural gas is called Micro turbines (MT). The merit of (MT) over internal combustion engines is low noise, less frequent maintenance, less vibration, more compact size, lower uncontrolled emissions, and an exemption from air quality permitting in many circumstances. Waste heat from 500 °F exhaust can be used to produce hot water with the addition of a waste heat recovery hot water heater. In some cases, micro turbines can be designed with waste heat recovery equipment to produce chilled water, or exhaust heat can be used directly in heating and drying applications.

The technology was originally developed for transportation applications, but is now finding a niche in power generation. One of the most striking technical characteristics of micro turbines is their extremely high rotational speed, up to 120,000 rpm. Micro turbines produce high frequency AC power. A power electronic inverter converts this high frequency power into a usable form. The individual unit of micro turbines ranges from 30 - 200 kW, but it can be combined readily into systems of multiple units. Low combustion temperatures can assure very low $NO_2$emission levels. They make much less noise than a turbine of comparable size [38].

### 2.6.1 Advantages of Micro Turbines

- They are very efficient (more than 80%) and have lower emissions (less than 10 ppm $NO_2$) with respect to large scale ones.
- They have well-known technology and they can start-up easily, have good load tracking characteristics and require less maintenance due their simple design [39].
- They have lower electricity costs and lower capital costs than any other DG technology costs [40].

- They have a small number of moving parts with small inertia not like a large gas turbine with large inertia.
- Modern power electronic interface between the MT and the load or grid increases its flexibility to be controlled efficiently [41].

## 2.7 Steam Turbines

Conventional steam turbines and combustion turbines are well-developed technologies that are widely used for medium sized systems (more than 500 kilowatts). Steam turbines have low maintenance and low operating cost relative to those of most other generating technologies as well as low emission. It is the most preferred technology of most conventional generation applications that generates more than 20 MW of power because of these qualities and shorter lead times needed to build units [42].

## 2.8 Gas Turbines

A device that comprise of compressor, combustor, and turbine-generator assembly that converts the rotational energy into electric power output is called Gas turbines. Gas turbines of all capacities are now widely used in the power industry. It finds application in other plant such as Small industrial gas turbines of 1 – 20 MW is commonly used in combined heat and power (CHP) applications. The maintenance cost is on the lower side than for reciprocating engines. Gas turbines can be noisy. "Emissions are somewhat lower than for combustion engines, and cost-effective NO$x$ emission-control technology is commercially available" [43].

## 2.9 Solar Thermal

Solar thermal systems generate electricity by concentrating the incoming sunlight and then trapping its heat, which increases the temperature of a working fluid to a very high degree to produce steam and then generate electricity. Notice that this process is different from that of a photovoltaic panel where the sunlight is directly converted into electricity without the involvement of heat collection [43]. Compared to solar photovoltaic, the solar thermal is more economical, as it eliminates the costly semiconductor cells [44]. One such commercial solar thermal power plant, rated 350 MW, is located in the California Mojave Desert and is connected to the Southern California Edison's transmission grid. This capacity is more than 90% of the world's solar thermal capacity up to 1999 [45].

## 2.10 Small Hydropower

Hydropower turbines were first used to generate electricity for large commercial use in the 1880s. Expansion and increasing access to transmission networks has led to concentrating power generation in large units benefiting from economies of scale. This resulted in a trend of constructing large hydropower installations rather than small hydropower systems for several decades. However, liberalization of the electricity industry has contributed in some ways to the development of small hydropower generating capacity by independent power producers [46]. Small hydropower (SHP) is commonly used to refer to hydropower with capacity less than 10 MW. Other terms that are normally used are mini hydropower for SHP with capacity between 100 kW and 1 MW and micro hydropower for SHP with capacity below 100 MW. The power generated from SHP plants is quite large. The European Small Hydropower Association reported that up to 2006, the total installed capacity of SHP in Europe is 13,000 MW [47].

## 2.11 Solar Photovoltaic

The type of direct conversion of sunlight to electricity without engagement of heat engines is called photovoltaic (PV) systems. PV found its application in calculator, remote buildings, communication satellite, watches as well as space vehicles. Photovoltaic (PV) system is a capital-intensive renewable technology with very low operating costs, compared to other DG technologies discussed above. Application of PV systems can also be more suitable during peak demand periods [38].

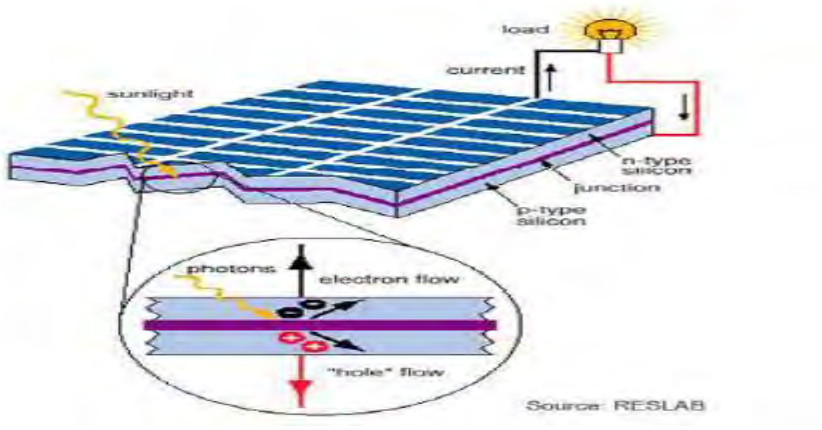


Figure 2.6: Photovoltaic system schematic diagram [25]

Driven by advances in technology and increases in manufacturing scale and sophistication, the cost of photovoltaic has declined steadily since the first solar cells were

manufactured [48] and the levelized cost of electricity (LCOE) from PV is competitive with conventional electricity sources in an expanding list of geographic regions [49]. The PV implementation is encouraged by the almost unlimited availability of sunlight, long life cycle, high modularity and mobility, easy maintainability (since there are no moving parts), very low operation cost, environmentally friendly, ability for off-grid application and short time for design, installation and start up. Mostly, individual PV modules range from 20 W to 100 kW. The disadvantages of PV systems include significant area requirements due to the diffuse nature of the solar resource, higher installation cost than other DG technologies, and intermittent output with a low load factor [50].

Photovoltaic arrays are often associated with buildings: either integrated into them, mounted on them or mounted nearby on the ground. Arrays most often retrofit into existing buildings, usually mounted on top of the existing roof structure or on the existing walls. Alternatively, an array can be located separately from the building, but connected by cable to supply power to the building, this arrangement is called a stocks cell. In 2010, more than four-fifths of the 9,000 MW of solar PV operating in Germany were installed on rooftops [51]. Building-integrated photovoltaic (BIPV) are increasingly incorporated into new domestic and industrial buildings as a principal or ancillary source of electrical power.



### 2.11.1 Important Merit of Photovoltaic PV Systems

- Photovoltaic (PV) systems provide green, non-dispatchable power by exploiting solar energy.
- Photovoltaic (PV) panels constitute a reliable, industrially matured, green technology for the exploitation of solar energy.
- With respect to operating costs and maintenance costs, Photovoltaic (PV) panels, unlike other renewable energy technologies, require minimum operating or maintenance costs [52].

### 2.11.2 Demerits of Photovoltaic (PV) Panels

- The enormous demerits of Photovoltaic (PV) panels is their limited efficiency levels; compared to other renewable energy sources such as solar thermal. The efficiency of PV rages from 12 – 20 %.
- Solar Photovoltaic (PV) panels' demerits also includes it inability to store excess amounts of produced energy for later use [2].

## 2.12 Wind Power

The sail of humans into the wind can best identify the existence of wind power [36]. Wind energy is growing at a rapid rate, and it has been described as one of the fastest growing energy technologies. It has more than 30% yearly growth and at the end of 2008 about 121,000 MW has been installed globally, 45% of this installed capacity are located in EU countries. It global growth chart as at year 2013 stand at 21% as shown in Figure 2.7. Wind powered pumps drained the borders of the Netherlands, and in arid regions such as the American Midwest or the Australian outback, wind pumps provided water for livestock and steam engines.

Production of mechanical or electrical power from flow of air can be achieved using wind turbines or sails. Mechanical power is obtained through windmills, wind pumps for water pumping as well as sails to propel ships. Wind is readily available, is plentiful, renewable, clean, emit no gas such as $CO_2$ and widely distributed which make them an alternative to fossil fuels. Intermittency and grid reliability is regarded as the major challenge facing wind power technology [36]. However, the price of wind power is therefore much more stable than the volatile prices of fossil fuel sources, which leads to its growth globally as shown in the Figure 2.7 below. Study shows that the marginal cost of wind energy after construction has been concluded is less than 1 cent per kWh [46].

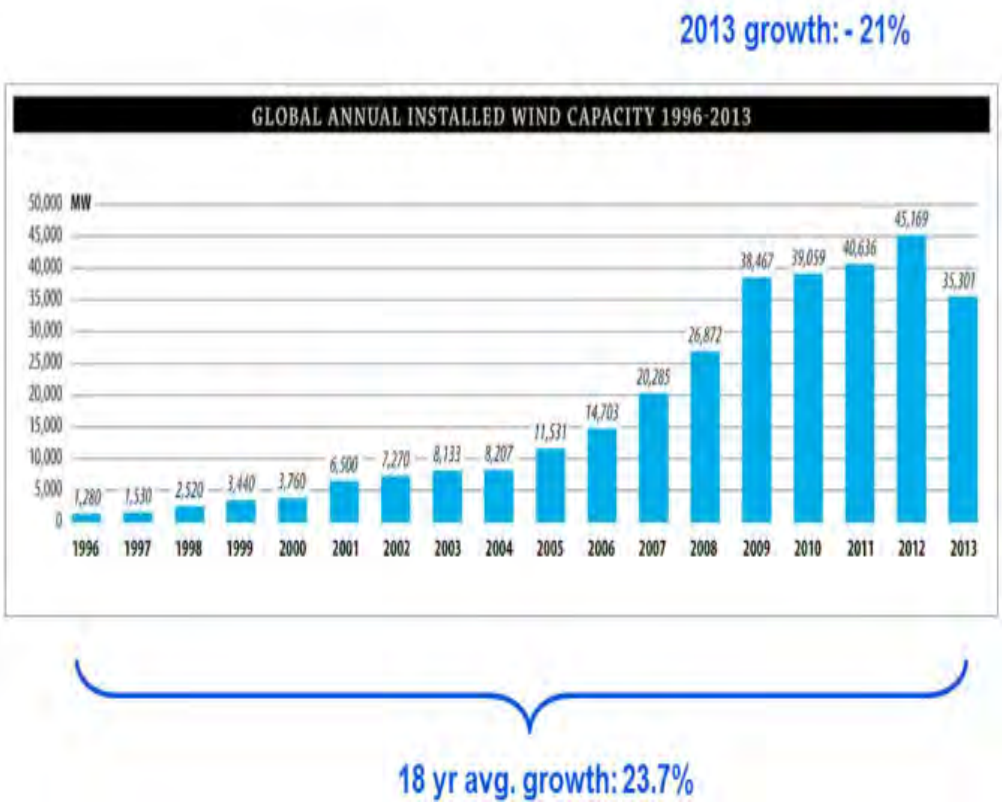


Figure 2.7: The global growth chart of wind power [53]

### 2.12.1 Operation

Wind rotates the windmill-like blades, which in turn rotate their attached shaft. This shaft operates a pump or a generator that produces electricity. Although the energy characteristics of larger wind turbine farms are closer to the centralized energy sources, small wind turbines (working as modules) can be combined with PV and battery systems to serve an area requiring 25–100 kW as shown in Figure 2.9 below [54].

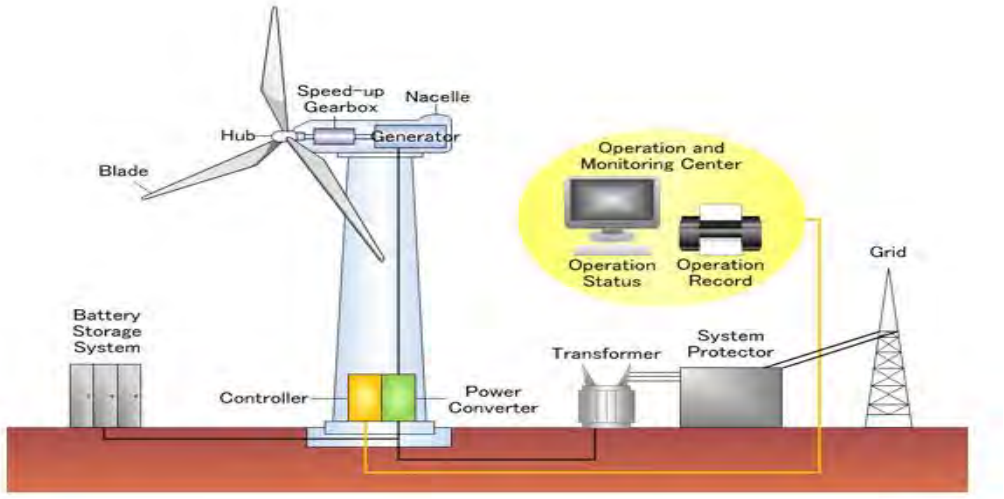


Figure 2.8: Schematic operation diagram of a wind turbine [54]

### 2.12.2 Advantages of Wind Power Include:

- It forestalls or replaces the need to build potentially more polluting conventional power plants.
- It produces virtually no pollution of air, water or soil.
- Because of its modular nature, it is easy to add capacity as needed.
- Installing wind turbines is relatively quick.

## 2.13 Distributed Generation Benefits

Distributed generation offers a lot benefits, both economic, environmental and technical can be drawn through the interconnection of DG units into electric power networks. An overview on these benefits can be seen in Figure 2.10 below. The major benefits of the integrations of DG into electric power networks are as follows [54].

### 2.13.1 Economical Benefits

The act of integrating DG units closer to load centre leads to avoidance of the need for building new T&D lines, upgrading the existing power supply system and reducing T&D capacity during network planning. Thus, DG can be a least-cost planning alternative[54]. Some economic benefits of DG are discussed as follows:


Figure 2.9: Distributed Generation Benefits [54]

- DGs can be assembled easily anywhere as modules which have different advantages as they can be installed in a very short period at any location. Total capacity of DG can be increased or decreased by adding or removing more modules, respectively.
- DGs can be installed in small increments to meet an increase in load growth, by sizing it in small increments to supply the load requirement.
- Integration of DG reduce power demand from central plant, which reduce the wholesale power price by supplying power to the grid.

### 2.13.2 Technical Benefits

DGs can provide different technical benefits based on different factors, for example, location and technology. The following are some of the technical benefits [54].

- Improving availability and reliability of the power supply network,
- Voltage regulation support and power quality improvement
- Power-loss reduction
- Reducing power flow inside the transmission network to fit certain constraints and improve its voltage profile
- DGs can help in "peak load shaving" and load management programs,
- Other benefits of DG include providing ancillary service, and adding self-generation to customer options
- DGs could prove invaluable for developing countries. Thus, micro power is an attractive option for those countries. DGs such as grid-free renewable may be particularly suitable for remote areas.

### 2.13.3 Environmental Benefits

Generation of Electric power account for 40% of carbon dioxide emission, a major contributor to climate change. The need to reduce carbon emission into the environment, also to reduce noise pollution and protect other creatures can be made possible by DG power source. Recent DG technologies offer an environmentally friendly source of electrical energy through limiting the Green house Gas (GHG) emissions. By 2050 a widespread installation of micro generation could reduce the household carbon emissions by approximately 15% [55]. Also, another benefit is that it reduce the tendency of construction of new transmission circuits and large networks.

## 2.14 Summary

This chapter reviews the definition of distributed generation as proffered by different bodies and authors in the field of electrical power system. It also gives detailed information about DG technologies that are available and the general benefits. The types of DG discussed above, as well as the advantages they offer and their benefits, will help to mitigate the effect of power loss reduction and poor voltage profile. The next chapter presents the impact of DG on power system distribution networks and their technology for integration to the grid.

# Chapter 3

# DISTRIBUTED GENERATION IMPACTS AND INTEGRATION TECHNOLOGY

## 3. Introduction

This chapter serves to review the major positive and negative impacts of Distributed Generation on the operation of distribution networks, it presents technical integration of Distributed Generation to the grid and various interface technologies currently in use.

## 3.1 Impact of Distributed Generation

The primary aim for design of Distribution network is to deliver electrical power to load at reasonable voltage and quality power. Consequently, in case of output fluctuation or a reverse flow from generators arises on the grid because of DG, there might be some effect on the entire system in terms of power quality or protection and safety [6]. Passive network is turn active when DG is installed, it changes the normal characteristics of the distribution system. The design of distribution system is arranged in such a way that power flows in direction. The installation of a DG however, introduces another source in the system which influenced the traditional characteristic of distribution network. When the DG power is more than the downstream load, it sends power upstream reversing the direction of power flow, and at some point between the DG and substation, the real power flow is zero due to back flow of power from DG [56]. The impacts of DG on Distribution networks includes, but are not limited to; impact on voltage Regulation, Power losses, Power security, Harmonics, Power quality, and Environment.

### 3.1.1 Impact of DG on Voltage Regulation

In a distribution system voltage regulation takes place at substation with the aid of load tap changing (LTC) transformers, regulators on distribution feeders and shunt capacitor on feeders or along the line in a radial distribution. The magnitude of real and reactive power flows as well as the voltage profile along a feeder changes occur when distributed generation (DG) is integrated into a distribution system. The change in power flow makes the Distribution network active and non-unidirectional. However, depending on the characteristic, location and size of DG as well as distribution system, its impact on voltage regulation can either be negative or positive. [57]. In Figure 3.1 the integration of DG shows an improved voltage profile, but for the situation without DG possible solutions include but are not limited to, moving the DG

unit to the optimal location side of the network, while the second solution is adding regulator controls to compensate for the DG output. However in the context of this work proper DG placement is appropriate.

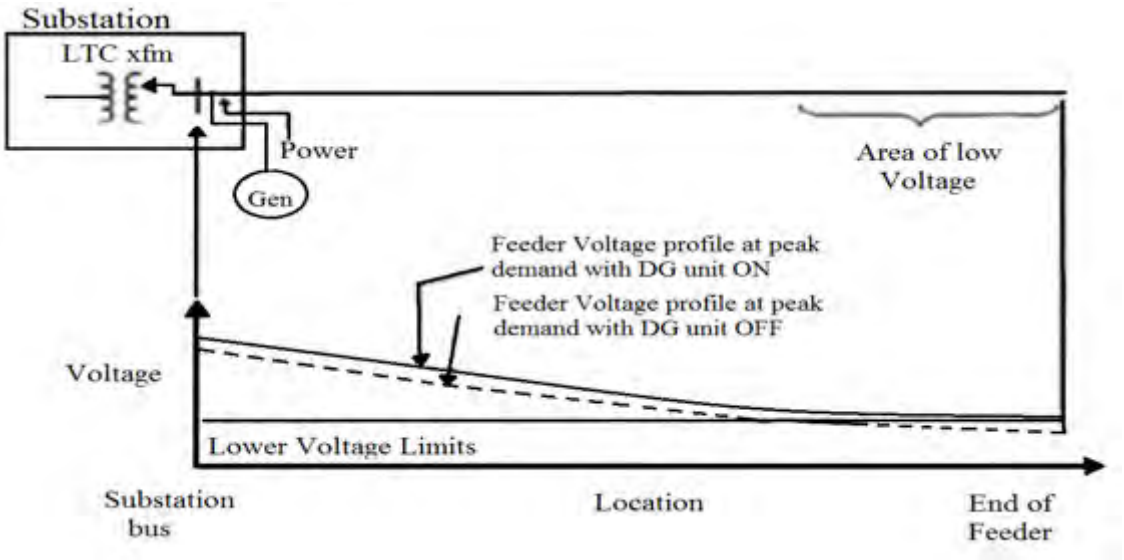


Figure 3.1: Voltage profiles with and without DG [57]

DG impact on primary feeder is negligible for small unit of range (< 10MW). However, if the aggregate capacity increases to critical thresholds, then voltage regulation analysis is required to make sure that the feeder voltage will be fixed within suitable limits [58].

### 3.1.2 Impact of Distributed Generation on Losses

Power losses on the feeder is another impact of distributed generation on distribution network. Optimal allocation of the DG units is an important criterion that must be analyzed to achieve a better reliability of distribution system. Capacitor allocation on distribution network is similar to DG placement and sizing for losses reduction. The main difference between both situations is that DG may contribute both active power and reactive power (P and Q). On the other hand, capacitor banks only contribute with reactive power flow (Q). Mainly, generators in the system operate with a power factor range between 0.85 lagging and unity, but the presence of inverters and synchronous generators provides a contribution to reactive power compensation (leading current) [59].

The optimum location of DG can be obtained using load flow analysis software, which is able to investigate the suitable location of DG within the system in order to reduce the losses. For instance, if feeders have high losses, adding a number of small capacity DGs will show an

important positive effect on the losses and have a great benefit to the system. On the other hand, if higher units are added, they must be connected considering the feeder capacity limits [3]. For example: the feeder capacity may be restricted as overhead lines and cables have thermal characteristic they should not exceed [58].

### 3.1.3 Impact of Distributed Generation on Power Security

Distributed Generation causes an increase in short-circuit current. When a short-circuit fault occurs, fault current is supplied from both the power system and DG to the fault point. If the total fault current exceeds the capacity of the feeder circuit breaker, the fault cannot be clear, and so continues. Increase in fault current deteriorates sensitivity to faults, depending on the location of the fault, the sensitivity of the relay system is liable to deteriorate. When fault current decreases on the feeder at the substation by supplying fault current from DG, the relay system either may not be able to detect the fault or may be slow to detect it [60].

### 3.1.4 Impact of Distributed Generation on Power Quality

Distributed Generation can also result in excess voltage. The voltage of substation distribution lines is controlled by a programmed timer or line drop compensator (LDC). Generally, a single distribution transformer has several feeder lines, and the voltage in these lines is adjusted in a block. Additionally, an SVR compensates the voltage midway along the line in heavy power-flow or long transmission lines. The load of each feeder should be balanced proportionally to utilize these voltage control systems. If there are many DG connections concentrated on a specific line, the gap in the power flow between feeder lines increases because of the back-flow from the DG. There is of particular concern when generating systems that depend on natural conditions, such as wind power or solar photovoltaic generators, are interconnected to the local system [60].

### 3.1.5 Impact of Distributed Generation on Harmonics

A wave that does not follow a “pure” sinusoidal wave is considered as harmonically distorted, Figure 3.2 shows that harmonics are always present in power systems to some extent. They can be caused by, for instance, non-linearity in transformer exciting impedance or loads such as fluorescent lights, AC to DC conversion equipment, variable-speed drives, switch mode power equipment, arc furnaces, and other equipment.

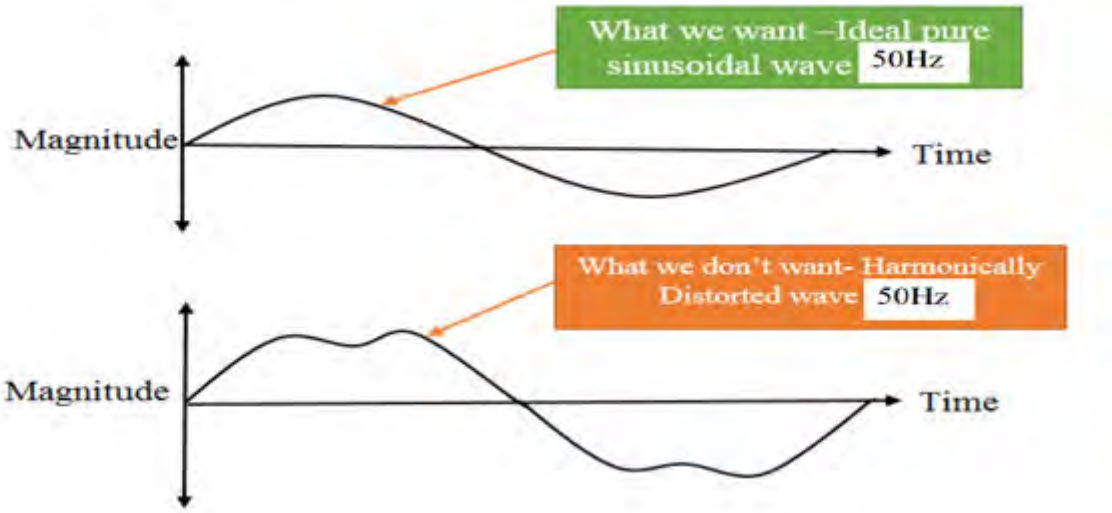


Figure 3.2: Comparison between pure sinusoidal wave and distorted wave [61]

DG can be a source of harmonics to the network. Harmonics produced can be from either the generation unit itself (synchronous generator) or from the power electronics equipment such as inverters. In the case of inverters, their contribution to the harmonic currents is in part due to the SCR (Silicon Controlled-Rectifier) power inverters that produce high levels of harmonic currents. Nowadays, inverters are designed with IGBT (Insulated Gate Bipolar Transistor) technology that use pulse width modulation to generate the injected "pure" sinusoidal wave. This new technology produces a cleaner output with fewer harmonics that should satisfy the IEEE 1547-2003 standards [57]. This problem of harmonics is usually caused by resonance with capacitor banks, or problems with equipment that are sensitive to harmonics. In the worst case, the equipment at the DG may need to be disconnected as a consequence of the extra heating caused by the harmonics.

### 3.1.6 Impact of DG on Short Circuit Levels of the Network

The presence of DG in a system affects the short circuit levels of the network. It creates an increase in the fault currents when compared to normal conditions at which no DG is installed in the network [62]. The fault contribution from a single small DG is not large, but even so, there will be an increase in the fault current. In the case of many small units, or few large units, the short circuit levels can be altered enough to cause miss coordination between protective devices, like fuses or relays. The influence of DG on faults depends on some factors such as the generating size of the DG, the distance of the DG from the fault location and the type of DG. In the case of one small DG embedded in the system, it will have little effect on the increase of the level of short circuit currents. On the other hand, if many small units or a

few large units are installed in the system, they can alter the short circuit levels sufficiently to cause fuse-breaker mis-coordination. This could affect the reliability and safety of the distribution system. Figure 3.3 shows a typical fused lateral on a feeder where fuse saving (fault selective relaying) is utilized and DGs are embedded in the system. In this case if the fault current is large enough, the fuse may no longer coordinate with the feeder circuit breaker during a fault. This can lead to unnecessary fuse operations and decreased reliability on the lateral [57].

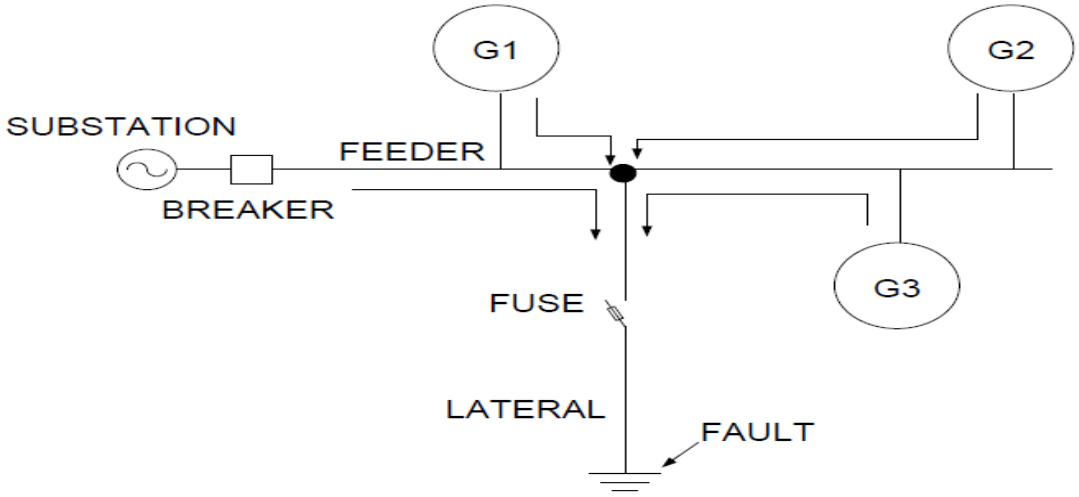


Figure 3.3: Fault contribution due to embedded DG in the system [57].

If the DG is located between the utility substation and the fault, a decrease in fault current from the utility substation may be observed. This decrease needs to be investigated for minimum tripping or coordination problems. On the other hand, if the DG source (or combined DG sources) is strong compared to the utility substation source, it may have a significant impact on the fault current coming from the utility substation. This may cause failure to trip, sequential tripping, or coordination problems [61].

The type of the DG also affects the short circuit levels. The highest contributing DG to faults is the synchronous generator. During the first few cycles the contribution is equal from the induction generator and self-excited synchronous generator, while after the first few cycles the synchronous generator is the most fault current contributing DG type. The DG type that contributes the least amount of fault current is the inverter interfaced DG type; in some inverter types the fault contribution lasts for less than one cycle. Even though a few cycles may be a short time, it may be long enough to impact fuse breaker coordination and breaker duties in some cases [63].

### 3.1.7 Impact of Distributed Generation on Reliability

DG units can have a positive impact on distribution system reliability if they are properly coordinated with the rest of the network. A common example of DG use is as generation backup, in which the unit operates in the case of main supply interruption [64]. For example, a utility can install DG to provide additional capacity to feeders or substations. Additionally, DG can be used to improve the restoration capability of the distribution networks, that is, DG can eliminate network constraints (voltage drop or feeder loading) during the restoration process [65]. In lieu of this, impact on reliability is of great importance to power system optimization which will be detailed in the next chapter.

### 3.1.8 Impact of Distributed Generation on the Environment

Renewable DG such as wind, solar PV and other low carbon like Micro CHP system have a positive impact on the environment by effective reduction of emission and warming. Aside from the market attractiveness, environmental friendliness is one of the major criteria that support DG operation. Towards eco-friendly operation improvement, there is need to program the central controller (CC) to make operational decisions based on the net lowest emission production, in view of both local emission and displaced emission from micro sources.

The structure of emission tariffs is a combined function of season, time and location so the tariffs would be most attractive at worst pollution time and location. This would send signal to the central controller to operate the micro source optimally for minimizing emission. In lieu of this, existing environmental regulation should be strictly adhere to.



## 3.2 Distributed Generation Interface with the Grid

The point of connection of energy sources to the grid is usually regarded as the point of common connection (PCC). Interface technology may comprise of a transformer and converters, which is the technology used at the point of common connection (PCC).

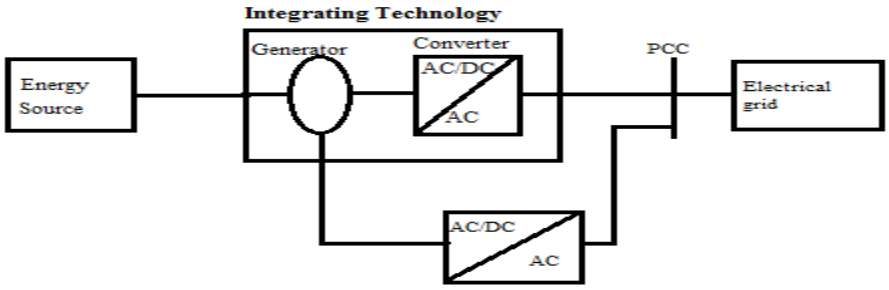


Figure 3.4: Interface technology of energy sources with the grid [66]

Various types of interfacing technologies are used; the use of power electronics converters and generators is common as shown in Figure 3.4. Interfacing technology main objective is to meet the energy requirements of the grid. DG interfacing technologies can be classified into four categories:

- DG direct machine coupling
- DG full power electronics coupling
- DG partial power electronics coupling
- Modular or distributed generation power electronics coupling [66]

### 3.2.1 DG Direct Machine Coupling

Mechanical power can be converted into electrical more efficiently using direct machines coupling to the grid without any transitional stage. The nature of mechanical power supply dictates the type of machines coupling to be used in any case. Synchronous machine is the right candidate for constant mechanical power that rotates at fixed speed while induction machines is suitable for strongly variable power that rotates at variable speed. Wind energy source is good example of these machines, connected as shown in Figure 3.5.

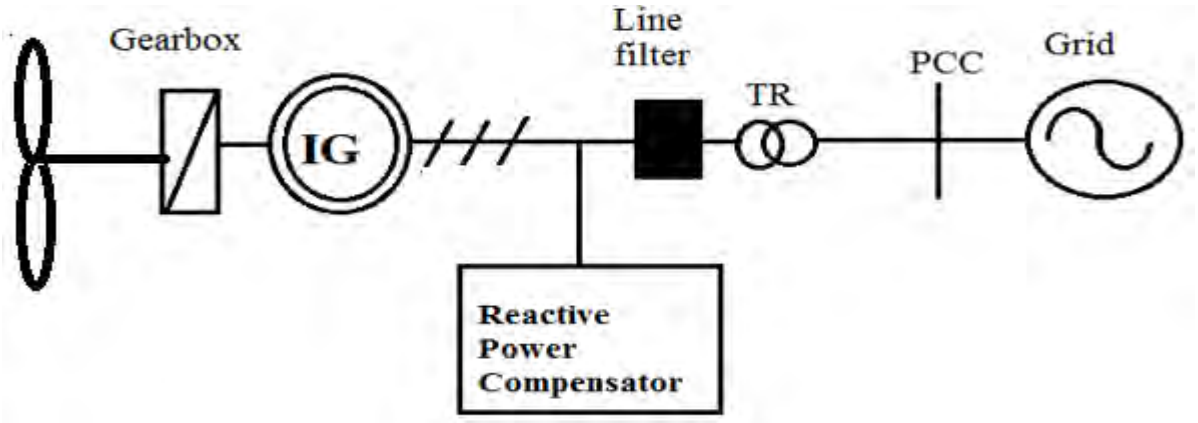


Figure 3.5: Direct induction generator coupling for a wind turbine [67]

### 3.2.2 Distributed Generation Full Power Electronics Coupling

The energy supplied by the distributed generator is condition by the power electronics interface to accommodate the grid requirements and to improve the performance of the energy source. However, the ability of power electronics equipment to transform power from one form to another with use of electronics controlled switches is called power electronics converter. In the coupling process, direct current (DC) power converters (inverter) to alternating current (AC) power that matches the grid requirements using the power electronic converters. Such converters can be called an inverter or DC/AC converters. With a source that produce DC energy, the power electronics may consist of one DC/AC converter or an intermediate DC/DC conversion stage can be added to achieve a specific goal, for instance, in an attempt to stabilize the output voltage so that the maximum available power is extracted as in the case of PV systems**.**

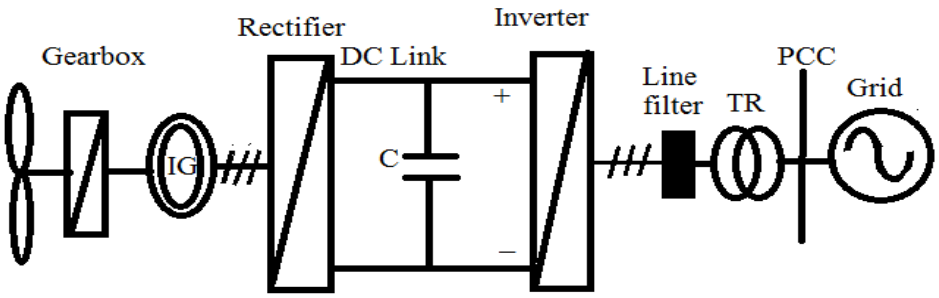


Figure 3.6: Full power electronics interfaced wind turbine with induction generator [68]

The arrangement that consists of AC/DC and DC/AC converters is also referred to as a frequency converter, since it connects together two different AC systems with possibly two different frequencies. The frequency converter is in a back-to-back configuration, where the DC is directly connecting the two converters together as shown in Figure 3.6 or an HVDC/MVDC system configuration when there is a transmission DC cable in the DC link for either HV or MV applications.

### 3.2.3 Distributed Generation Partial Power Electronics Coupling

Another coupling arrangement for grid integration is a partial power electronics interface, where the rating of the converter is proportional to a certain percentage of the apparent power of the DG. Typical example is shown in Figure 3.7, a connection of a doubly-fed induction generator into the grid through partial power electronic interface.

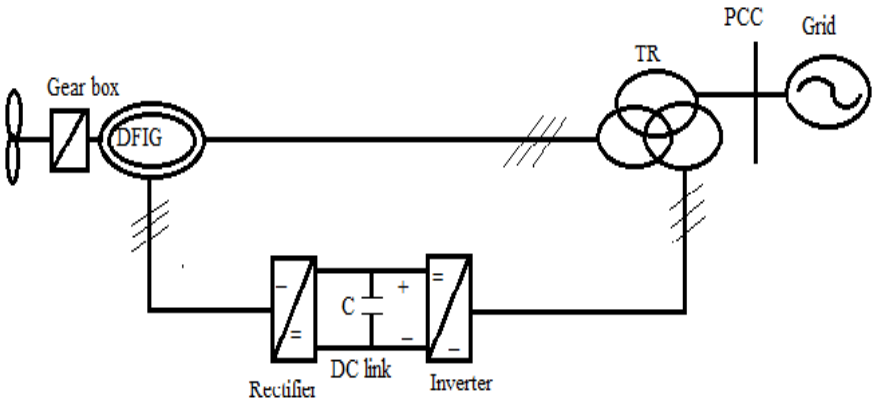


Figure 3.7: Double-fed induction generator connection of a wind turbine [67]

A partially rated power electronics converter at the connection point of a wind farm (or any aggregate of sources) is usually needed to mainly provide a voltage dip ride-through capability, which is a required feature regarding different grid codes, and possible reactive power support.

### 3.2.4 Power Electronics DG Interface

Distributed power electronics interfaces refer to a number of distributed generation that are connected to the same local grid through power electronics converters. If such units belong to the same owner, their operation can be coordinated in a way to achieve certain benefits such as regulating the local voltage.

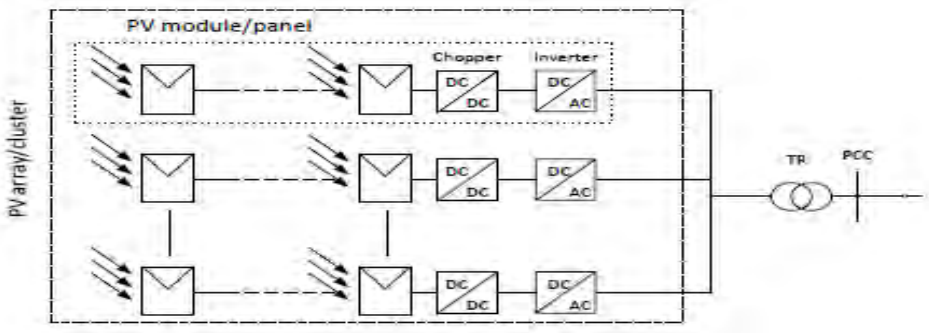


Figure 3.8: Photovoltaic array interface through modular conversion [18]

The module-integrated photovoltaic system, shown in Figure 3.8 is also a type of distributed active interface structure that has been developed in order to increase the efficiency and reliability of the solar power cells. This is made possible when different solar cells, in an array or a cluster are exposed to different irradiation. Hence, operating each integrated converter at a different point that is related to the MPP results in better reliability compared to using a central conversion. Another example is a wind farm with full power electronics-interfaced wind

turbines. Implementing a proper control architecture that makes use of the distributed controllability of the converters makes such setup reliable, reconfigurable, and self-healing.

### 3.3 Summary

From the above, it can be seen that Distributed Generation impacts the Distribution Network differently, both negatively and positively depending on the fact to be considered, which can result in economical or technical benefit. Positive impact can be achieved by proper integration of the Distributed Generation via optimal allocation. Also, various Distributed generation integration technologies, through which better power loss reduction and improved voltage can achieve has been reviewed. The next chapter will dwell on problem formulation of the objective function of this research and modelling of equipment used.

# Chapter 4

# MODELLING AND PROBLEM FORMULATIONS

## 4. Introduction

This chapter deals with the problem formulation, the formulations of the system sensitivity factors and the multi-objective optimization. The constraints to which the multi-objective function is subjected to are also defined here. Generally, both real and reactive power flow and power loss sensitivity factors are formulated using the full Newton-Raphson load flow Jacobian matrix, while the multi-objective optimization is formulated taking into consideration the three key factors, that is, real power loss reduction index, reactive power loss reduction index and voltage profile improvement index. Both equality and inequality constraints are defined.

## 4.1 Load Modelling

The distribution system under study is assumed to follow the normalized 24-hour load profile of the IEEE system as shown in Figure 4.1 [69]. The constant P and Q load in load characteristic incorporate through load factor LF in the equation below.

$$LF = \sum_{t=1}^{24} \frac{p.u.demand(t)}{24} \tag{4.1}$$

where,

LF = is the load factor

t = is time in hours

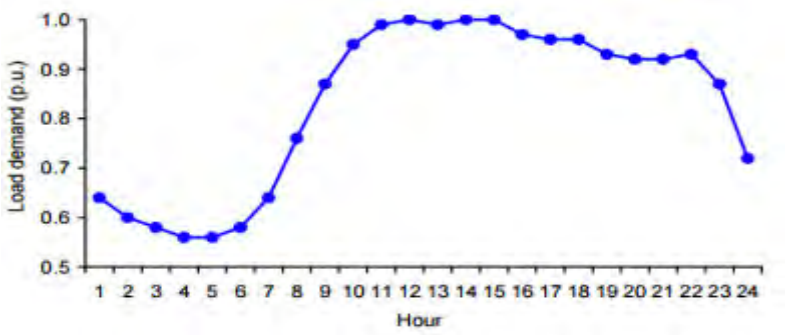


Figure 4.1: Normalized daily load demand curve [69]

## 4.2 Renewable DG Modelling

In this research, two types of renewable DG units described in Chapter 2, namely wind (or wind power) and solar PV are considered. The outputs of wind DG and PV-based DG are assumed to follow the normalized average output curve depicted in Figure 4.2 [70]. Each curve provides an hourly generation output as a percentage of the daily peak output itself. The capacity factor (CF) of each type of DG is estimated as the ratio of the area under the output curve in p.u. to the total duration as shown in figure 4.2 below:

$$CF = \sum_{t=1}^{24} \frac{p.u.DGoutput(t)}{24} \tag{4.2}$$

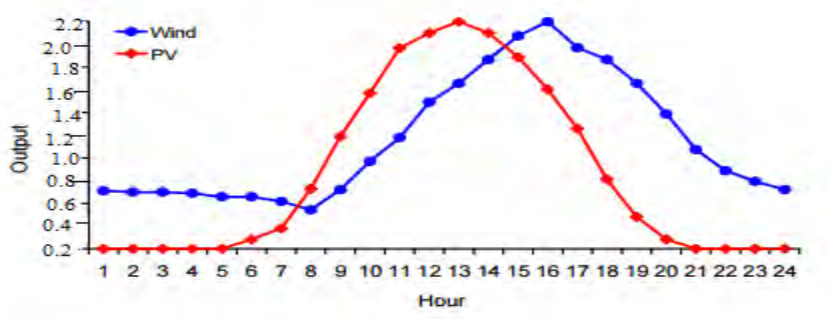


Figure 4.2: Normalized daily wind and PV output curves [70]

Wind energy is extracted through wind turbine blades and then transferred through a gearbox and the rotor hub to the mechanical energy in the shaft. The shaft drives the generator to convert the mechanical energy to electrical. The turbine model is based on the output power characteristics, expressed as [71] [72].

$$P_m = C_p(\lambda, \beta).\frac{1}{2}\rho A v^3 \tag{4.3}$$

and

$$\lambda = \frac{R_{blade} w_r}{v} \tag{4.4}$$

where,

$R_{blade}$ is

$v$ is wind speed

$\rho$ is air density

A is area of rotor

$P_m$ is maximum power

$C_p$ is performance coefficient

$\lambda$ is speed ratio

$\beta$ blade pitch angle

$w_r$ angular frequency of rotational turbine

Production from a wind turbine depends on wind speed $v_w^3$, density of the air $\rho$ and the swept area of the rotor $A$. Therefore, the maximum power $P_m$ available from the wind can be expressed as equation (4.4).

$$P_m = \frac{1}{2}\rho A v_w^3 \tag{4.5}$$

The output power from the PV module at solar irradiance $s$, $P_{PVo}(s)$ can be expressed as follows [73]:

$$P_{PVo}(s) = N \times FF \times V_y \times I_y \tag{4.6}$$

where $FF = \frac{V_{MPP} \times I_{MPP}}{V_{oc} \times I_{sc}}$; $V_y = V_{oc} - K_v \times T_{cy}$

$$I_y = s\left[I_{sc} + K_i \times \left(T_{cy} - 25\right)\right];\ T_{cy} = T_A + s\left(\frac{N_{OT}-20}{0.8}\right)$$

where, $N$ are the number of modules; $T_{cy}$ and $T_A$ are respectively cell and ambient temperature ($^oC$); $K_i$ and $K_v$ are respectively current and voltage temperature coefficients (A/$^oC$and V/$^oC$); $N_{OT}$ is the nominal operating temperature of cell in ($^oC$); $FF$ is fill factor; $V_{oc}$ and $I_{sc}$ are respectively the open circuit voltage (V) and short circuit current (A); $V_{MPP}$ and $I_{MPP}$ are respectively the voltage and current at maximum power point.

### 4.3 Total System Power Loss

Since one of the main objectives of the proposed approach is to minimize the total system power loss by optimal sizing and siting of distributed generation in radial distribution system, the objective function is mathematically formulated as follows:

$$\text{Minimize } S_{loss} = \sqrt{P_{loss}^2 + Q_{loss}^2} \tag{4.7}$$

Total active power loss in a Radial distribution system is given by.

$$P_{loss} = \left(\sum_{i=1}^{n} (I_i)^2 * R_i\right) \tag{4.8}$$

Total reactive power loss in a distribution system is also given by.

$$Q_{loss} = \left(\sum_{i=1}^{n} (I_i)^2 * X_i\right) \tag{4.9}$$

where,

$n$ is the number of lines at bus i ,

$I_i$ Is the line current at bus $i$ in amps,

$R_i$ is the line resistance in ohms,

$X_i$ is line reactance at bus i in ohms respectively.

The total system power loss is also formulated as exact loss formula which includes real and reactive power losses respectively. The exact real and reactive power loss are given by equation (4.10) and (4.11) respectively and the details of their formulation is given in Appendix IX [74] .

$$P_{loss} = \sum_{i=1}^{n}\sum_{j=1}^{n}[a_{ij}(P_iP_j + Q_iQ_j) + b_{ij}(Q_iP_j - P_iQ_j)] \quad (4.10)$$

and $$Q_{loss} = \sum_{i=1}^{n}\sum_{j=1}^{n}[c_{ij}(P_iP_j + Q_iQ_j) + d_{ij}(Q_iP_j - P_iQ_j)] \quad (4.11)$$

where,

$$a_{ij} = \frac{R_{ij}}{V_iV_j}\cos(\delta_i - \delta_j)\ ;\ b_{ij} = \frac{R_{ij}}{V_iV_j}\sin(\delta_i - \delta_j)$$

$$c_{ij} = \frac{X_{ij}}{V_iV_j} * \cos(\delta_i - \delta_j);\ \ d_{ij} = \frac{X_{ij}}{V_iV_j} * \sin(\delta_i - \delta_j)$$

$n$ is the bus number

$a_{ij},\ b_{ij}, c_{ij}$ and $d_{ij}$ are function of loss coefficient between bus $i\ and\ j$.

$P_i$ is real power flow at bus in kW

$Q_i$ is reactive power flow at bus $i$ in kVAR

$P_j$ is real power flow at bus j in kW

$Q_j$ is reactive power flow at bus j in kVAR

$R_{ij}$ is Resistance of the line connecting bus i and j in Ohms

$X_{ij}$ is Reactance of the line connecting bus i and j in Ohms

$V_i\ and\ V_j$ are bus voltage magnitude at bus i and j in PU

$\delta_i\ and\ \delta_j$ are bus voltage angle at bus i and j

The total impedance between the bus $i$ and bus j is given by:

$$Z_{ij} = R_{ij} + jX_{ij} \tag{4.12}$$

## 4.4 System Power Flow Sensitivity Factors

System power flow sensitivity is the change in power flow in a transmission or distribution line connected between two buses say bus *i* and bus *j* due to a unit change in the power injected at any bus in the system.

The complex power injected by a source into a bus, say $i^{th}$ bus of a power system is given by;

$$S_i = P_i + jQ_i = V_i J_i^* ; \quad i = 1,2, \ldots\ldots, n \tag{4.13}$$

Where,

$V_i$ is the voltage at the $i^{th}$ bus with respect to ground

$J_i$ is the source current injected into the bus

So as to handle the load flow problem more conveniently the use of $J_i$ rather than $J_i^*$ is encouraged [75]. As a result the complex conjugate of the above equation is considered, to be:

$$S_i^* = P_i - jQ_i = V_i^* J_i; \;\; i = 1,2, \ldots\ldots n \tag{4.14}$$

The source current is given by;

$$J_i = \sum_{j=1}^{n} Y_{ij} V_j; \;\; i = 1, \;\; 2, \ldots\ldots, n \tag{4.15}$$

Thus by substituting this equation into the complex conjugate equation of power injection we have:

$$P_i - jQ_i = V_i^* \sum_{j=1}^{n} Y_{ij} V_j ; \;\; i = 1, 2, \ldots\ldots n \tag{4.16}$$

Equating real and imaginary parts of the above equation we get:

$$P_i = Re\{V_I^* \sum_{j=1}^{n} Y_{ij} V_j\} \tag{4.17}$$

$$Q_i = -Im\{V_I^* \sum_{j=1}^{n} Y_{ij} V_j\} \tag{4.18}$$

In polar form $V_i$ and $Y_{ij}$ can be expressed as:

$$V_i = |V_i| e^{j\delta_i} \tag{4.19}$$

$$Y_{ij} = |Y_{ij}| e^{j\theta_{ij}} \tag{4.20}$$

From the polar representations given above the real and reactive powers can be expressed in general as shown;

$$P_i = |V_i| \sum_{j=1}^{n} |V_j||Y_{ij}| \cos(\theta_{ij} - \delta_i + \delta_j) \; ; \; i = 1, 2, \ldots\ldots, n \tag{4.21}$$

$$Q_i = -|V_i| \sum_{j=1}^{n} |V_j||Y_{ij}| \sin(\theta_{ij} - \delta_i + \delta_j) \; ; \; i = 1, 2, \ldots\ldots, n \tag{4.22}$$

### 4.4.1 Change in Real Power Flow Analysis.

The real power flow in a line *k* connecting two buses, bus *i* and bus *j* can be expressed as [76]:

$$P_i = V_i V_j Y_{ij} \cos(\theta_{ij} + \delta_j - \delta_i) + V_i^2 Y_{ii} cos\theta_{ii} \tag{4.23}$$

where,

$V_i \; and \; V_j$ are the voltage magnitudes at buses $i$ and $j$ respectively

$\delta_i$ and $\delta_j$ are the voltage angles at buses $i$ and $j$ respectively

$Y_{ii}$ is the magnitude of $i^{th}$ element of the $Y_{Bus}$ matrix

$Y_{ij}$ is the magnitude of the $ij^{th}$ element of the $Y_{Bus}$ matrix

$\theta_{ii}$ is the angle of the $i^{th}$ element of the $Y_{Bus}$ matrix

$\theta_{ij}$ is the angle of the $ij^{th}$ element of the $Y_{Bus}$ matrix

Mathematically, the real power flow sensitivity can be written as:

$$\begin{bmatrix} \frac{\Delta P_{ij}}{\Delta P_n} \\ \frac{\Delta Q_{ij}}{\Delta Q_n} \end{bmatrix} \tag{4.24}$$

Using Taylor series approximation while ignoring the second and higher order terms the change in real line flow can be expressed as:

$$\Delta P_{ij} = \frac{\partial P_{ij}}{\partial \delta_i} \Delta\delta_i + \frac{\partial P_{ij}}{\partial \delta_j} \Delta\delta_j + \frac{\partial P_{ij}}{\partial V_i} \Delta V_i + \frac{\partial P_{ij}}{\partial V_j} \Delta V_j \tag{4.25}$$

The coefficients appearing in the above equation can be obtained using the partial derivatives of real power flow with respect to variables $\delta$ and $V$ as shown below:

$$\frac{\partial P_{ij}}{\partial \delta_i} = -V_i V_j Y_{ij} \sin(\theta_{ij} + \delta_{ij}) \tag{4.26}$$

$$\frac{\partial P_{ij}}{\partial \delta_j} = V_i V_j Y_{ij} \sin(\theta_{ij} + \delta_{ij}) \tag{4.27}$$

$$\frac{\partial P_{ij}}{\partial V_i} = V_j Y_{ij} \cos(\theta_{ij} + \delta_{ij}) - 2V_i Y_{ij} cos\theta_{ij} \tag{4.28}$$

$$\frac{\partial P_{ij}}{\partial V_j} = -V_i Y_{ij} \cos(\theta_{ij} + \delta_{ij}) \tag{4.29}$$

### 4.4.2 Change in Reactive Power Flow Analysis.

The reactive power flow in a line $k$ connecting two buses, bus $i$ and bus $j$ can be expressed as [76]:

$$Q_i = -V_i V_j Y_{ij} \sin(\theta_{ij} + \delta_j - \delta_i) - V_i^2 Y_{ii} sin\theta_{ii} \tag{4.30}$$

where,

$V_i \; and \; V_j$ are the voltage magnitudes at buses $i$ and $j$ respectively

$\delta_i$ and $\delta_j$ are the voltage angles at buses $i$ and $j$ respectively

$Y_{ii}$ is the magnitude of $i^{th}$ element of the $Y_{Bus}$ matrix

$Y_{ij}$ is magnitude of the $ij^{th}$ element of the $Y_{Bus}$ matrix

$\theta_{ii}$ is the angle of the $i^{th}$ element of the $Y_{Bus}$ matrix

$\theta_{ij}$ is the angle of the $ij^{th}$ element of the $Y_{Bus}$ matrix

Mathematically, the reactive power flow sensitivity can be written as:

$$\begin{bmatrix} \frac{\Delta Q_{ij}}{\Delta P_n} \\ \frac{\Delta Q_{ij}}{\Delta Q_n} \end{bmatrix} \tag{4.31}$$

Using Taylor series approximation while ignoring second and higher order terms the change in reactive line flow can be expressed as:

$$\Delta Q_{ij} = \frac{\partial Q_{ij}}{\partial \delta_i}\Delta\delta_i + \frac{\partial Q_{ij}}{\partial \delta_j}\Delta\delta_j + \frac{\partial Q_{ij}}{\partial V_i}\Delta V_i + \frac{\partial Q_{ij}}{\partial V_j}\Delta V_j \tag{4.32}$$

The coefficients appearing in the above equation can be obtained using the partial derivatives of reactive power flow with respect to variables and $V$ as shown;

$$\frac{\partial Q_{ij}}{\partial \delta_i} = -V_i V_j Y_{ij} \cos(\theta_{ij} + \delta_{ij}) \tag{4.33}$$

$$\frac{\partial Q_{ij}}{\partial \delta_j} = V_i V_j Y_{ij} \cos(\theta_{ij} + \delta_{ij}) \tag{4.34}$$

$$\frac{\partial Q_{ij}}{\partial V_i} = -V_j Y_{ij} \sin(\theta_{ij} + \delta_{ij}) - 2V_i Y_{ij} cos\theta_{ij} - V_i Y_{sh} \tag{4.35}$$

$$\frac{\partial Q_{ij}}{\partial V_j} = -V_i Y_{ij} \sin(\theta_{ij} + \delta_{ij}) \tag{4.36}$$

### 4.4.3 Formulating the Power Flow Sensitivity Factors

The power flow sensitivity factors represent the change in the real reactive power flow over a distribution line that connects bus-*i* and bus-*j* due to the change in active and reactive

power injected at any other bus-n. The equations for the changes in the line flows can be arranged in matrix form and expressed as;

$$\begin{bmatrix}\frac{\Delta P_{ij}}{\Delta Q_{ij}}\end{bmatrix}=\begin{bmatrix}\frac{\partial P_{ij}}{\partial \delta} & \frac{\partial P_{ij}}{\partial V}\\ \frac{\partial Q_{ij}}{\partial \delta} & \frac{\partial Q_{ij}}{\partial V}\end{bmatrix}\begin{bmatrix}\Delta\delta\\ \Delta V\end{bmatrix} \tag{4.37}$$

The variables $\Delta\delta$ and $\Delta V$ can be obtained from load flow solution using Newton Raphson technique as follows;

The full newton-raphson load flow Jacobian matrix is expressed as;

$$\begin{bmatrix}\Delta P\\ \Delta Q\end{bmatrix}=[J]\begin{bmatrix}\Delta\delta\\ \Delta V\end{bmatrix}=\begin{bmatrix}J_{11} & J_{12}\\ J_{21} & J_{22}\end{bmatrix}\begin{bmatrix}\Delta\delta\\ \Delta V\end{bmatrix} \tag{4.38}$$

Thus from this equation the variables $\Delta\delta$ and $\Delta V$ can be obtained:

$$\begin{bmatrix}\Delta\delta\\ \Delta V\end{bmatrix}=[J]^{-1}\begin{bmatrix}\Delta P\\ \Delta Q\end{bmatrix}=\begin{bmatrix}J_{11} & J_{12}\\ J_{21} & J_{22}\end{bmatrix}^{-1}\begin{bmatrix}\Delta P\\ \Delta Q\end{bmatrix} \tag{4.39}$$

Now substituting the obtained equation for $\Delta\delta$ and $\Delta V$ in the equation for the change in line flow we have:

$$\begin{bmatrix}\frac{\Delta P_{ij}}{\Delta Q_{ij}}\end{bmatrix}=\begin{bmatrix}\frac{\partial P_{ij}}{\partial \delta} & \frac{\partial P_{ij}}{\partial V}\\ \frac{\partial Q_{ij}}{\partial \delta} & \frac{\partial Q_{ij}}{\partial V}\end{bmatrix}[J]^{-1}\begin{bmatrix}\Delta P\\ \Delta Q\end{bmatrix} \tag{4.40}$$

The above equation gives the change in both real and reactive power flow and thus using this equation the real and reactive power flow sensitivity factors can be determined as given in

Appendix VII

The real power flow sensitivity factors are represented as;

$$\begin{bmatrix}\frac{\partial P_{ij}}{\partial P_n}\\ \frac{\partial P_{ij}}{\partial Q_n}\end{bmatrix}=\begin{bmatrix}F_{P-P}\\ F_{P-Q}\end{bmatrix}=[J^T]^{-1}\begin{bmatrix}\frac{\partial P_{ij}}{\partial \delta}\\ \frac{\partial P_{ij}}{\partial V}\end{bmatrix} \tag{4.41}$$

$$\begin{bmatrix}\frac{\partial Q_{ij}}{\partial P_n}\\ \frac{\partial Q_{ij}}{\partial Q_n}\end{bmatrix}=\begin{bmatrix}F_{Q-P}\\ F_{Q-Q}\end{bmatrix}=[J^T]^{-1}\begin{bmatrix}\frac{\partial Q_{ij}}{\partial \delta}\\ \frac{\partial Q_{ij}}{\partial V}\end{bmatrix} \tag{4.42}$$

where,

$F_{P-P}$ is the real power flow sensitivity related to the real power injection.

$F_{P-Q}$ is the active flow sensitivity related to the reactive power injection.

$F_{Q-P}$ is the reactive power flow sensitivity related to the active power injection.

$F_{Q-Q}$ is the reactive power flow sensitivity related to the reactive power injection.

$J^T$ is the Jacobian matrix of power flow, and the superscript *T* indicates the transposition.

Here the four sensitivities are column vectors with dimension of number of the system buses

### 4.5 System Power Loss Sensitivity Factors

From the circuit diagram shown in Figure 4.3 both real and reactive power loss sensitivity factors can be calculated.

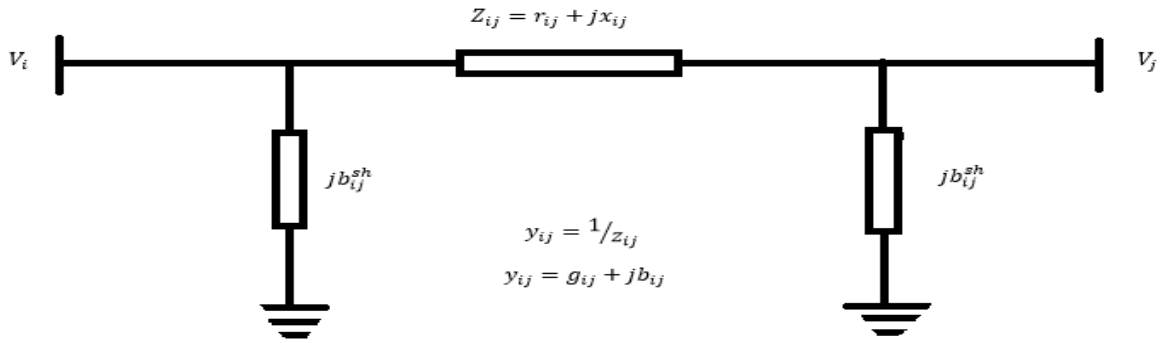


Figure 4.3: Circuit diagram of a line lumped model

#### 4.5.1 Change in Real Power Loss Analysis

The active power loss of the line lumped model shown in the line-*(pie)* circuit is Figure 4.3 given by [76] :

$$P_{L(ij)} = g_{ij}(V_i^2 + V_j^2 - 2V_iV_jcos\delta_{ij}) \quad (4.43)$$

Thus the total active power loss in the circuit can be expressed as;

$$P_{L(total)} = \sum_{l=1}^{nl}[\, g_{ij}(V_i^2 + V_j^2 - 2V_iV_jcos\delta_{ij}] \quad (4.44)$$

where,

$nl$ is the number of lines of the network;

$g_{ij}$ is the conductance of the line i-j

$V_i$ is the node voltage of bus i

$V_j$ is the node voltage of bus j

$\delta_{ij}$ is the phase angle difference between the buses i and j

Mathematically, the reactive power loss sensitivity can be written as:

$$\begin{bmatrix} \frac{\Delta P_{L(ij)}}{\Delta P_n} \\ \frac{\Delta P_{L(ij)}}{\Delta Q_n} \end{bmatrix} \tag{4.45}$$

Using Taylor series approximation while ignoring second and higher order terms the change in real power loss can be expressed as:

$$\Delta P_{L(ij)} = \frac{\partial P_{L(ij)}}{\partial \delta_i}\Delta\delta_i + \frac{\partial P_{L(ij)}}{\partial \delta_j}\Delta\delta_j + \frac{\partial P_{L(ij)}}{\partial V_i}\Delta V_i + \frac{\partial P_{L(ij)}}{\partial V_j}\Delta V_j \tag{4.46}$$

The coefficients appearing in the above equation can be obtained using the partial derivatives of the real power loss with respect to variables δ and *V* as shown below:

$$\frac{\partial P_{L(ij)}}{\partial \delta_i} = 2g_{ij}V_iV_jsin\delta_{ij} \tag{4.47}$$

$$\frac{\partial P_{L(ij)}}{\partial \delta_j} = -2g_{ij}V_iV_jsin\delta_{ij} \tag{4.48}$$

$$\frac{\partial P_{L(ij)}}{\partial V_i} = g_{ij}(2V_i - 2V_jcos\delta_{ij})$$

$$= 2g_{ij}(V_i - V_jcos\delta_{ij}) \tag{4.49}$$

$$\frac{\partial P_{L(ij)}}{\partial V_j} = g_{ij}(2V_j - 2V_icos\delta_{ij})$$

$$= 2g_{ij}(V_j - V_icos\delta_{ij}) \tag{4.50}$$

The sensitivity power factor of real power loss in equation (4.44) with respect to real power flow in equation (4.23) is given by

$$\alpha_{i=}\frac{P_{L(total)}}{P_i} = \frac{\sum_{l=1}^{nl}[g_{ij}(V_i^2 + V_j^2 - 2V_iV_jcos\delta_{ij}]}{V_iV_jY_{ij}\,cos(\theta_{ij} + \delta_j - \delta_i) - V_i^2Y_{ii}cos\theta_{ii}} \tag{4.51}$$

It can be reduced to;

$$\alpha_{i=}\frac{\partial PL}{\partial Pi}2\sum_{l=1}^{nl}(a_{ij}P_j - b_{ij}Q_j) \tag{4.52}$$

### 4.5.2 Change in Reactive Power Loss Analysis.

The reactive power loss in a line *l* connecting two buses, bus *i* and bus *j* can be expressed as:

$$Q_{L(ij)} = b_{ij}(V_i^2 + V_j^2 - 2V_iV_jcos\delta_{ij}) \tag{4.53}$$

Thus the total reactive power loss in the circuit can be expressed as;

$$Q_{L(total)} = \sum_{l=1}^{nl}[-b_{ij}^{sh}(V_i^2 + V_j^2) - b_{ij}(V_i^2 - V_j^2 - 2V_iV_jcos\delta_{ij})] \tag{4.54}$$

where,

$nl$ is the number of lines of the network;

$b_{ij}^{sh}$ is the shunt susceptance of the line i-j

$V_i$ is the node voltage of bus i

$V_j$ is the node voltage of bus j

$\delta_{ij}$ is the phase angle difference between the buses i and j

Mathematically, the reactive power loss sensitivity can be written as:

$$\begin{bmatrix} \frac{\Delta P_{L(ij)}}{\Delta P_n} \\ \frac{\Delta P_{L(ij)}}{\Delta Q_n} \end{bmatrix} \tag{4.55}$$

Using Taylor series approximation while ignoring second and higher order terms the change in real power loss can be expressed as:

$$\Delta Q_{L(ij)} = \frac{\partial Q_{L(ij)}}{\partial \delta_i}\Delta\delta_i + \frac{\partial Q_{L(ij)}}{\partial \delta_j}\Delta\delta_j + \frac{\partial Q_{L(ij)}}{\partial V_i}\Delta V_i + \frac{\partial Q_{L(ij)}}{\partial V_j}\Delta V_j \tag{4.56}$$

Partial derivatives of real power loss with respect to variable δ and $V$ can be is used to obtain the coefficients equation above as shown below:

$$\frac{\partial Q_{L(ij)}}{\partial \delta_i} = -2b_{ij}V_iV_jsin\delta_{ij} \tag{4.57}$$

$$\frac{\partial Q_{L(ij)}}{\partial \delta_j} = 2b_{ij}V_iV_jsin\delta_{ij} \tag{4.58}$$

$$\begin{aligned} \frac{\partial Q_{L(ij)}}{\partial V_i} &= -2b_{ij}^{sh}V_i - b_{ij}(2V_i - 2V_jcos\delta_{ij}) \\ &= -2[b_{ij}^{sh}V_i + b_{ij}(V_i - V_jcos\delta_{ij})] \end{aligned} \tag{4.59}$$

$$\begin{aligned} \frac{\partial Q_{L(ij)}}{\partial V_j} &= -2b_{ij}^{sh}V_j - b_{ij}(2V_j - 2V_jcos\delta_{ij}) \\ &= -2[b_{ij}^{sh}V_j + b_{ij}(V_j - V_icos\delta_{ij})] \end{aligned} \tag{4.60}$$

### 4.5.3 Formulating the Power Loss Sensitivity Factors

The real power loss sensitivity factors represent the change in the real power loss over a transmission or distribution line connected between bus-*i* and bus-*j* due to the change in active power or reactive power injected at any other bus-n while the reactive power loss sensitivity factors represent the change in the reactive power loss over a transmission or distribution line connected between bus-*i* and bus-*j* due to the change in reactive power or real power injected at any other bus-n. The equations for the changes in the line flows can be arranged in matrix form and expressed as:

$$\begin{bmatrix}\frac{\Delta P_{L(ij)}}{\Delta Q_{L(ij)}}\end{bmatrix}=\begin{bmatrix}\frac{\partial P_{ij}}{\partial \delta} & \frac{\partial P_{ij}}{\partial V}\\ \frac{\partial Q_{ij}}{\partial \delta} & \frac{\partial Q_{ij}}{\partial V}\end{bmatrix}\begin{bmatrix}\Delta\delta\\ \Delta V\end{bmatrix} \tag{4.61}$$

The variables $\Delta\delta$ and $\Delta V$ can be obtained from load flow solution using the Newton-Raphson technique as follows:

The full N-R load flow Jacobian matrix is expressed as;

$$\begin{bmatrix}\Delta P\\ \Delta Q\end{bmatrix}=[J]\begin{bmatrix}\Delta\delta\\ \Delta V\end{bmatrix}=\begin{bmatrix}J_{11} & J_{12}\\ J_{21} & J_{22}\end{bmatrix}\begin{bmatrix}\Delta\delta\\ \Delta V\end{bmatrix} \tag{4.62}$$

Thus from this equation the variables $\Delta\delta$ and $\Delta V$ can be obtained:

$$\begin{bmatrix}\Delta\delta\\ \Delta V\end{bmatrix}=[J]^{-1}\begin{bmatrix}\Delta P\\ \Delta Q\end{bmatrix}=\begin{bmatrix}J_{11} & J_{12}\\ J_{21} & J_{22}\end{bmatrix}^{-1}\begin{bmatrix}\Delta P\\ \Delta Q\end{bmatrix} \tag{4.63}$$

Now substituting the obtained equation for $\Delta\delta$ and $\Delta V$ in the equation for the change in line flow we have:

$$\begin{bmatrix}\frac{\Delta P_{L(ij)}}{\Delta Q_{L(ij)}}\end{bmatrix}=\begin{bmatrix}\frac{\partial P_{L(ij)}}{\partial \delta} & \frac{\partial P_{L(ij)}}{\partial V}\\ \frac{\partial Q_{L(ij)}}{\partial \delta} & \frac{\partial Q_{L(ij)}}{\partial V}\end{bmatrix}[J]^{-1}\begin{bmatrix}\Delta P\\ \Delta Q\end{bmatrix} \tag{4.64}$$

Equation (4.64) gives the change in both real and reactive power flow and thus using this equation the real and reactive power flow sensitivity factors can be determined as given in Appendix VIII

The real power flow sensitivity factors are represented as;

$$\begin{bmatrix}\frac{\partial P_{L(ij)}}{\partial P_n}\\ \frac{\partial P_{L(ij)}}{\partial Q_n}\end{bmatrix}=\begin{bmatrix}S_{P-P}\\ S_{P-Q}\end{bmatrix}=[J^T]^{-1}\begin{bmatrix}\frac{\partial P_{L(ij)}}{\partial \delta}\\ \frac{\partial P_{L(ij)}}{\partial V}\end{bmatrix} \tag{4.65}$$

The reactive power loss sensitivity factors are expressed as;

$$\begin{bmatrix}\frac{\partial Q_{L(ij)}}{\partial P_n}\\ \frac{\partial Q_{L(ij)}}{\partial Q_n}\end{bmatrix}=\begin{bmatrix}S_{Q-P}\\ S_{Q-Q}\end{bmatrix}=[J^T]^{-1}\begin{bmatrix}\frac{\partial Q_{L(ij)}}{\partial \delta}\\ \frac{\partial Q_{L(ij)}}{\partial V}\end{bmatrix} \tag{4.66}$$

where,

$S_{P-P}$ is the real power flow sensitivity related to the real power injection.

$S_{P-Q}$ is the active flow sensitivity related to the reactive power injection.

$S_{Q-P}$ is the reactive power flow sensitivity related to the active power injection.

$S_{Q-Q}$ is the reactive power flow sensitivity related to the reactive power injection.

$J$ is the Jacobian matrix of power flow, and the superscript $T$ indicates the transposition.

Here the four sensitivities are column vectors with dimension of number of the system buses.

## 4.6 Objective Function

The multi-objective index for the performance calculation of distribution systems for DG size and location planning with load models considers the below mentioned indices (equation 4.74) by giving a weight to each index.

Recall the generalized objective function

$$\text{Minimize } f(x) = \{f_1(x), f_2(x), \ldots\ldots\ldots, f_k(x)\} \tag{4.67}$$

where,

$f_1(x)$, $f_2$(x)……..$f_k(x)$ are variables in the objective function

Subject to

Equality Constraints $g(x) = g_i(x), g_2(x), \ldots\ldots\ldots g_k(x) = 0$

Inequality Constraints $h(x) = h_j(x), h_2(x), \ldots\ldots\ldots h_k(x) \geq 0$

### 4.6.1 Operational Constraints Formulation

The above formulated multi-objective function is minimized subject to various operational constraints so as satisfy the electrical requirements for the distribution network. The operational

constraints are classified into two types.

- Equality Constraints $g_i(x) = 0$ (4.68)
- Inequality Constraints $h_j(x) \geq 0$ (4.69)

where, $k$ is the number of objective functions and $x$ is the vector of control variables

### 4.6.2 Real Power Loss Reduction Index

A common strategy for sizing and placement of DG is to minimize system power loss of the power system. Real power loss reduction factor index per node is defined as the ratio of percentage reduction in real power loss from base case when a DG is installed at bus i. Real Power Loss Reduction Index (PLRI) is expressed as:

$$f_1 = PLRI = \frac{P_{L(base)} - P_{L(dg)}}{P_{L(base)}} \tag{4.70}$$

where,

$P_{L(base)}$ is the active power loss before DG installation

$P_{L(dg)}$ is the real power loss in the system after installation of DG

### 4.6.3 Reactive Power Loss Reduction Index

In order to determine the effect of DG on reactive power losses, Reactive Power Loss Reduction Factor Index is incorporated in the objective function. This refers to the ratio of percentage reduction in reactive power loss from base case when a DG is installed at bus i. Reactive Power Loss Reduction Index (QLRI) is expressed as [75];

$$f_2 = QLRI = \frac{Q_{L(base)} - Q_{L(dg)}}{Q_{L(base)}} \tag{4.71}$$

where,

$Q_{L(base)}$ is the active power loss before DG installation

$Q_{L(dg)}$ is the real power loss in the system after installation of DG

### 4.6.4 Voltage Profile Improvement Index

In a power system the voltage at each bus should be within the acceptable range and the line flow within the limits. These limits are important so that integration of DG into the system does not increase the cost for voltage control or replacement of existing lines. The Voltage Profile Improvement Index help identify the size-location pair which gives higher voltage deviations from the base voltage. The Voltage Profile Improvement Index (VPII) is defined as;

$$f_3 = VPII = \frac{1}{\lambda + max_{1=2}^{n}(|1 - V_{(DG)}|)} \tag{4.72}$$

where,

$V_{(DG)}$ is the voltage value after DG installation.

$\lambda$ is a scalar value.

## 4.7 Formulation of Multi-objective Function

Multi-Objective Function (MOF) require to achieve the performance calculation of distributed systems for DG size and location is given by;

$$MOF = w_1 PLRI + w_2 QLRI + w_3 VPII \tag{4.73}$$

where,

$w_1, w_2$ and $w_3$ are the respective weights assigned to each factor.

The total sum of the weight assigned to all parameters of (MOF) should be equal to one;

That is:

$$|w_1| + |w_2| + |w_3| = 1 \tag{4.74}$$

These weights are indicated to give the corresponding importance to each impact index for the penetration of DG depending on the required analysis. The weights vary according to the engineer's concerns. The index whose impact outperforms the others in terms of importance and benefits is given a larger weight and vice versa.

### 4.7.1 Equality Constraints

Real and Reactive power constraints are similar to the non-linear power flow equations. The constraints for power balance can be formulated as follows

$$P_i = P_{DGi} - P_{Di} \tag{4.75}$$

$$Q_i = Q_{DGi} - Q_{Di} \tag{4.76}$$

where,

$P_i$ is real power flow at bus $i$ in kW

$Q_i$ is reactive power flow at bus $i$ in kVAR.

$P_{DGi}$ is real power generation from DG placed at bus$i$in kW

$Q_{DGi}$ is reactive power generation from DG placed at bus $i$ in kVAR

$P_{Di}$ is real power demand at bus $i$ in kW

$Q_{Di}$ is reactive power demand at bus $i$ in kVAR

$P_i$ is also written as

$$P_i = -\frac{1}{[a_{ij}]}\sum_{j=1}^{n}\sum_{j\neq 1}[(a_{ij})P_j - b_{ij}Q_j] \tag{4.77}$$

The above equation is rewritten as equation for optimal sizing of DG

$$P_{DGi} = P_{Di} + [\frac{1}{[a_{ij}]}\sum_{j=1}^{n}\sum_{j\neq 1}[(a_{ij})P_j - b_{ij}Q_j]] \tag{4.78}$$

Consequently for reactive power

$$Q_{DGi} = Q_{Di} + [\frac{1}{[c_{ij}]}\sum_{j=1}^{n}\sum_{j\neq 1}[(c_{ij})Q_j - b_{ij}P_i]] \tag{4.79}$$

where,

$P_i$ is real power flow at bus $i$ in kW

$Q_i$ is reactive power flow at bus $i$ in kVAR.

$P_{DGi}$ is real power generation from DG placed at bus$i$in kW

$Q_{DGi}$ is reactive power generation from DG placed at bus $i$ in kVAR

$P_{Di}$ is real power demand at bus $i$ in kW

$Q_{Di}$ is reactive power demand at bus $i$ in kVAR

### 4.7.2 Inequality Constraints

The inequality constraints are those associated with the bus voltages and DG to be installed.

Inequality constraints lies between acceptable limits to satisfy the objective function.

#### 4.7.2.1 Bus Voltage limits

This includes the upper and lower voltage magnitude limit, $V_{imin}$ and $V_{imax}$ at bus $i$. Bus Voltage magnitude is to be kept within acceptable operating limits throughout the optimization process, then the bus voltage limit is given by

$$V_{imin} \leq V_i \leq V_{imax} \tag{4.80}$$

where,

$V_{imin}$ and $V_{imax}$ are lower and upper bound bus voltage limits in p. u.

#### 4.7.2.2 DG Capacities

The DG capacity of each unit should be defined around its nominal value. So that each DG unit is maintained within an acceptable limit. This includes the upper and lower real and reactive power generation limits of distributed generators (DGs) connected at bus i. The capacity of DG is given as follows:

$$P_{DGmin} \leq P_{DGi} \leq P_{DGmax} \tag{4.81}$$

$$Q_{DGmin} \leq Q_{DGi} \leq Q_{DGmax} \tag{4.82}$$

where,

$P_{DGmin}$ is the minimum real power generation from DG capacity in kW.

$P_{DGmax}$ is the maximum real power generation from DG capacity in kW.

$Q_{DGmin}$ is the minimum reactive power generation from DG capacity in kVAR.

$Q_{DGmax}$ is the maximum reactive power generation from DG capacity in kVAR.

## 4.8 Grid Code

In order to connect RES to the grid, there are certain requirement that need to be met for the stability of the network and maintenance of power quality, hence the need for grid connection codes. The South Africa grid connection code for DG aims to specify the minimum technical and design grid connection requirements for DG connection to South Africa transmission or distribution system [77].

Table 4.1: DGs classification into distribution network [78]

| Sub-categories of Renewable power plant (RPP) | Power Range | Connection Voltage | Voltage Limits % |
|---|---|---|---|
| A1 | $0 < DG \leq 13.8$ kVA | LV | -15+10 |
| A2 | 13.8<DG<100 kVA | LV | -15+10 |
| A3 | 100≤ $DG$ <1 MVA | LV | -15+10 |
| B | $DG$ ≤20 MVA | MV | ±10 |
| C | DG≥20 MVA | HV | ±10 |

### 4.8.1 Grid connection of DGs

The voltage at the point of connection according to the South Africa grid connection code must be in the range of -15 % to +10 % (0.85 to 1.1p.u.) for low voltage network and ±10 (0.9 to 1.1p.u.) for medium and high voltage networks around the nominal voltage [7]. This condition is taken into consideration in this thesis.

## 4.9 Summary

In this chapter both system power flow sensitivity factors and system power loss sensitivity factors have been formulated to be used in getting the combined sensitivity factors. The combined sensitivity factors will be used to get the candidate buses for DG allocation. The multi-objective function to be used in calculating fitness for solutions during optimization has also been formulated in this chapter. The chapter ends by defining the systems operational constraints and grid codes. The next chapter will discuss OPF programming and Optimization methods with its theory.

# Chapter 5

# THEORY OF OPTIMIZATION AND OPF PROGRAMMING

## 5. Introduction

The need for proper integration of DG in a large distribution system requires some special optimal power flow Optimal Power flow (OPF) programming and Evolutionary Techniques as well as other methods in order to reduce losses and improve the voltage profile. Researchers have optimized DG size and location with different techniques. Some of these techniques are reviewed below.

## 5.1 OPF Programming Techniques for DG Allocation

In the recent past, application of optimization techniques to integration Distributed Generation in power system operation as gain considerable popularity in power system research. Universal term used to describe the extensive class of problem in which we seek to optimize is called optimal power flow. Typical OPF formulations aim at reducing the operating cost of thermal resources subject to some constraints represented by bus active and reactive power balances in terms of bus voltages and phase angles. OPF problems have been solve with various type of optimization approach. The techniques can be classified as:

- Nonlinear programming (NLP) examples are

  -Quadratic programming (QP) and

  -Newton-based solution of optimality conditions.

- Linear programming (LP) examples are

  -Hybrid linear and integer programming and

  -Interior point methods.

### 5.1.1 Non-Linear Programming (NLP)

This programming is the earliest formation category since it fits nicely within the framework presented by the physical models of the electric network. In 1962, Carpentia first introduced a generalized, nonlinear programming formulation of the economic dispatch problem, including voltage and other operational constraints. A problem which involves nonlinear objective and constraint functions normally adopt non-linear programming (NLP). The constraints may consist of equality and/or inequality formulations. They contains specified

bounded constraints called inequality and specified equality constraints. [79]. In the same year, Dommel and Tinney's work cited in [80] tried to improve the convergence of the Newton-based approach. This optimization work was used to confirm the convergence at every stage of the process. Due to the similarity of this method to the Lagrange and Kuhn-Tucker methods, the efficiency is reduce due to issue of wandering phenomena. This method was applied on IEEE 30-bus system and is contrained by being incapable of handling more than two constraints per node.

Shoults and Sun in 1982, [81] presented a problem of OPF which was centered upon the decomposition algorithm of real and reactive (P/Q). The P-Problem formulation parameter includes cost minimization of hourly production by regulating generator real power outputs and phase shifting transformers tap setting. The Q-Problem formulation parameter includes losses minimization of real power transmission by regulating generator terminal voltages, shunt capacitor/reactors and transformer tap settings. The constraints for this problem include bus voltage limits, generator reactive power limit and line flow capacity rating. The results obtained shows that decomposition algorithms give the same solution going by the results. Also, gradient method nonlinear optimization strategy employing the Sequential Unconstrained Minimization Technique (SUMT) was developed mainly for OPF problems. An outside of penalty function is defined (since the starting point is not required to be feasible) to force the dependent functions to be feasible at the optimal point. A 5-bus system was used to demonstrate that the P- and Q-sub-problems have solutions. This method has the capability of solving large systems such as 1500 buses and 2500 transmission lines and was actually tested on a practical 962 bus system. Different initial starting points gave the same results; the practical 962- bus system was solved in 46 seconds and the 5-bus system took 2.3 seconds. An initial starting point is necessary to obtain a feasible solution and the method decomposes large into smaller sub-problems and, hence, less computation time is required. This method is useful for on-line operation [82].

#### 5.1.1.1 Quadratic Programming Method

In 1973, Reid and Hasdorf [83] presented a quadratic programming method to solve QPF problems. The method employs Wolfe's algorithm specialized to solve the economic dispatch problem which does not require penalty factors or the determination of the gradient step size. The method was developed purely for research purposes; therefore, the model used is limited and employs the classical economic dispatch with voltage, real, and reactive power

as constraints. The CPU time required was very reasonable; however, the time increased as the system size increased. Convergence is very fast and does not depend upon the selection of gradient step size or penalty factors. The method did not integrate the power flow as constraint and economic dispatch; therefore, they have to be solved separately, which can affect the CPU time required [84]. In 1981, Giras presented a quadratic programming approach which employs a Quasi-Newton based on the Han-Powell algorithm. This algorithm provides a solution even from an infeasible initial starting point. However, when tested on small synthetic systems, the method appears to be fast because of its power flow super linear convergence qualities. The method converges rapidly for small-scale problems; however the convergence criteria do not seem to be practical [85].

#### 5.1.1.2 Newton-Based Solutions

In this approach, the necessary conditions of optimality commonly referred to as the Kuhn-Tucker conditions are obtained. In general, these are nonlinear equations requiring iterative method. The Newton method is favored for its quadratic convergence properties.

### 5.1.2 Linear Programming (LP)

Linear programming treats problems with constraints as objective function formulated in linear forms with non-negative variables. The simplex method is known to be quite effective for solving LP problems.

#### 5.1.2.1 Mixed Integer Programming (MIP)

Mixed integer programming (MIP) is a particular type of linear programming whose constraint equations involve variables restricted to being integers. Integer programming, and mixed integer programming, like nonlinear programming are extremely demanding of computer resources and the number of discrete variables is an important indicator of how difficult an MIP problem will be to solve OPF.

## 5.2 Optimization Methods for DG Allocation

In the recent past, much effort has been contributed to solving the optimal DG placement problem, utilizing different algorithms and considering different objectives. The DG placement problem could be formulated as an optimization problem. Various algorithms are used to solve the problem. The methods used to solve this problem can be divided into three categories;

- Analytical Methods
- Computational Methods

- Artificial Intelligence Methods

### 5.2.1 Analytical Methods

Although the analytical methods suffer from many drawbacks, they are still used in optimizing the location and size of DGs in distribution systems. This is because they are easy to work with and their logical analysis can easily be followed.

Graham et al [86] applied Loss Sensitivity Factor method (LSF) based on the principle of linearization of the original nonlinear equation (loss equation) around the initial operating point, which helps to reduce the amount of solution space. Total loss were minimized by optimal placement of DG unit exclusively at various optimal location of test system. They iteratively increased the size of the DG unit at all buses and then calculated the losses; based on loss calculation they ranked the nodes. Top ranked nodes are selected for DG unit placement [87]. Also in [88] Ashwani and Gao proposed the use of power flow and power loss sensitivity factors in identifying the most suitable zone and then optimized the solution by maximizing the voltage improvement and minimizing the line losses in the network. This work did not consider reactive power loss in optimization. This same approach was tested in [89] [90] [91] .

Sirish [92] implemented a KVS- Direct Search Algorithm to determine the optimal size Distributed Generators (DG) and Static Capacitors together with their optimal locations in a 69 Bus Radial Distribution Systems to obtain maximum real power loss reduction. The optimal sizes of capacitors and DGs are chosen to be standard sizes that are available in the market that is, discrete sizes of capacitors and DGs are considered. Direct Search Algorithm was also used in [93].

### 5.2.2 Computational Methods

Another class of techniques used for optimizing the location and size of DGs in a power system is the computational methods. Although these methods are fast compared to the other classes of techniques, their drawback is that they are complex and reproduction of their results may be difficult or sometimes impossible. Le and Kashem [94] addressed the issue of optimizing DG planning in terms of DG size and location to reduce the amount of line losses in distribution networks. Their optimization methodology, which was based on the Sequential Quadratic Programming (SQP) algorithm, assessed the compatibility of different generation schemes upon the level of power loss reduction and DG cost. In [95], [96] this same approach was used for optimal decision making.

### 5.2.3 Artificial Intelligence Methods

Artificial intelligent (AI) methods such as Genetic Algorithms (GAs) are adaptive heuristic search algorithms based on the evolutionary ideas of natural selection and genetics. Artificial intelligent represent an intelligent exploitation of solving optimization problems through a random search. Also particle swarm optimization is inspired from the natural swarms with communications based on evolutionary computations. Therefore, analytical and the computational optimization methods are being phased out by the most promising artificial intelligence methods such as PSO, GA, ABC to obtain more accuracy in optimization process. This is because, among other benefits the artificial intelligence techniques are not gradient based and thus are not prone to being trapped in local minima. The results from the artificial intelligence, optimization algorithms are also easily reproducible. Some of the artificial intelligence methods mentioned above are further discuss below.

#### 5.2.3.1 Particle Swarm Optimization (PSO)

The Particle Swarm Optimization (PSO) algorithm, as one of the state-of-the-art algorithms inspired by the nature, was introduced in the mid-1990s by Kennedy and Eberhart [97]. Ever since then, it has gain popularity in solving several optimization problems in different area of studies such as biological/medical, computer graphics and music. [98]. The nature of swarms interprets the particles of PSO with computational evolution based communication scheme. The robust solution offer by particle swarm optimization make it possible for it to handle multi objective optimization problem conveniently. One of the merit offer by PSO is that they are impressively resistant to the local optima problem. PSO algorithm has been used for optimal sitting and sizing of DG in distribution systems, as well as voltage profile improvement, loss reduction, and Total Harmonic Distortion (THD) decrease in the distribution network [97] [99]. Figure 5.1 shows the basic block diagram of Particle Swarm Optimization

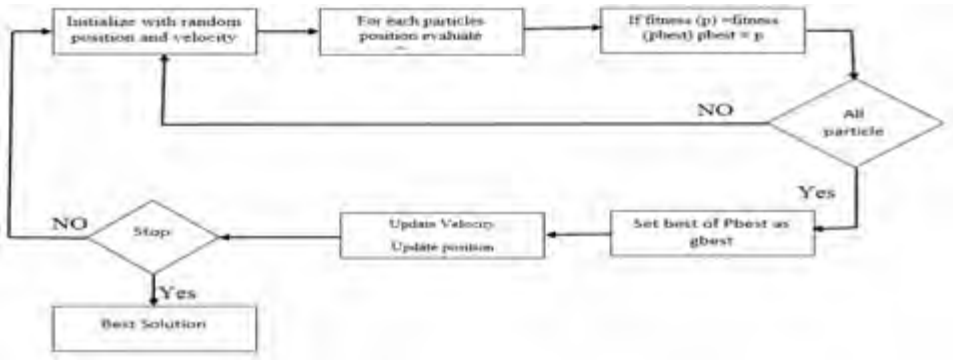


Figure 5.1: Basic block diagram of Particle Swarm Optimization [99]

Sedighi et al [100] and Alinejad-Beromi [99] utilized PSO to evaluate the optimal placement and sizing for single and multiple DGs in order to achieve different goals, including improving voltage profile, reducing active power loss and related DG costs and minimizing THD (Total Harmonic Distortion) in distribution networks. A composing constraints overall objective function and goals was formulated by using properly weighted factors. The authors of the two papers applied load flow and the harmonic load flow algorithm to evaluate fitness values sensitivity in the PSO algorithm process [100]. Other works in which the PSO approach was used are [101] [102] [103].

Jain et al [104] presented a method for optimal siting and sizing of multiple DGs using PSO by minimizing power loss while maintaining the voltage profile and stability margin. Their results showed that the method performed better or at least similar in comparison to other classical and analytical methods for the single DG placement problem. However, in the placement of the third DG it violated some of the constraints. Varesi [105] proposed a PSO based technique for the optimal allocation of DG units in the power system to help in power loss reduction and voltage profile improvement. Load flow algorithm was combined appropriately with the PSO to determine the optimal number, type, size and location of DG units. He only considered two DG units in his work.

Mohammad and Nasab [106] suggested a PSO based multi-objective methodology for optimal allocation of DG. A hybrid objective function was used which had two parts, in the first part the Power Loss Reduction Index was considered while in the second part Reliability Improvement Index was considered. The research considered only active power losses.

Jamian et al. [107] implemented an Evolutionary PSO for sizing DGs to achieve power loss reduction. They argued that though EPSO and PSO give the same performance in finding the optimal size of DG, EPSO can give superior results by having less number of iterations and shorter computation time. Besides that, EPSO avoids the problem of being stuck in a local minimum by selecting the survival particles to remain in the next iteration. Afraz et al [108] also proposed a PSO based approach to optimize the sizing and siting of DGs in radial distribution systems with an objective of reducing line losses and improving the voltage profile. The proposed objective function was a multi-objective one considering active and reactive power losses of the system and the voltage profile. In their research they considered a DG generating active power only. Khan et al., in [109], presented a Novel Binary Particle Swarm Optimization (NBPSO) and Heydari et al. [110] discrete particle swarm optimization (DPSO) approach for the optimal placement and sizing of distributed generations and capacitors in

distribution systems for simultaneous voltage profile improvement, loss and total harmonic distortion (THD) reduction. Their objective function had a term which prevented harmonic resonance between capacitor reactance and system reactance. Constraints included voltage limit, voltage THD, number and size of capacitors and generators. The IEEE 33-bus test system was modified and employed in testing the proposed algorithm. PSO has many advantages which include:

- PSO has an advantage of a fast convergence rate in comparison to most optimization techniques including Genetic Algorithm
- The search can be carried out by the speed of the particle, since it has no overlapping and mutation calculation like GA
- Optimist particle can transmit information onto other particle during the development of several generations, and it has a very fast searching speed.

The only major demerit of PSO are:

- They produce less accurate results at regulation speed, this is because they easily suffers from partials optimism.
- Non-coordinate problems such as the solution to the energy field and the moving rules of the particles in the energy field, application of the method may not work out properly.

#### 5.2.3.2 Fuzzy Optimization Theory

Fuzzy stochastic optimization deals with situations where fuzziness and randomness co-occur in an optimal setting. Research and many other fields are in one way or another concerned with optimization of design, decisions, structures, procedure or information processes. Analysis of such problems along with construction of algorithms for solving them constitutes the disciplinary matrix of mathematical programming. In case of classical models the vague data are replaced by "average data", Fuzzy optimization techniques offer the opportunity to model subjective imaginations of the decision maker as precisely as a decision maker will be able to describe it.

Hong et al. [111] sought the optimal allocation of DG in a smart grid via a multi-objective optimization model. The objectives of the proposed method were to minimize costs of operation of DG and network active power loss and to increase environmental benefits. First, the optimal DG placement was determined by performing a network power loss sensitivity

analysis, where a bus with high sensitivity was selected to install a DG unit. To solve the sizing problem, fuzzy theory was proposed. The multi-objective planning was changed into single-objective planning by employing fuzzy optimization.

#### 5.2.3.3 Artificial Bee Colony (ABC)

The (ABC) algorithm has been a recently introduced population-based meta-heuristic optimization technique inspired by the intelligent foraging behavior of honeybee swarms. Optimization algorithms based on swarm intelligence, known as meta-heuristic algorithms, gained popularity in solving complex and high dimensional optimization problems. Since most of the meta-heuristic methods are independent of the initial solutions and are derivative-free, they overcome the main limitations of deterministic or conventional optimization methods, i.e., getting trapped in local extremer and divergence situations, respectively [112]. The ABC algorithm was introduced to handle unconstrained benchmark optimization functions [113] [114] similar to other well-known meta-heuristic algorithms. An extended version of the ABC algorithm was then offered to handle constrained optimization problems [115]. The colony of artificial bees consists of three groups: employed, onlookers, and scout bees. The merit of artificial bee colony (ABC) are listed as follows:

- ABC dose not converge prematurely.
- It has the ability to discover good solution more rapidly.
- It produce good solution at reasonable time.

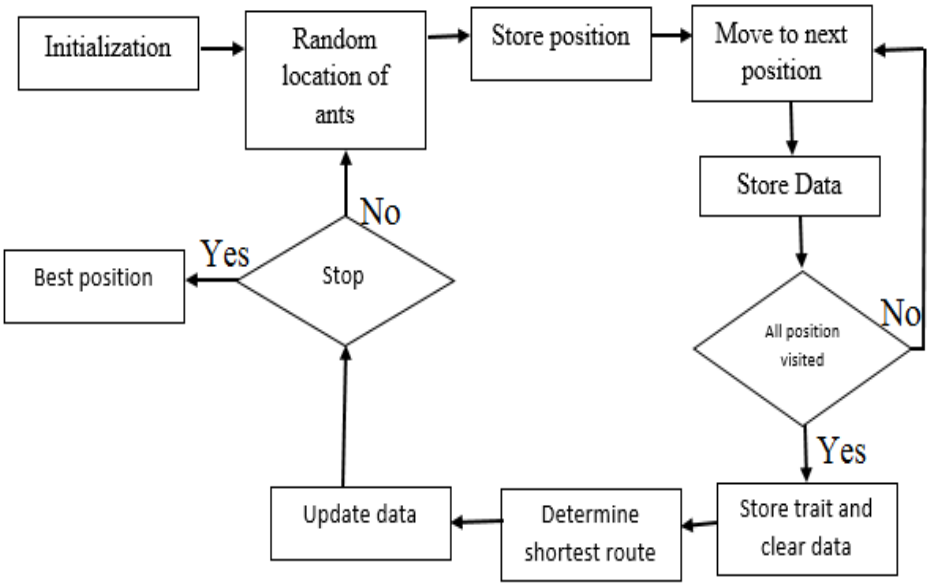


Figure 5.2: Basic block diagram of Ant Bee Colony Optimization [115]

ABC algorithm is represented in the Figure 5.2. This algorithm counts on discrete time steps and memory allocation of the positions visited by artificial ants. Solution quality is evaluated through artificial ant trails and the shortest route determines the best solution that can be achieved employing this algorithm. Implemented in power systems to determine the optimal values of transformer tap setting for voltage control and loss minimization, the (ABC) method achieved optimal solution using the IEEE 30 bus test system [116]. Abu-Mouti and El-Hawary [117] proposed a heuristic technique to find the optimal DG siting and sizing. In this work, the total system power loss for radial distribution networks was the optimization objective. The problem was divided into two sub-problems and each part was treated independently. The authors employed a sufficient sensitivity analysis based on power flow in the first portion to determine the best bus to allocate the DG unit while the optimal DG capacity was chosen by using a heuristic curve-fitted technique. However, the proposed method did not address the multiple DG installation.

#### 5.2.3.4 Genetic Algorithm

Artificial intelligence approach that mimics the process of natural selection of gene is called Genetic Algorithm (GA). This heuristic (also sometimes called a metaheuristic) is routinely used to generate useful solutions to optimization and search problems. Genetic Algorithm is an evolutionary algorithm (EA) which generate solution to optimization problems using techniques inspired by nature evolution, such as mutation, selection, and crossover. GA has been used by several authors to optimize the location and size of DGs in power systems. The flow chart of the algorithm is presented in Figure 5.3. A genetic algorithm approach, using parameters such as generator voltages, static VAR Compensators and On Load Transformer tap Changers of transformer, is employed to optimize the effect on the generator reactive power [118] [119]. It works by its own internal rules.

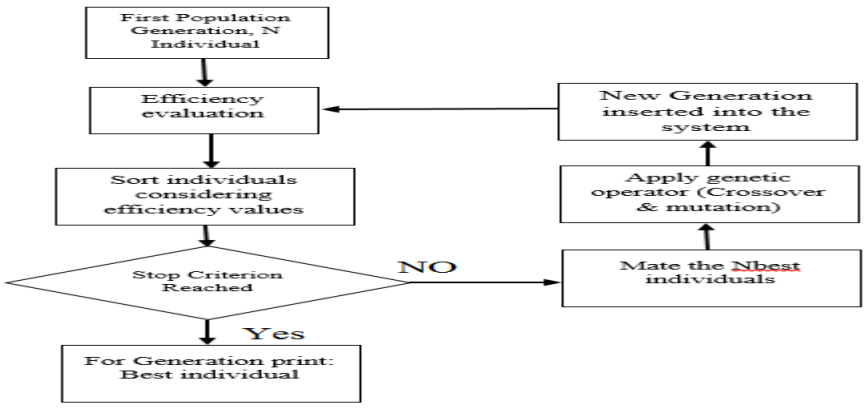


Figure 5.3: Basic Genetic Algorithm flow chart [86]

Ault and McDonald in [86] used a Genetic Algorithm (GA) based method to determine the size and location of DG units. They addressed the problem in terms of cost, considering that the cost function may lead to deviation of the exact size of the DG unit at suitable location. It always gives a near optimal solution, but it is computationally demanding and slow in convergence. This same approach was applied in [120] [121] [122]. Beromi et al [123] present optimal allocation of DG for voltage profile improvement and loss reduction. GA was used as the optimization technique. Load flow was applied for decision making which combined appropriately with GA. The following are some of the advantages of GA [124]:

- It requires no knowledge of gradient information about the response surface.
- It is resistant to becoming trapped in local optima therefore can be employed for a wide variety of optimization problems.
- It can rapidly examine a vast solution set.
- Bad proposals do not affect the end solution negatively as they are simply discarded.
- It doesn't have to know any rules of the problem, it runs by its own internal rules [125].

Phases of search in GA includes:

- Generate an initial population,
- Evaluating a fitness function,
- Producing a new population.

A genetic search begins with a randomly generated initial population within which each individual is evaluated by means of a fitness function. The individual in this and subsequent generations are reproduce or discarded with respect to their fitness values. More generations are produce by applying GA operators. This eventually leads to a generation of high performing individuals. There are usually three operators in a typical genetic algorithm [125]: production operator (elitism), recombination (also known as the crossover) operator and mutation operator.

GAs may have a tendency to converge towards local optima or even arbitrary points rather than the global optimum of the problem, hence there is need to combine a method that have good convergence such as PSO to obtain a robust solution for the problem at hand.

## 5.3 Theory of GA and PSO Techniques

This thesis presents GA as a technique which has the ability to search a vast area for possible solution and come up with reliable results. This is because as stated previously, bad solutions do not affect GAs' end solution negatively since they are discarded as the iterations progress but let to it convergence, there is need for PSO that offer good convergence. On the other hand, the work of Ashari and Soeprijanto [126] formed a key basis in choosing PSO as the other optimization technique. In this thesis, the strengths of PSO as an optimization technique and its flexibility to absorb other parameters for improvement are clearly presented. As a result GA was selected to be used in the initial stages for exploration purposes and PSO is used to improve the optimal solution by incorporating crossover and mutation parameters. Given these strengths for the two optimization techniques the hybridization was deemed to give excellent results.

### 5.3.1 Genetic Algorithm

The Genetic Algorithm initiates the mechanism of the natural selection and evolution and aims to solve an optimization problem with objective function $f(x)$

where,

$x = x_1, x_2, \ldots\ldots, x_n$ is the N-dimensional vector of optimization parameters.

Genes and chromosomes are the basic building blocks of the GA. The conventional standard GA encodes the optimization parameters into a binary code string. A gene in GA is a binary code. A chromosome is a concatenation of genes that takes the form;

Chromosome = $[g_1^1 g_2^1 \ldots g_{L1}^1 g_1^2 g_2^2 \ldots g_1^N g_2^N \ldots\ g_{LN}^N = [x_1 x_2 \ldots\ x_n]$

Where,

$g_j^i$ is a gene.

$L_i$ is the length of the code string of the $i^{th}$optimization parameter

$$x_k = g_1^k g_2^k \ldots\ g_{lk}^k$$

In depth description of the method is not provided here as GA has been applied in several problems. The reader is referred to excellent publications and textbooks such as [127] [128] [129] [130]. GA is one of the effective parameter search techniques which are considered when

conventional techniques have not achieved the desired speed, accuracy or efficiency. GA is different from conventional optimization and search operations in the following ways.

- GA usually works with the coding of parameters rather than the parameters themselves.
- This technique searches from a population of points rather than a single point.
- It uses only objective functions rather than additional information such as their differential coefficients.
- GA use probabilistic transition rules, and not deterministic rules.

### 5.3.2 Choice of GA Parameters

GA parameters is crucial for its faster convergence, depend on its selection. In the absence of any guiding rule to choose these parameters, some mechanism has to be developed. The GA parameters include:

- Population size

The nature of the problem dictates population size, but mostly have several hundreds or thousands of possible solutions. Often, the initial population size is generated randomly, granting the full range of possible solutions (the *search space*). Periodically, the solutions may be "seeded" in areas where optimal solutions are likely to be found

- Selection

This is a genetic operator that selects chromosomes on the basis of their fitness values and produces a new offspring (temporary population), namely, the mating pool. This obtainable by many different schemes, but the most common method is Roulette Wheel Selection. The roulette wheel is biased with the fitness of each of the solution candidates. The wheel is spun M-times where M is the number of strings in the population. This operation generates a measure that reflects the fitness of the previous generation's candidates.

- Crossover

In genetic algorithms, a genetic operator used to vary the programming of a chromosome or chromosomes from one generation to the next called. It is analogous to reproduction and biological crossover, upon which genetic algorithms are based. Cross over is a process of taking more than one parent solutions and producing a child solution from them. There are approach for selection of the chromosomes. Generally, the types of crossover are one-point, two-point

and N-point, and random multipoint crossover and the choice of mutation depend on user. The crossover operator is the main search tool. It mates chromosomes in the mating pool by pairs and generates candidate offspring by crossing over the mated pairs with probability crossover. Typically the probability of parent-chromosome crossover is assumed to be between 0.6 and 1.0.

- Mutation

The diversity transformation gene from one generation of a population of genetic algorithm chromosomes to the next is called mutation. It is analogous to biological mutation. Mutation changes one or more gene values in a chromosome from its initial state. In mutation, the answer may change completely from the old result. Hence GA can come to a better solution by using mutation. Mutation occurs during evolution according to a user-definable mutation probability. After crossover, some of the genes in the candidate offspring are inverted with the probability $P_{mut}$. Typically, the probability of mutation $P_{mut}$ is assumed to be between 0.01 and 0.1.

- Elitism

The worst chromosome in the newly generated population is replaced by the best chromosome in the old population if the best number in the newly generated population is worse than that in the old population. This is adopted to ensure the algorithm's convergence. This method of preserving the elite parent is called elitism.

### 5.3.3 GA Implementation Steps

In GA algorithm, the population has n chromosomes that represent candidate solutions, each chromosome is an m dimensional real value vector where m is the number of optimized parameters. GA methodology discussed above is implemented using the following steps.

Step 1: (initialization): Set the iteration counter k = 1 and generate randomly n chromosomes.

Step 2: (fitness): Evaluate each chromosome in the initial population using the objective function, F.

Step 3: (Selection): Depending on individual chromosome fitness and using a given selection scheme (for example, roulette wheel method) select two parent chromosomes from the population for mating.

Step 4: (Crossover and Mutation): With a crossover probability, cross over the selected parents to form a new child. With a selected mutation probability and method, mutate the genes in the new child at each chromosome.

Step 5: (new population): Create a new population by repeating steps 3 and 4 while accepting the new formed child until the new population is completed.

Step 6: (Elitism): Replace the least chromosome in the newly generated population by the best chromosome in the old population if the best one in the newly generated population is worse than that in the old population. This is adopted to ensure the algorithm's convergence.

Step 7: (replacement): Replace old population with new generated population for a further run of algorithm.

Step 8: (Iteration updating): Update the iterations counter k = k+1

Step 9: If stopping criteria is satisfied go to step 10 else go to step 2.

Step 10: Stop, the optimized solution is the chromosome with the best fitness in the present population.

### 5.3.4 Particle Swarm Optimization

A velocity is defined which directs each particle's position and gets updated in each iteration. Particles gradually move near the optima due to their best position they have ever experienced and the outstanding solution which the group has accomplished. The velocity of a particle is updated due to three factors i.e. the past velocity of the particle, the best position the particle has experienced so far and the best position the entire swarm has experienced so far as shown in Figures 5.4 and 5.5.

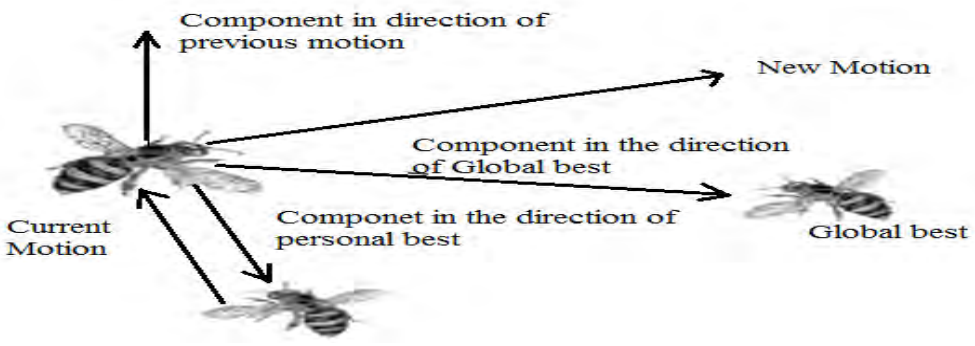


Figure 5.4: Concept of a searching point by PSO [106]

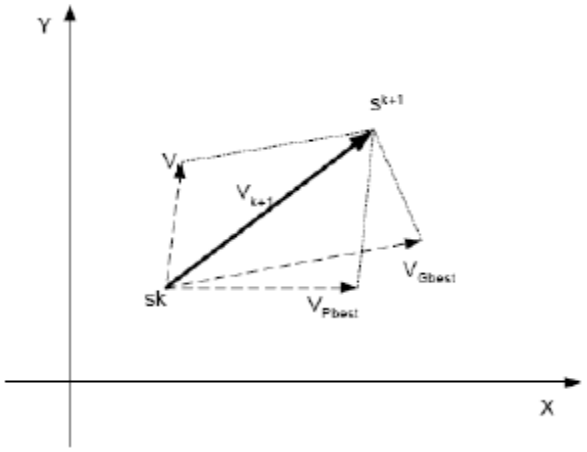


Figure 5.5: Velocity updating in PSO [106]

### 5.3.5 Mathematical Modification of PSO

Mathematical modification steps can may be expressed as follows:

$$V_{id}^{k+1} = w_k V_{id}^{k} + c_1 r\left(Pbest_{id} - S_{id}^{k}\right) + c_2 r(Gbest_{id} - S_{id}^{k}) \quad (5.1)$$

$$S_{id}^{k+1} = S_{id}^{k} + V_{id}^{K+1};\ i = 1,2,\dots,n\ \&\ d = 1,2,\dots,m \quad (5.2)$$

where,

$V_{id}^{k+1}$ is modified velocity of agent $i$

$w_k$ is weight function for velocity of agent

$V_{id}^{k}$ is current velocity

$c_1$ and $c_2$ are weight coefficients for each term respectively

$r$ is a random number.

P$best_{id}$ is the particles best position

$S_{id}^{k}$ is current searching point

$S_{id}^{k+1}$ is the modified searching point

G$best_{id}$ is the group best position

$n$ is number of particles in a group

$m$ is number of members in a particle

The following weight function is used:

$$w_k = w_{max} - \frac{w_{max} - w_{min}}{k_{max}} . k \tag{5.3}$$

where,

$w_{min}$ and $w_{max}$ are the minimum and maximum weights respectively.

$k$ and $k_{max}$ are the current and maximum iteration.

### 5.3.6 Choice of PSO Parameters

The most important parameters in the PSO algorithm include:

- Particle Velocity

The current velocity $V_{id}^{k}$ is constrained in the limits $V_{id}^{min} \leq V_{id}^{k} \leq V_{id}^{max}$. The parameter $V^{max}$ determines the resolution, or fitness, showing which regions are to be searched between the present position and the target position. If $V^{max}$ is very high, particles might fly past good solutions. This is because the particles move in larger steps and the solution reached may not be optimal. Similarly if $V^{max}$ is too small, particles take a longer time to reach desired solutions. They may even not explore sufficiently hence being captured in local minimum solutions. In many experiences with PSO, $V^{max}$ is often set at 12–25% of the dynamic range of the variables on each dimension [106].

- Random Numbers

The uniform random values are in the range [0, 1]. They help in achieving the stochastic behavior of PSO.

- Weighting Coefficients

The parameters $c_1$ and $c_2$ represent the weighting of the stochastic acceleration terms. High values result in abrupt movement toward, or past, target regions. On the other hand, low values allow particles to roam far from the target regions before being tugged back. The parameters $c_1$ and $c_2$may be adopted in the range 0 to 2 [106] [131] as the number of iterations increases, but in many applications $c_1$ and $c_2$are often constants. Parameters $c_1$ and $c_2$control the rate of relative influence of the memory of other particles and their typical values are $c_1 = c_2 = 2$ .

- Inertia Weight

Suitable choice of the inertia weight *w* can supply a balance between global and local explorations. That is a balancing factor between exploration and exploitation. For faster convergence, inertia weight is usually selected to be high at the beginning and is decreased in the course of optimization. In general, the inertia weight w is adjusted according to equation (5.3) above.

- Termination criterion

After the initial phase, several iterations of update and evaluation steps are performed until a stopping condition is met. Generally, the stopping condition is the attainment of a predefined maximum numbers of iterations or the attainment of certain accuracy in the solution.

### 5.3.7 PSO Implementation Steps

In PSO algorithm, the number of population n particles that represent solutions candidate. Every particle is an m dimensional real value vector where m is the number of parameters to be optimized. Consequently, each optimized parameter denotes a dimension of the problem space. The PSO technique can be described in the following steps.

Step 1: Start the process: Set the iteration counter k = 1. Generates randomly an initial population of n particles. Initial velocity of each particle is randomly generated for evaluation of the objective function $k_{max}, w_{min}, w_{max}, c_1$ and $c_2$ are assigned.

Step 2: Objective function calculation: Calculate the objective function and fitness value of each particle. The fitness value of each particle during the first iteration becomes its $P_{best}$. The best fitness value among all the $P_{best}$ is denoted as $G_{best}$

Step 3: Velocity modification: Modify the velocity of each particle using the below equation (5.1)

Then generate the new particles based on equation (5.2)

Step 4: Upgrading of $P_{best}, G_{best}$ Compute the fitness value of each new offspring. Compare the calculated fitness value of each new particle with its $P_{best}$. If the fitness value of a particle is better than the previous $P_{best}$, then $P_{best}$ is updated with the current value. If the best $P_{best}$ is better than $G_{best}$ , then $G_{best}$ is substituted with the best $P_{best}$ .

Step 5: Iteration updating: Update the iteration counter, k = k+1.

Step 6: If stopping criteria is satisfied go to step 7, else go to step 3.

Step 7: Stop. The particle that generates the latest $G_{best}$ is the optimal solution of PSO.

## 5.4 Summary

This chapter discussed the OPF programming methods and optimization methods for DG allocation and sizing. It also reviewed and explained the theory of GA and PSO in relationship with their operators. The next chapter will develop the hybridization of GA and PSO to form GA-IPSO and show in a flow chat how they can be used for optimal allocation of DG.

# Chapter 6

# HYBRIDIZATION OF GA AND PSO FOR OPTIMAL DG ALLOCATION

## 6. Introduction

This chapter covers the hybridization tools used in this research and the proposed methodology for hybridization. There are different methods by which these two optimization techniques can be hybridized so as to come up with a better method to solve the problem at hand. The details of the proposed methodology are given in this chapter, which includes the selection approach. The steps of the proposed algorithm are also shown.

## 6.1 Roulette Wheel Selection Method

Roulette Wheel selection, also known as the Fitness proportionate selection, is a genetic operator used in genetic algorithms for selecting potentially useful solutions for recombination. The idea behind the roulette wheel selection technique is that each individual is given a chance to become a parent in proportion to its fitness. Thus, this fitness level is used to associate a probability of selection with each individual chromosome. If $f_i$ is the fitness of individual $i$ in the population, its probability of being selected is given by;

$$p_i = \frac{f_i}{\Sigma_{j=1}^{N} f_j} \tag{6.1}$$

where,

$p_i$ is the probability of selecting individuals.

$N$ is the number of individuals in the population.

$f_i$ is the fitness of individual

It is called roulette wheel selection as the chances of selecting a parent can be seen as spinning a roulette wheel in a casino with the size of the slot for each parent being proportional to its fitness. Obviously those with the largest fitness (slot sizes) have more chance of being chosen. Although candidate solutions with a higher fitness will be less likely to be eliminated, there chance of surviving the selection process is very high. Therefore, in contrast to a less sophisticated selection algorithm, such as truncation selection, which will eliminate a fixed percentage of the weakest candidates; with roulette wheel selection there is a chance some weaker solutions may survive the selection process. This is an advantage, as though a solution may be weak, it may include some component which could prove useful following the

recombination process. In the same vain, it is possible for one member to dominate all the others and get selected a high proportion of the time.

In this research work roulette wheel selection method was employed in the Genetic Algorithm. This is because as evident later in the steps of the proposed methodology, the algorithm first used Genetic Algorithm to do exploration thus making this selection method the most favorable one.

### 6.2 Greedy Selection Method

A greedy selection algorithm always makes the choice that looks good at the moment. The hope is that a locally optimal choice will lead to a globally optimal solution. This technique might also be called a "single-minded" technique or a technique that gobbles up all of its favourites first. The idea behind a greedy algorithm is to perform a single procedure in the recipe over and over again until it can not be done any more and see what kind of results it will produce. It may not produce the very best solution, but it is one way of approaching the problem and sometimes yields very good (or even the best possible) results.

The choice made by a greedy selection may depend on choices made so far, but not on future choices. It iteratively makes one greedy choice after another, reducing each given problem into a smaller one. In other words, a greedy algorithm never reconsiders its choices in the iteration. This is the main difference from roulette wheel selection method which is exhaustive and is guaranteed to find the solution in most cases. After every stage, roulette wheel selection method makes decisions based on all the algorithmic paths to a solution.

Greedy selection is one of the most straightforward design techniques. Most problems have *n* inputs and a solution to these problems contains a subset of inputs that satisfies a given constraint. A feasible solution is therefore any subset that satisfies the constraint; that is a solution that maximizes or minimizes a given objective function. Greedy selection is used to determine a feasible solution that may or may not be optimal. At every point, a decision is made that is locally optimal and in the hope that it leads to a globally optimal solution. This leads to a powerful method for getting a solution that works well for a wide range of applications.

After exploration is done in the GA section of the algorithm, there is need for exploitation of the already partially optimized solutions so as to come up with the most optimal solution(s). This exploitation section was done in the IPSO section and thus greedy selection method was used to facilitate this due to its nature.

### 6.3 Arithmetic Crossover (AC) and Mutation

In this research Arithmetic Crossover (AC) was applied to both GA and PSO sections in the hybridized algorithm. It creates offspring which is the weighted arithmetic mean of two initial parents. The flexibility of offspring depend of constraints and bounds. Alpha is a random value between [0, 1]. If parent1 and parent2 are the parents, and parent1 has the better fitness value, the function returns the child defined *arithmetic crossover* as the combination of two parent chromosomes $X_{p1}$ and $X_{p1}$ to give two children chromosomes $X_{c1}$ and $X_{c2}$ as follows [132], [133] :

$$X_{c1} = \lambda X_{p1} + (1 - \lambda) X_{p2} \tag{6.2}$$

$$X_{c2} = \lambda X_{p2} + (1 - \lambda) X_{p1} \tag{6.3}$$

$\lambda \epsilon (0,1)$ is generated randomly between 0 and 1 and used to compute the children

For a given child;

$$X_{cl}^{k} = X_{l1},,,X_{lj},,,X_{lm}^{k} \tag{6.4}$$

where,

$$l = 1,2,\dots,N; j = 1,2,\dots,m$$

If the element $X_{lj}^{k}$ is selected for mutation, the resulting offspring is given by;

$$X_{cl}^{k} = X_{l1},,,X_{lj}^{k*},,,X_{lm}^{k} \tag{6.5}$$

where,

$$X_{lj}^{k*} = X_{lj}^{k} + \Delta X_{lj}^{k} \tag{6.6}$$

$\Delta X_{lj}^{k}$ is randomly selected from the two possible choices:

$$\Delta X_{lj}^{k} = r(X_{lj}^{max} - X_{lj}^{k})(1 - \frac{k}{k_{max}}) \tag{6.7}$$

where,

$r$ is a random number between 0 and 1

Arithmetic crossover and mutation was employed because it enabled the use of real coded chromosomes in the algorithm. Thus the encoding of chromosomes from real values to binary numbers and decoding them back was avoided making the algorithm not only less complex but also reducing its computation time.

In this research, the following values were used for different parameters:

A crossover probability of 0.95

A mutation probability of 0.05

Number of generation is 20

Population size 50

Weighting Coefficients $c_1 = c_2 = 2$

Number of iteration 60

These are the best values to work with during optimization.

### 6.4 Choice of Weights values for Multi-objective Function

As mentioned earlier, the allocation of the various weights in a given multi-objective function varies according to the engineer's requirements. In this thesis, more emphasis is given to real power loss reduction since this leads to a considerable decrease in total cost of operation, although, this is not mean that the other two factors are not important. Thus, a study of the effect of the weights on the fitness was done so as to determine the best weights combination to adopt in coming up with the multi-objective function. During this study, the values of the weights are assumed positive and restricted as follows:

- $w_1$ is restricted between 0.5 and 0.8
- $w_2$ and $w_3$ are restricted between 0.1 and 0.4

This is done so as to ensure that much emphasis is given to the real power loss reduction index as earlier stated while at the same time ensuring that all the three indices are taken into consideration in formulating the multi-objective function.

It is also important to note that the condition $|w_1| + |w_2| + |w_3| = 1$ has to be satisfied in each case. Table 6.1 below gives the results obtained in this study.

Table 6.1: Effects of weights on fitness

| $w_1$ | $w_2$ | $w_3$ | Best Fitness |
|---|---|---|---|
| **0.5** | 0.1 | 0.4 | 0.9094 |
| **0.5** | 0.2 | 0.3 | 0.9102 |
| **0.5** | 0.3 | 0.2 | 0.9099 |
| **0.5** | 0.4 | 0.1 | 0.9103 |
| **0.6** | 0.1 | 0.3 | 0.9107 |
| **0.6** | 0.2 | 0.2 | 0.9091 |
| **0.6** | 0.3 | 0.1 | 0.9096 |
| **0.7** | 0.1 | 0.2 | 0.9101 |
| **0.7** | 0.2 | 0.1 | 0.9102 |
| **0.8** | **0.1** | **0.1** | **0.9092** |

From the results presented in Table 6.1 above the combination of weights chosen is the one which gave the minimum best fitness. Thus the weights chosen were: $w_1 = 0.6, w_2 = 0.2, w_3 = 0.2$ and the multi objective function (MOF) is given by equation (4.75).

## 6.5 Load Flow Program

Base case power-flow for the system under actual and projected normal operating conditions was done with load flow program. The results of base case create a criterion for comparison of changes in network flows and voltages under changing network topology. System instability such as low voltages, line over-loads, or loading conditions deemed excessive can be discovered and taken into consideration by making a design. The load flow program in matrix and script code for this work is done in Matlab.

## 6.6 Genetic Algorithm and IPSO Methods Main Program

The proposed methodology is composed mainly of applying Load flow program interacted with GA and GA-IPSO program using Input System Data in MATLAB Matlab in simulations. The main modules of the proposed technique are explained as follows:

Input system data module includes:

- Network data
- Buses data
- Lines data
- DG data
- Number of locations
- number of DGs
- DG types
- Constraints
- Objective function data
- Weights.

## 6.7 Methodology of approach Used

The aim is to reduce system losses and improving the voltage profile by optimal location of DG in the distribution system.

System power flow and power loss sensitivity factors have been used in order to come up with the candidate buses for DG location. This helps in reducing the search space for the

algorithm and thus making it to converge faster. The results of these sensitivity factors are then passed to GA which gives possible DG sizes for each location. This is done by randomly initializing the DG sizes for each location and then optimizing these values using a predefined multi-objective function. In general GA performs exploration and comes up with promising solutions which are passed to IPSO for fine tuning.

The output from GA, which is transferred to IPSO comprises some sets of optimal solutions with a DG location and the associated DG size. The GA optimized results was used as its set of initial particles for IPSO. This assists in achieving faster convergence. IPSO fine tune the solutions from Genetic Algorithm so as to come up with an optimal solution. The block diagram in Figure 6.1 shows the general procedure of the proposed methodology.

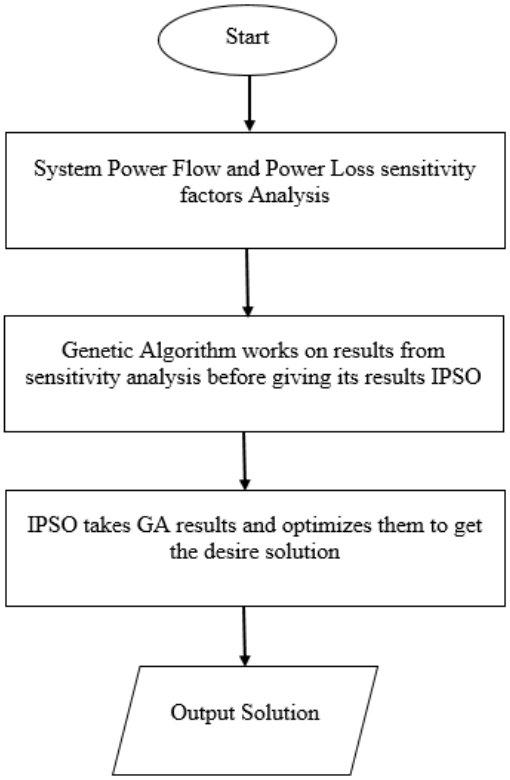


Figure 6.1: A block diagram showing general procedure of the proposed methodology

## 6.8 Steps of the GA-IPSO Algorithm

The step of GA-IPSO approach for optimal allocation of DG units in the distribution systems is as detailed in the following implementation steps;

1. Get system data by reading the power system parameters.

2. Employ Newton-Raphson method for load flow studies to calculate system base case power loss.

3. Compute CSF for each bus and arrange buses in order of sensitivity.

$$CSF = \left(F_{p-pi} \times F_{Q-pi}\right) + \left(F_{p-Qi} \times F_{Q-Qi}\right) + \left(S_{P-Pi} \times S_{Q-Pi}\right) + \left(S_{P-Qi} \times S_{Q-Qi}\right) \quad (6.7)$$

4. Buses with high sensitivities are chosen as candidate buses.

5. Input both GA and IPSO control parameters.

6. Set candidate bus count $i = 1$

7. While $i \leq n$

(i) Initialize N chromosomes with random values to represent possible DG sizes.

$$P_{DG}^{min} \leq P_{DGj} \leq P_{DG}^{max} \text{ and } Q_{DG}^{min} \leq Q_{DGj} \leq Q_{DG}^{max}, j = 1,2, \ldots N$$

(ii) Set iteration count (for GA)$k = 1$

(iii) While $k \leq k_{max}$

a) Evaluate each chromosome's fitness using the multi-objective.

b) Using roulette wheel selection method, select two chromosomes ($X_{P1}$and $X_{P2}$).

c) Evaluate mutation and crossover based on the probabilities and

d) Create a new population by repeating steps (b) and (c) while accepting the newly formed children until the new population is complete.

e) Replace old population with new population.

f) Update the iterations counter $k = k + 1$

(iv) Stop and pass current chromosomes (partially optimized) to IPSO.

(v) Use GA optimized chromosomes as initial IPSO particles.

(vi) The fitness value eas evaluated for each particle using multi-objective function. The value of each particle becomes its $P_{best}$. The particle value with the best fitness among all the $P_{best}$ is denoted as $G_{best}$

(vii) Set iteration count (for IPSO) $iter = 1$

(viii) While $iter \leq iter_{max}$

a) Modify the velocity of each particle element as shown.

$$V_{id}^{k+1} = w_k V_{id}^{k} + c_1 r\left(Pbest_{id} - S_{id}^{k}\right) + c_2 r\left(Gbest_{id} - S_{id}^{k}\right) \quad (6.8)$$

where,

$$w_k = w_{max} - \frac{w_{max} - w_{min}}{iter_{max}}.iter \quad (6.9)$$

Then generate the new position for each particle element.

$$S_{id}^{iter+1} = S_{id}^{iter} + V_{id}^{iter+1} \quad (6.10)$$

b) Using greedy selection method select two chromosomes ($S_{p1}$ and $S_{p2}$ ).

c) Perform crossover and mutation based on the probabilities ($P_{cross}$ and $P_{mut}$)

d) Create a new population by repeating steps (c) and (d) while accepting the newly formed children until the new population is complete.

f) Compute the fitness value of each new particle and update $P_{best}$ as shown;

$$p_{best(j)}^{iter+1} = \begin{cases} S_{(j)}^{iter+1} \; if & MOF_j^{iter+1} < MOF_j^{iter} \\ p_{best(j)}^{iter+1} \; if & MOF_j^{iter+1} \geq MOF_j^{iter} \end{cases} \quad (6.11)$$

$$G_{best(j)}^{iter+1} = \begin{cases} p_{(j)}^{iter+1} \; if & MOF^{iter+1} < MOF^{iter} \\ q_{best(j)}^{iter+1} \; if & MOF^{iter+1} \geq MOF^{iter} \end{cases}$$

g) Update the iteration counter, $iter = iter + 1$

(ix) Stop the particle that produce the latest $G_{best}$ is the optimal solution.

(x) With the latest $G_{best}$ in the network, calculate system power loss and bus voltages

$$(P_{L(DGi)}, Q_{L(DGi)}, and\ V_{(DGi)}) \quad (6.12)$$

(xi) Update the candidate bus $i = i + 1$

8. Compare the fitness of candidate buses $G_{best}$ and get the most minimized one at highest Iteration.

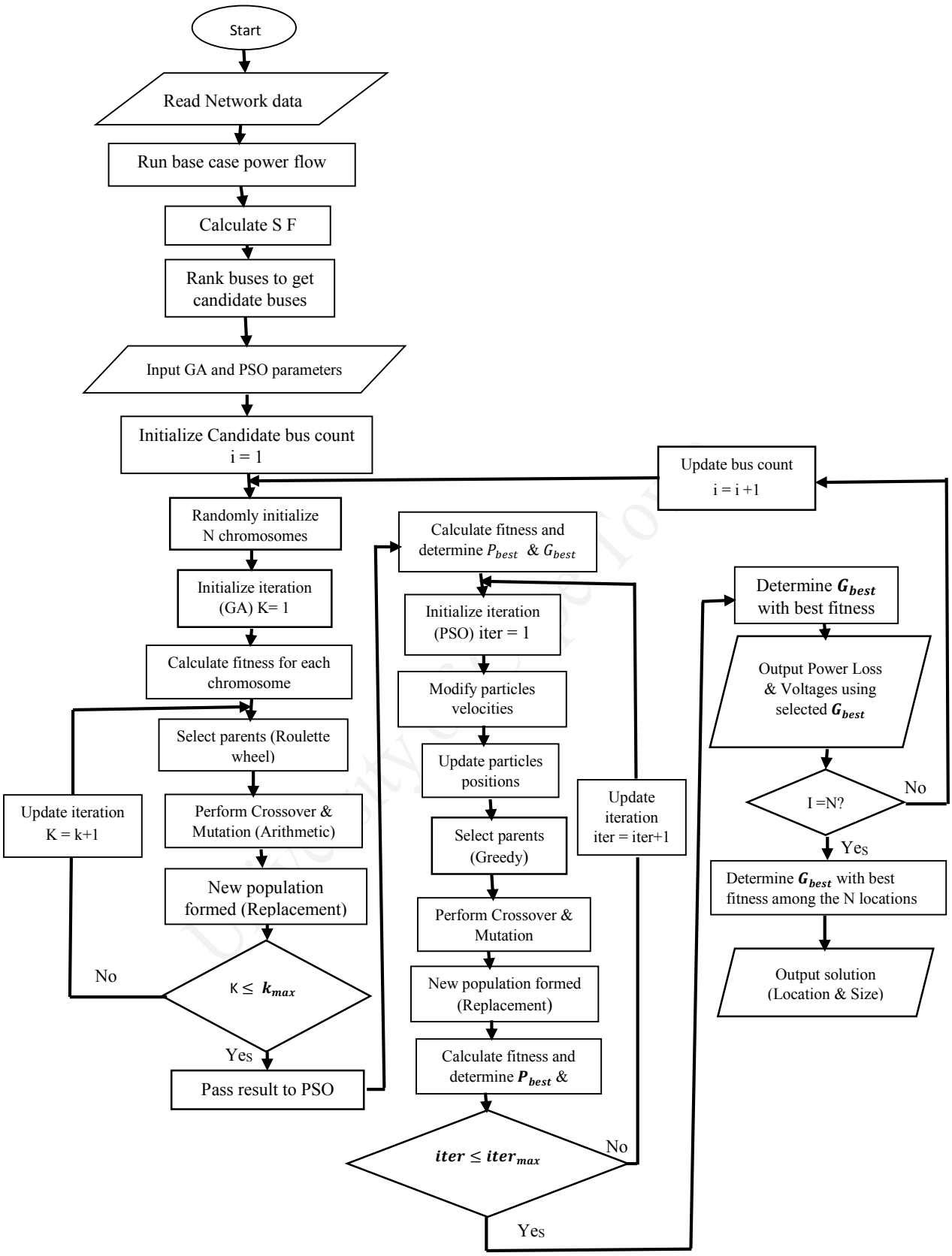


Figure 6.2: A flow chart for GA-IPSO algorithm [74].

9. Optimal locations results and their respective optimal DG when there no more changes as show in typical convergence characteristic in appendix XI.

## 6.9 Summary

This chapter dealt with the hybridization of the already chosen optimization techniques and their step implementation. The next chapter will discuss the simulation procedures and results obtained using the proposed approach and GA.

# Chapter 7

# SIMULATION RESULTS

## 7. Introduction

This chapter presents the results obtained using GA and GA-IPSO methods. The algorithm outlined in the previous chapter was implemented and programmed in Matlab 2013. The main codes programmed according to the implementation steps of the GA-IPSO algorithm are given in Matlab. The results are subdivided into two sub sections, section one used IEEE 33-bus under peak and base load condition and section two use Western Cape real network under peak and base load condition. An analytical approach was used in section one under peak load condition using one unit of DG, also the three of DG units were optimized using GA and GA-IPSO respectively. Also in section two, two unit of DG were optimized using GA and GA-IPSO under peak and base load condition. In both sections, voltage profile graph were drawn and loss reduction percentage presented on a table for both GA and GA-IPSO respectively.

## 7.1 Types of DGs used

In this research, two types of DGs were used (Photovoltaic and Wind), the first one was made to generate active power while the latter can generate both active and reactive power. Photovoltaic PV is considered as the DG type one and wind generator is the DG type two as discussed in the literature review. In addition, DG type one is operating at unity power factor (pf) while the type two is operating at 0.9 pf.

## 7.2 Test System Description

In these results, the DG(s) were assumed to be located in an IEEE 33-bus test system. The test system is a radial system with a total load of 3.72 MW and 2.3 MVAR. The total real power loss 211.20 kW and reactive power loss is 101.10 kVAR, are obtained using Newton-Raphson method. The diagram of this network is given in Appendix I while its line and bus data are as shown in Appendices II and III respectively.

Also, a modified South African real network (Western Cape network), with total local load of 400 MW and 204.40 MVAR was used. The real power loss is 180 kW and reactive

power loss is 40 kVAR. The line and bus data are as shown in Appendices IV and V respectively, while the diagram of this network is given in Appendix VI.

## 7.3 Section 1: Results using IEEE 33-bus test system under peak load

In this section, the results of optimal allocation two types of distributed generation (wind and PV) in IEEE 33-bus is given in this section considering the stochastic nature of their supply. The peak load within a period of 24-hours as presented in chapter 4, Figure 4.1 were used. Also, results from GA-IPSO compared with the GA optimization method are presented. Finally, study cases are defined as:

Case 1: One unit of PV DG (type1) Using Analytical Approach.

Case 2: One unit of Wind DG (type2) Using Analytical Approach.

Case 3: Three units of PV DG using GA.

Case 4: Three units of wind DG using GA.

Case 5: Three units of PV DG using GA-IPSO.

Case 6: Three units of Wind DG using GA-IPSO.

### 7.3.1 Result of Case 1, for PV (type1) DG Using Analytical approach

The base case was run using Newton-Raphson load flow to obtain the bus voltage magnitude, real and reactive power loss respectively. After the load flow, optimum size of DG for each bus was identified using equation (4.80) and the approximate loss for each bus was found using equation (4.50) by placing DG at the corresponding location with the optimum sizing obtained from above. Also the optimum location at which the loss is minimum after DG placement is obtained. As far as one location is concerned, in a distribution test system, the range of DG sizes for the test system at various locations is between 0.1–3.99 MW. Figure 7.1 shows optimum sizes of DG at various nodes for the 33-bus distribution test system.

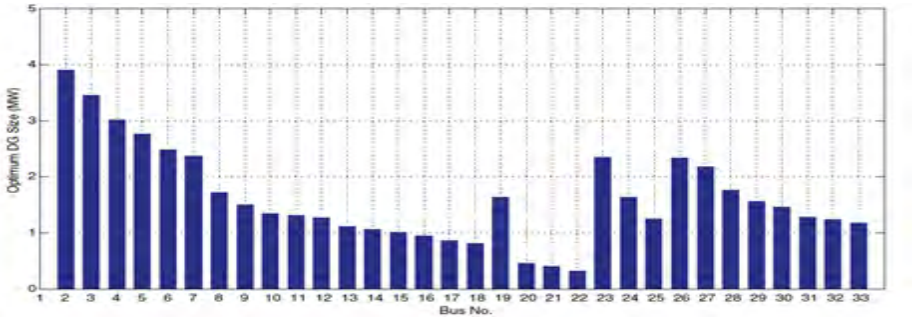


Figure 7.1: Optimum size of DG at various locations for the 33-bus Network.

In Figure 7.2, the trend of the losses is captured with the help of the approximate solution which is good enough to identify the location that would lead to the least total power losses.

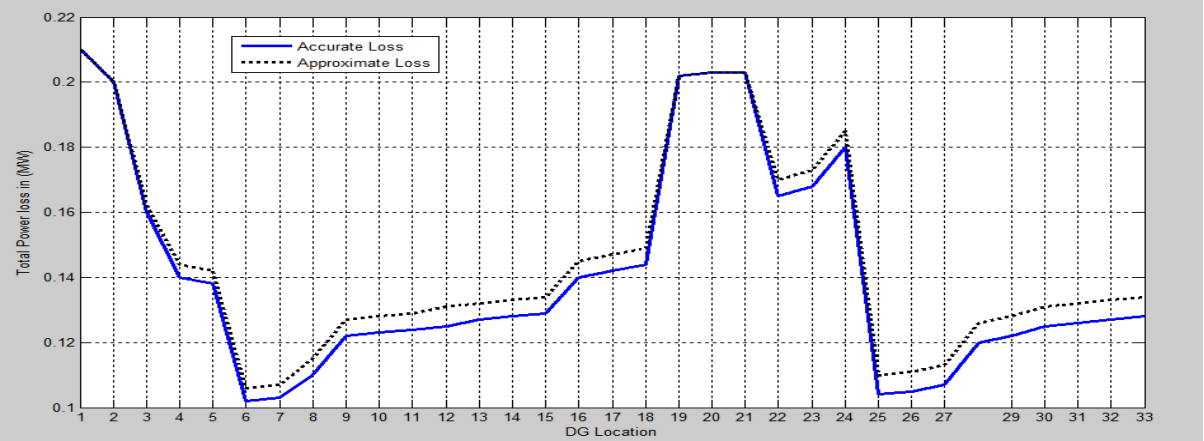


Figure 7.2: Approximate and accurate losses of the 33-bus test system using PV DG.

The best location is bus 6 with a total real power loss reduction of 111.24 kW and the second best location is bus 7 with slightly higher total power losses as shown in Table 7.1 below. The percentage real power loss reduction are 52.7 % and 47.9 % at bus 6 and 7 respectively with respect to base case loss.

Table 7.1: Summary of Optimal Location for one unit of PV DG

| Test System | Optimum Location | Optimum Size (MW) | Power loss (kW) | | % loss Reduction |
|---|---|---|---|---|---|
| | | | Without DG | With DG | |
| 33-bus | Bus 6 | 2.49 | 211.20 | 99.96 | 52.6 |
| | Bus 7 | 2.12 | 211.20 | 109.95 | 47.9 |

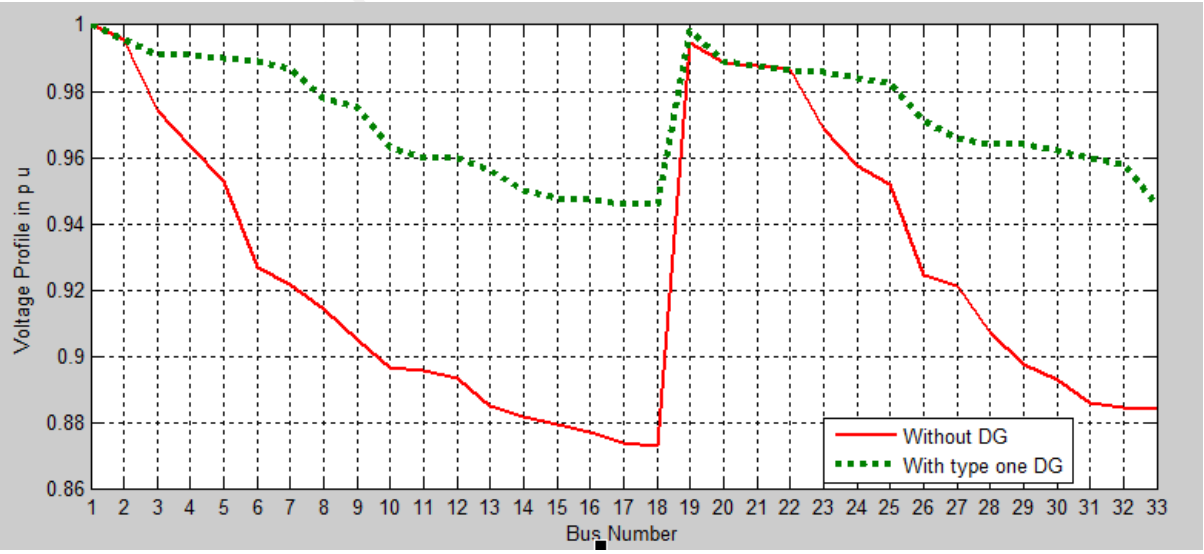


Figure 7.3: Voltage profile of 33-bus test system after integration of PV DG at bus 6

Voltage profile improvement in the network is displayed above in Figure 7.3. After integration of DG it can be observed that buses 15, 16, 17, 18 and 33 are still outside the standard limit of ±5% voltage deviation despite the power losses reduction recorded.

### 7.3.2 Result of Case 2, for Wind (type2) DG Using Analytical approach

As shown in Figure 7.4, the trend of the losses is captured with the help of approximate solution which is good enough to identify the location that would lead to the least total power losses. From Table 7.2, bus 12 is shown as the optimal location with percentage power loss reduction of 51.4% and 23% for active and reactive power respectively.

Table 7.2: Summary of Optimal Location for one unit of Wind DG

| Test System | Optimal location | Optimal Size | | Power loss | | % loss Reduction | |
|---|---|---|---|---|---|---|---|
| | | MW | MVAR | kW | kVAR | | |
| 33-bus | Without DG | | | 211.2 | 101.1 | | |
| 33-bus | Bus 12 | 2.04 | 0.51 | 102.68 | 78 | 51.4 | 23 |

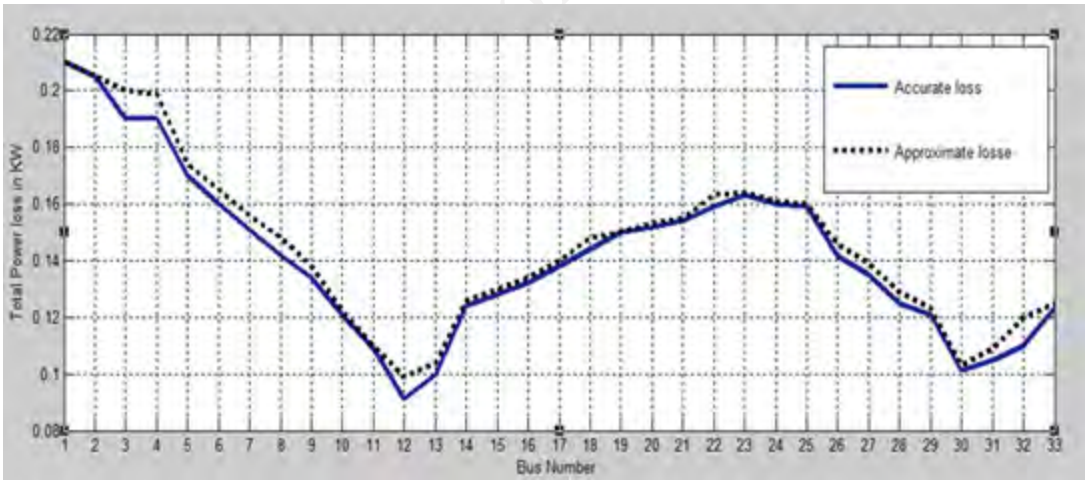


Figure 7.4: Approximate and accurate losses of 33-bus test system using Wind DG.

Bus 12 in Figure 7.4 above has the minimum loss and is a prospective DG candidate bus in the 33-bus network. Voltage profile improvement in the network is displayed below in Figure 7.5. After integration of DG it can be observed that buses 17, 18 and 33 are still outside the standard limit of ±5% voltage deviation despite the power losses reduction recorded. Hence there is a need for a more accurate, robust, less time consuming new approach.

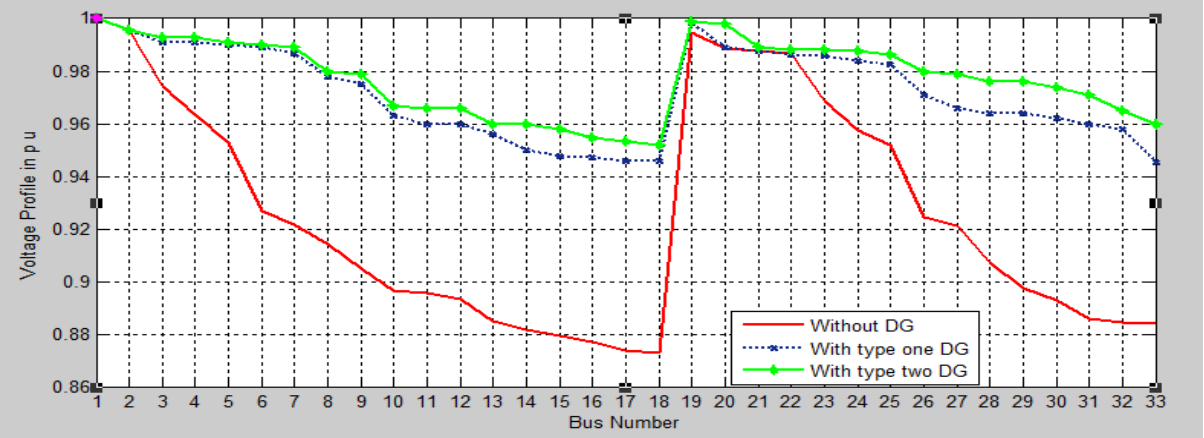


Figure 7.5: Voltage profile of 33-bus test system after integration of Wind DG bus 12.

### 7.3.3 Result of Case 3, three units of PV DG using GA

Optimal placement and sizing of three units of DG was investigated using the GA implementation steps in Chapter 5 as well as the network parameters in Chapter 6 to obtain the optimized solution of chromosome with the best fitness in the population. With the chosen DG candidate buses and sizes, a load flow study was done using Newton Raphson method so as to determine the associated power losses and voltage levels.

Table 7.3: Best ten optimal solutions for installing three units of DG type one.

| DG Bus | DG Size MW | DG Bus | DG2 Size MW | DG Bus | DG Size MW | P loss (kW) | % Losses reduction |
|---|---|---|---|---|---|---|---|
| **10** | 1.50 | 25 | 0.86 | 32 | 1.05 | 87.43 | 58.6 |
| **8** | 2.15 | 25 | 1.60 | 31 | 2.10 | 89.02 | 57.9 |
| **9** | 1.47 | 24 | 2.20 | 32 | 1.50 | 91.04 | 56.9 |
| **8** | 2.16 | 25 | 2.18 | 33 | 1.07 | 94.00 | 55.5 |
| **9** | 2.15 | 25 | 2.00 | 31 | 2.01 | 94.09 | 55.4 |
| **10** | 1.55 | 29 | 0.95 | 32 | 1.21 | 96.51 | 54.3 |
| **9** | 1.50 | 24 | 2.05 | 30 | 0.66 | 97.80 | 53.7 |
| **12** | 2.15 | 25 | 1.75 | 32 | 2.21 | 99.00 | 53.1 |
| **11** | 1.40 | 25 | 1.80 | 32 | 2.05 | 99.89 | 52.7 |
| **8** | 2.05 | 29 | 0.95 | 33 | 1.07 | 102.50 | 51.5 |

The results of ten candidate buses with best fitness are given in Table 7.3 above. The optimal solution that minimizes the objective function was found at buses 10, 25 and 32, with sizes of the PVs at 1.50 MW, 0.863 MW and 1.05 MW respectively. Here, total real power losses were reduced to 87.43 kW from 211.2 kW. This indicates a reduction of about 58 6 % from the pre-installation case.

### 7.3.3.1 Bus Voltage Profile for PV DG using GA

Table 7.4 gives the voltage comparison for the case without a DG in the system and then with DGs optimally located at buses 10, 25 and 32 and sized (see Table 7.3) using GA. The voltage improves from 0.873 p.u. lowest voltage at bus 18 to 0.9480 p.u. at bus 32 as shown in Table 7.4 and Figure 7.6.

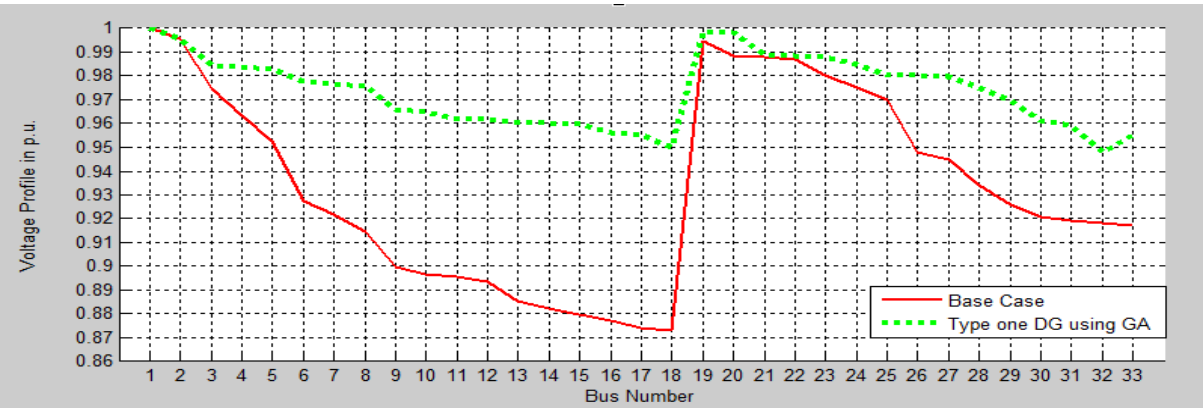


Figure 7.6: Voltage Profile for PV (type1) DG Using Genetic Algorithm

Table 7.4: Voltage Profile of PV DG Using Genetic Algorithm

| Bus No | Base Case | Voltage Profile with DG Type One | Bus No | Base Case | Voltage Profile with DG Type One | Bus No | Base Case | Voltage Profile with DG Type One |
|---|---|---|---|---|---|---|---|---|
| | Load Flow | GA | | Load flow | GA | | Load Flow | GA |
| **1** | 1 | 1 | 12 | 0.8936 | 0.9616 | 23 | 0.9800 | 0.9881 |
| **2** | 0.9955 | 0.9955 | 13 | 0.8852 | 0.9605 | 24 | 0.9750 | 0.9851 |
| **3** | 0.9744 | 0.9845 | 14 | 0.8821 | 0.9601 | 25 | 0.9700 | 0.9801 |
| **4** | 0.9635 | 0.9637 | 15 | 0.8797 | 0.9597 | 26 | 0.9480 | 0.9800 |
| **5** | 0.9528 | 0.9829 | 16 | 0.8774 | 0.9560 | 27 | 0.9450 | 0.9795 |
| **6** | 0.9272 | 0.9775 | 17 | 0.8740 | 0.9550 | 28 | 0.9340 | 0.9750 |
| **7** | 0.9217 | 0.9769 | 18 | 0.8730 | 0.9500 | 29 | 0.9260 | 0.9695 |
| **8** | 0.9145 | 0.9755 | 19 | 0.9947 | 0.9989 | 30 | 0.9210 | 0.9611 |
| **9** | 0.8999 | 0.9659 | 20 | 0.9887 | 0.9980 | 31 | 0.9190 | 0.9590 |
| **10** | 0.8969 | 0.9650 | 21 | 0.9878 | 0.9889 | 32 | 0.9180 | 0.9480 |
| **11** | 0.8957 | 0.9617 | 22 | 0.9867 | 0.9885 | 33 | 0.9170 | 0.9550 |

### 7.3.4 Result of Case 4, three units of wind DG using GA

The optimal solution that minimizes the objective function was found at buses 10, 18 and 32, with a real power output of 1.04 MW, 1.95 MW and 1.21 MW and a reactive output of 0.79 MVAR, 0.10 MVAR and 0.92 MVAR respectively. Here, total real power losses were reduced to 85.41 kW from 211.2 kW and reactive power losses also reduced to 39.06 kVAR from 101.1 kVAR. This indicates a reduction of about 59 % and 61 % respectively, from the pre-installation case as shown in Table 7.5.

Table 7.5: Best ten optimal solutions for installing three DGs of type two.

| DG Bus | DG Size | | DG Bus | DG2 Size | | DG3 Bus | DG3 Size | | $P_{loss}$ | | % Losses reduction | |
|---|---|---|---|---|---|---|---|---|---|---|---|---|
| | MW | MVar | | MW | MVar | | MW | MVar | (KW) | KVAR | KW | KVAR |
| **10** | 1.04 | 0.79 | 18 | 1.95 | 0.10 | 32 | 1.21 | 0.92 | 85.41 | 39.06 | 59 | 61 |
| **8** | 1.05 | 0.91 | 29 | 0.95 | 0.10 | 33 | 1.06 | 0.09 | 88.02 | 40.05 | 58 | 60 |
| **9** | 1.05 | 0.68 | 25 | 2.02 | 0.95 | 31 | 2.05 | 0.42 | 91.14 | 41.09 | 56 | 60 |
| **11** | 2.10 | 0.40 | 25 | 0.98 | 0.31 | 32 | 2.04 | 0.41 | 95.00 | 42.95 | 55 | 58 |
| **12** | 2.05 | 0.51 | 25 | 2.07 | 0.41 | 32 | 1.21 | 0.52 | 95.09 | 44.00 | 55 | 57 |
| **10** | 1.04 | 0.87 | 25 | 0.60 | 0.42 | 32 | 0.55 | 0.13 | 96.51 | 48.05 | 54 | 53 |
| **9** | 2.10 | 0.42 | 24 | 2.02 | 0.43 | 30 | 0.66 | 0.10 | 97.80 | 50.42 | 74 | 50 |
| **9** | 2.07 | 0.98 | 24 | 1.40 | 0.50 | 32 | 1.50 | 0.45 | 99.00 | 52.04 | 53 | 48 |
| **8** | 1.16 | 0.53 | 25 | 1.65 | 0.95 | 33 | 1.07 | 0.25 | 99.89 | 54.06 | 53 | 46 |
| **8** | 1.05 | 0.42 | 25 | 0.90 | 0.20 | 31 | 2.10 | 1.05 | 101.50 | 56.09 | 51 | 45 |

### 7.3.4.1 Bus Voltage Profile for PV and wind DG using GA

Table 7.6 gives the voltage comparison for the case without a DG in the system and then with DGs optimally located and sized using GA. The voltage level improved from 0.873 p.u. lowest voltage at bus 32 to 0.9480 p.u. for solar PV and 0.9505 p.u. for wind at bus 18 which is the weakest bus as shown in the Table 7.6 above. Figure 7.7 below also gives a graph for this comparison.

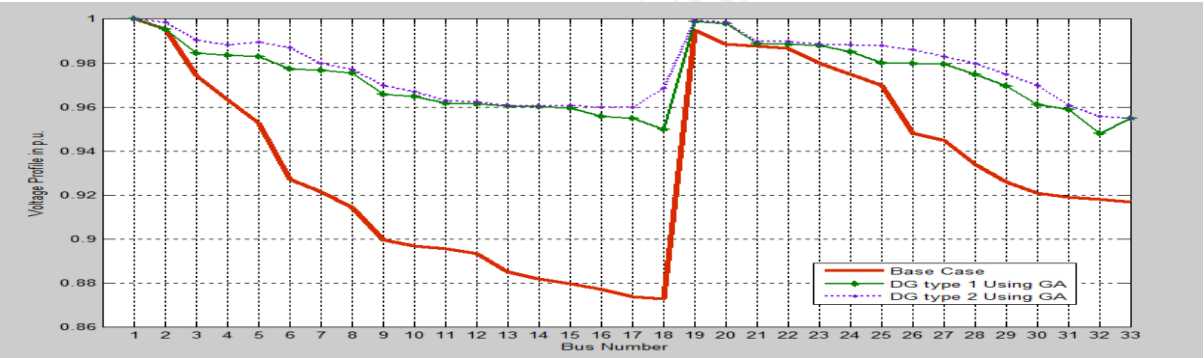


Figure 7.7: Voltage Profile for PV (type1) and Wind (type2) DG Using GA

Table 7.6: Voltage Profile for PV and wind DG using Genetic Algorithm

| Bus No | Base Case | Voltage Profile with DG Using GA | | Bus No | Base Case | Voltage Profile with DG Using GA | | Bus No | Base Case | Voltage Profile with DG Using GA | |
|---|---|---|---|---|---|---|---|---|---|---|---|
| | Load Flow | PV DG | Wind DG | | Load Flow | PV DG | Wind DG | | Load Flow | PV DG | Wind DG |
| **1** | 1 | 1 | 1 | 12 | 0.8936 | 0.9616 | 0.9625 | 23 | 0.9800 | 0.9881 | 0.9886 |
| **2** | 0.9955 | 0.9955 | 0.9985 | 13 | 0.8852 | 0.9605 | 0.9610 | 24 | 0.9750 | 0.9851 | 0.9859 |
| **3** | 0.9744 | 0.9845 | 0.9905 | 14 | 0.8821 | 0.9601 | 0.9606 | 25 | 0.9700 | 0.9801 | 0.9807 |
| **4** | 0.9635 | 0.9637 | 0.9884 | 15 | 0.8797 | 0.9597 | 0.9598 | 26 | 0.9480 | 0.9800 | 0.9806 |
| **5** | 0.9528 | 0.9829 | 0.9895 | 16 | 0.8774 | 0.9560 | 0.9565 | 27 | 0.9450 | 0.9795 | 0.9800 |
| **6** | 0.9272 | 0.9775 | 0.9872 | 17 | 0.8740 | 0.9550 | 0.9555 | 28 | 0.9340 | 0.9750 | 0.9775 |
| **7** | 0.9217 | 0.9769 | 0.9798 | 18 | 0.8730 | 0.9500 | 0.9505 | 29 | 0.9260 | 0.9695 | 0.9705 |
| **8** | 0.9145 | 0.9755 | 0.9771 | 19 | 0.9947 | 0.9989 | 0.9995 | 30 | 0.9210 | 0.9611 | 0.9616 |
| **9** | 0.8999 | 0.9659 | 0.9698 | 20 | 0.9887 | 0.9980 | 0.9985 | 31 | 0.9190 | 0.9590 | 0.9609 |
| **10** | 0.8969 | 0.9650 | 0.9698 | 21 | 0.9878 | 0.9889 | 0.9890 | 32 | 0.9180 | 0.9480 | 0.9559 |
| **11** | 0.8957 | 0.9617 | 0.9630 | 22 | 0.9867 | 0.9885 | 0.9888 | 33 | 0.9170 | 0.9550 | 0.9551 |

### 7.3.5 Placement and Sizing procedure Using GA-IPSO

System power flow and power loss sensitivity analysis was carried out for the base case. GA works on results from sensitivity analysis before giving its result to IPSO. IPSO takes GA results and optimizes them to get the solution of chromosome with the best fitness in the population as shown in Chapter 6 (Figure 6.1). The combined sensitivity factors (CSF) were analyzed for all the buses and the buses which gave a combined sensitivity factor of more than 0.8 and with the best fitness in the population were taken to be the candidate buses. Newton-Raphson load flow program was used to determine the power losses and voltage levels.

#### 7.3.5.1 Result of CSF for one solar PV and one wind DG Using GA-IPSO

CSF was done for each of the two types of DGs and the obtained results are as shown in Table 7.7 below.



Table 7.7: Results for CSF and fitness for candidate buses under peak load in 33-bus

| Candidate Bus | Sensitivity Factor | PV DG | | Wind DG | | |
|---|---|---|---|---|---|---|
| | | Fitness | DG Size (MW) | Fitness | DG Size (MW/MVAR) | |
| **10** | 0.8789 | 0.9176 | 2.500 | 0.9178 | 1.510 | 0.030 |
| **13** | 0.9236 | 0.9198 | 1.988 | 0.9198 | 0.988 | 0.060 |
| **15** | 0.8352 | 0.9165 | 1.863 | 0.9157 | 0.102 | 0.515 |
| **17** | 0.8733 | 0.9173 | 1.999 | 0.9167 | 0.120 | 0.056 |
| **18** | 1.022 | 0.9134 | 2.050 | 0.9125 | 2.087 | 0.083 |
| **19** | 1.0957 | 0.9118 | 0.710 | 0.9109 | 1.087 | 0.320 |
| **20** | 1.0637 | 0.9133 | 1.588 | 0.9125 | 2.073 | 0.009 |
| **21** | 0.9973 | 0.9128 | 1.994 | 0.9119 | 2.010 | 0.081 |
| **22** | 1.0558 | 0.9169 | 1.988 | 0.9163 | 2.128 | 0.059 |
| **23** | 0.9909 | 0.9129 | 2.081 | 0.9110 | 1.301 | 0.010 |
| **24** | 1.0349 | 0.9123 | 1.010 | 0.9112 | 1.301 | 1.010 |
| **25** | 0.8743 | 0.9175 | 1.523 | 0.9154 | 2.043 | 0.420 |
| **26** | 1.0064 | 0.9221 | 2.082 | 0.9198 | 2.076 | 1.011 |
| **32** | 0.8110 | 0.9091 | 1.504 | 0.9083 | 1.080 | 0.052 |

### 7.3.6 Result of Case 5, using three units of PV DG

The three selected optimal locations and their respective optimal DG sizes were as follows in order of effectiveness;

Bus number 19 with a DG size of 0.710 MW

Bus number 24 with a DG size of 1.010 MW

Bus number 32 with a DG size of 1.504 MW

In this case, total real power losses were reduced to 84.51 kW from 211.2 kW, which indicates a reduction of about 60 % from the pre-installation case as shown in Table 7.8.

Table 7.8: A comparison of results obtained using three units of PV DG

| Methodology | Bus Number | | DG Size | Power Loss | Power loss Reduction | % Power loss Reduction |
|---|---|---|---|---|---|---|
| | | | MW | kW | kW | kW |
| **Base Case** | | | - | 211.20 | - | - |
| **GA** | 10 | | 1.500 | 87.43 | 123.77 | 58.6 |
| | 25 | | 0.863 | | | |
| | 32 | | 1.050 | | | |
| **GA-IPSO** | 19 | | 0.710 | 84.51 | 126.96 | 60.00 |
| | 24 | | 1.010 | | | |
| | 32 | | 1.504 | | | |

### 7.3.6.1 Bus Voltage Profile for three units of PV DG using GA-IPSO

Table 7.9 shows the voltage comparison for the case without a DG in the system and that with DGs optimally located and sized using GA-IPSO. The voltage level improves from 0.873 p.u. lowest voltage to 0.9580 p.u. at bus 32. Figure 7.8 below also gives a graph of this comparison.

Table 7.9: Voltage Profile of PV DG Using GA-IPSO

| Bus No | Base Case | Voltage Profile with PV DG | Bus No | Base Case | Voltage Profile with PV DG | Bus No | Base Case | Voltage Profile with PV DG |
|---|---|---|---|---|---|---|---|---|
| | Load flow | GA-IPSO | | Load flow | GA-IPSO | | Load flow | GA-IPSO |
| **1** | 1 | 1 | 12 | 0.8936 | 0.9750 | 23 | 0.9800 | 0.9890 |
| **2** | 0.9955 | 0.9998 | 13 | 0.8852 | 0.9701 | 24 | 0.9750 | 0.9862 |
| **3** | 0.9744 | 0.9990 | 14 | 0.8821 | 0.9698 | 25 | 0.9700 | 0.9809 |
| **4** | 0.9635 | 0.9989 | 15 | 0.8797 | 0.9672 | 26 | 0.9480 | 0.9801 |
| **5** | 0.9528 | 0.9980 | 16 | 0.8774 | 0.9644 | 27 | 0.9450 | 0.9798 |
| **6** | 0.9272 | 0.9899 | 17 | 0.8740 | 0.9602 | 28 | 0.9340 | 0.9780 |
| **7** | 0.9217 | 0.9855 | 18 | 0.8730 | 0.9600 | 29 | 0.9260 | 0.9698 |
| **8** | 0.9145 | 0.9831 | 19 | 0.9947 | 0.9989 | 30 | 0.9210 | 0.9650 |
| **9** | 0.8999 | 0.9789 | 20 | 0.9887 | 0.9987 | 31 | 0.9190 | 0.9601 |
| **10** | 0.8969 | 0.9750 | 21 | 0.9878 | 0.9940 | 32 | 0.9180 | 0.9589 |
| **11** | 0.8957 | 0.9690 | 22 | 0.9867 | 0.9898 | 33 | 0.9170 | 0.9580 |

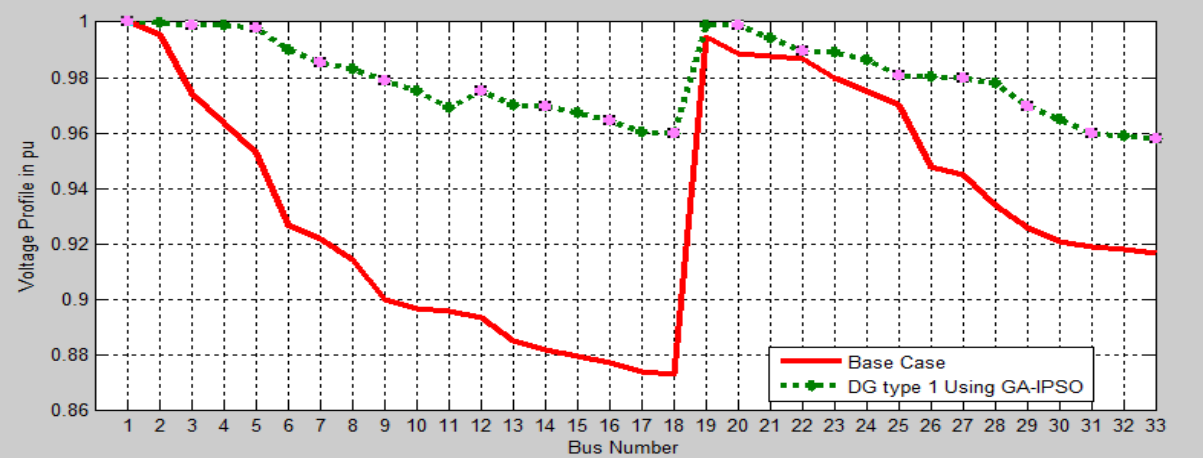


Figure 7.8: Voltage Profile of PV (type1) DG Using GA-IPSO

### 7.3.7 Result of Case 6, using three units of Wind DG

Similarly the three optimal locations for the wind DG and their respective optimal sizes were chosen using the respective columns for fitness and DG sizes in Table 7.7 above. The three selected optimal locations and their respective optimal DG sizes were as follows in order of effectiveness:

Bus number 19 with a DG generating 1.087 MW and 0.020 MVAR

Bus number 23 with a DG generating 1.301 MW and 1.010 MVAR

Bus number 32 with a DG generating 1.080 MW and 0.052 MVAR

The comparison of the results obtained for the power losses is given in Table 7.10 below. In this case, total real power losses were reduced to 83 kW from 211.2 kW and reactive power reduced to 36.72 kVAR from 101.1 kVAR, which indicates a reduction of about 61 % and 64 % from the pre-installation case respectively as shown in Table 7.10.

Table 7.10: A comparison of results obtained for Wind DG Using GA and GA-IPSO

| Methodology | Bus No | DG Size | | Power loss | | Power loss Reduction | | % Power loss Reduction | |
|---|---|---|---|---|---|---|---|---|---|
| | | MW | MVAR | kW | kVAR | kW | kVAR | kW | kVAR |
| **Base Case** | | - | - | 211.2 | 101.1 | - | - | - | - |
| **GA** | 10 | 0.96 | 0.73 | 85.41 | 39.06 | 125.79 | 62.04 | 59 | 61 |
| | 18 | 1.04 | 0.68 | | | | | | |
| | 31 | 1.07 | 0.73 | | | | | | |
| **GA-IPSO** | 19 | 1.087 | 0.320 | 83.00 | 36.72 | 128.20 | 64.38 | 61 | 64 |
| | 23 | 1.301 | 1.010 | | | | | | |
| | 32 | 1.080 | 0.052 | | | | | | |

### 7.3.7.1 Bus Voltage Profile for PV and Wind DG using GA-IPSO

A graph was plotted to facilitate this comparison as shown in Figure 7.9. With type two DG optimally located and sized at buses 19, 23, and 32 using GA-IPSO the voltage level improves from 0.873 p.u. to 0.9645 p.u. lowest voltage at bus 33 as shown in the Table 7.11 comparing voltage profile of both PV and wind with the base case.

Table 7.11: A comparison of Bus Voltages for PV and wind DG using GA-IPSO

| Bus No | Base Case V P | Voltage Profile with DG Using GA-PSO | | Bus No | Base Case | Voltage Profile with DG Using GA-PSO | | Bus No | Base Case | Voltage Profile with DG Using GA-PSO | |
|---|---|---|---|---|---|---|---|---|---|---|---|
| | Load flow | PV DG | Wind DG | | Load flow | PV DG | Wind DG | | Load flow | PV DG | Wind DG |
| **1** | 1 | 1 | 1 | **12** | 0.8936 | 0.9750 | 0.9770 | **23** | 0.9800 | 0.9890 | 0.9989 |
| **2** | 0.9955 | 0.9998 | 0.9999 | **13** | 0.8852 | 0.9701 | 0.9752 | **24** | 0.9750 | 0.9862 | 0.9901 |
| **3** | 0.9744 | 0.9990 | 0.9998 | **14** | 0.8821 | 0.9698 | 0.9735 | **25** | 0.9700 | 0.9809 | 0.9898 |
| **4** | 0.9635 | 0.9989 | 0.9992 | **15** | 0.8797 | 0.9672 | 0.9712 | **26** | 0.9480 | 0.9801 | 0.9872 |
| **5** | 0.9528 | 0.9980 | 0.9989 | **16** | 0.8774 | 0.9644 | 0.9709 | **27** | 0.9450 | 0.9798 | 0.9812 |
| **6** | 0.9272 | 0.9899 | 0.9970 | **17** | 0.8740 | 0.9602 | 0.9689 | **28** | 0.9340 | 0.9780 | 0.9780 |
| **7** | 0.9217 | 0.9855 | 0.9889 | **18** | 0.8730 | 0.9600 | 0.9689 | **29** | 0.9260 | 0.9698 | 0.9742 |
| **8** | 0.9145 | 0.9831 | 0.9864 | **19** | 0.9947 | 0.9989 | 0.9998 | **30** | 0.9210 | 0.9650 | 0.9705 |
| **9** | 0.8999 | 0.9789 | 0.9850 | **20** | 0.9887 | 0.9987 | 0.9995 | **31** | 0.9190 | 0.9601 | 0.9659 |
| **10** | 0.8969 | 0.9750 | 0.9813 | **21** | 0.9878 | 0.9840 | 0.9991 | **32** | 0.9180 | 0.9589 | 0.9651 |
| **11** | 0.8957 | 0.9690 | 0.9789 | **22** | 0.9867 | 0.9898 | 0.9990 | **33** | 0.9170 | 0.9580 | 0.9645 |

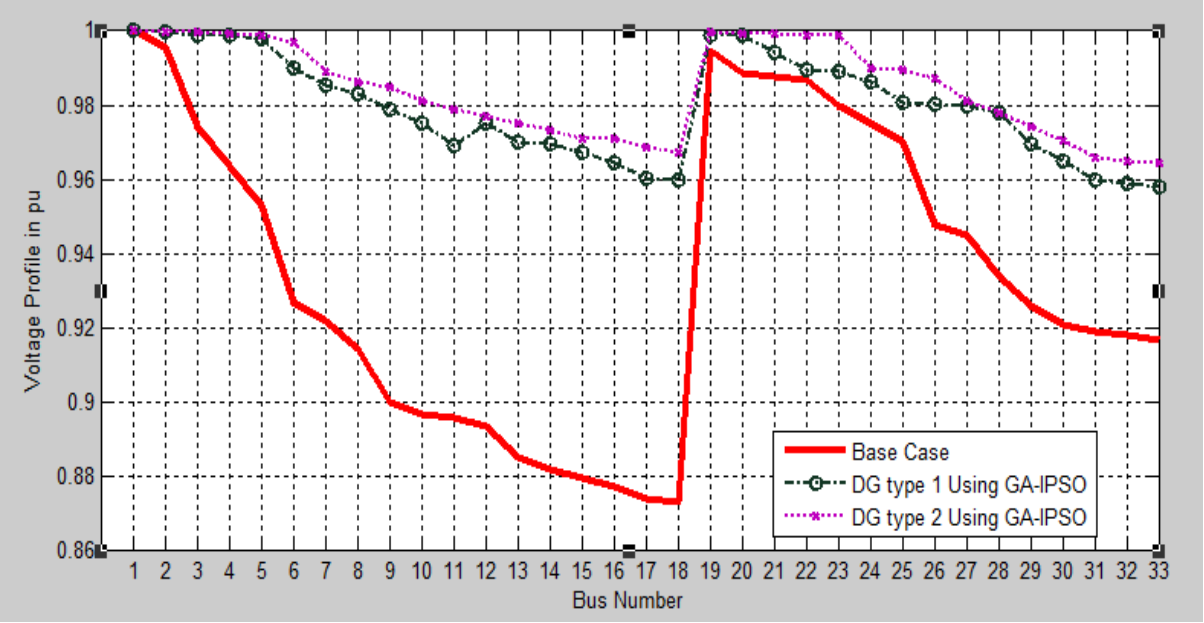


Figure 7.9: Voltage profile of PV (type1) and Wind (type2) DG Using GA-IPSO

## 7.4 Results of IEEE 33-bus under Base load condition

The results of two types of distributed generation (wind and PV) are given in the same chapter and the variation in their supply with the period under consideration. Also, results from GA-IPSO were compared with the GA optimization method and results presented. Finally, study cases are defined as:

Case 1: Three units of PV DG Using GA.

Case 2: Three units of Wind DG Using GA.

Case 3: Three units of PV DG Using GA-IPSO.

Case 4: Three units of Wind DG Using GA-IPSO.

### 7.4.1 Placement and Sizing for IEEE 33-bus system using Genetic Algorithm

Implementation of GA for this section is similar to steps used in the above, but the base load was used in this case considering the stochastic nature of DGs.

### 7.4.2 Result of Case 1, three units of PV DG (under base load) using GA.

The optimal solution that minimizes the objective function was found to be at buses 6, 20 and 31, with size of the DG being 0.80 MW, 0.63 MW and 0.60 MW respectively. Here, total real power losses were reduced to 69.24 kW from 211.2 kW from the results of ten candidate buses with best fitness given in Table 7.12. This indicates a reduction of about 67.2 % from the pre-installation case.

Table 7.12: Best ten optimal solutions for installing two units of PV DGs.

| DG1 Bus | DG Size MW | DG2 Bus | DG2 Size MW | DG 3 Bus | DG3 Size MW | P loss (kW) | % Losses reduction |
|---|---|---|---|---|---|---|---|
| **6** | 0.80 | **20** | 0.63 | **31** | 0.60 | 69.24 | 67.2 |
| **8** | 0.15 | **18** | 0.60 | **32** | 0.10 | 70.12 | 66.8 |
| **9** | 0.47 | **24** | 0.04 | **32** | 0.50 | 72.42 | 65.7 |
| **8** | 0.56 | **18** | 0.09 | **30** | 0.65 | 76.00 | 64.0 |
| **9** | 0.50 | **25** | 0.80 | **32** | 0.51 | 79.10 | 62.5 |
| **10** | 0.55 | **29** | 0.95 | **32** | 0.20 | 82.51 | 60.9 |
| **9** | 0.50 | **24** | 0.52 | **30** | 0.66 | 83.04 | 60.7 |
| **12** | 0.15 | **25** | 0.75 | **32** | 0.21 | 85.01 | 59.7 |
| **11** | 0.40 | **25** | 0.80 | **32** | 0.52 | 89.40 | 57.7 |
| **8** | 0.05 | **29** | 0.50 | **33** | 0.65 | 92.50 | 56.2 |

### 7.4.2.1 Bus Voltage Profile for PV DG under base load, using GA

Table 7.13 gives the voltage comparison for the case without a DG and with DGs optimally located and sized using GA. The lowest voltage level improves from 0.873 p.u. to 0.9509 p.u. at bus 18. Figure 7.10 below also gives a graph for this comparison.

Table 7.13: Voltage Profile of PV DG Using Genetic Algorithm

| Bus No | Base Case | Voltage Profile with DG Type One | Bus No | Base Case | Voltage Profile with DG Type One | Bus No | Base Case | Voltage Profile with DG Type One |
|---|---|---|---|---|---|---|---|---|
| | Load Flow | GA | | Load flow | GA | | Load Flow | GA |
| **1** | 1 | 1 | 12 | 0.8936 | 0.9620 | 23 | 0.9800 | 0.9888 |
| **2** | 0.9955 | 0.9956 | 13 | 0.8852 | 0.9608 | 24 | 0.9750 | 0.9889 |
| **3** | 0.9744 | 0.9846 | 14 | 0.8821 | 0.9605 | 25 | 0.9700 | 0.9884 |
| **4** | 0.9635 | 0.9840 | 15 | 0.8797 | 0.9599 | 26 | 0.9480 | 0.9880 |
| **5** | 0.9528 | 0.9830 | 16 | 0.8774 | 0.9569 | 27 | 0.9450 | 0.9799 |
| **6** | 0.9272 | 0.9777 | 17 | 0.8740 | 0.9553 | 28 | 0.9340 | 0.9750 |
| **7** | 0.9217 | 0.9770 | 18 | 0.8730 | 0.9509 | 29 | 0.9260 | 0.9721 |
| **8** | 0.9145 | 0.9760 | 19 | 0.9947 | 0.9989 | 30 | 0.9210 | 0.9698 |
| **9** | 0.8999 | 0.9659 | 20 | 0.9887 | 0.9989 | 31 | 0.9190 | 0.9640 |
| **10** | 0.8969 | 0.9655 | 21 | 0.9878 | 0.9898 | 32 | 0.9180 | 0.9580 |
| **11** | 0.8957 | 0.9625 | 22 | 0.9867 | 0.9893 | 33 | 0.9170 | 0.9550 |

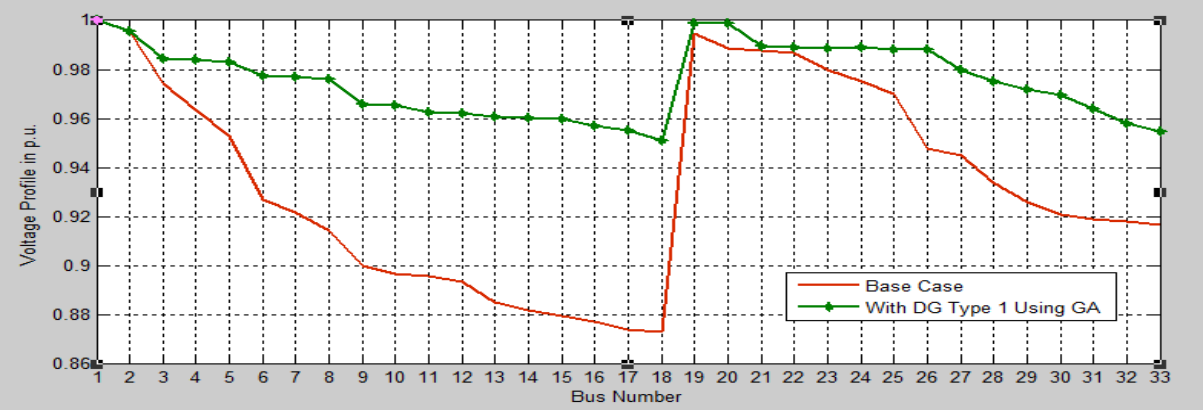


Figure 7.10: Voltage Profile for PV DG under base load, using GA

### 7.4.3 Result of Case 2, for three units of Wind DG (under base load) using GA

The optimal solution that minimizes the objective function was found at buses 10, 17 and 32, with a real power output of 0.74 MW, 0.65 MW and 0.25 MW and a reactive output of 0.09 MVAR, 0.01 MVAR and 0.09 MVAR respectively. Here, total real power losses were reduced to 50.43 kW and reactive power losses also reduce to 29.05 kVAR from the results of ten candidate buses with best fitness tabulated in Table 7.14. This indicates a reduction of about 76 % and 71 % from the pre-installation case as shown in Table 7.14 below.

Table 7.14: Best ten optimal solutions for installing three units of wind DGs

| DG Bus | DG Size | | DG Bus | DG2 Size | | DG3 Bus | DG3 Size | | $P_{loss}$ | | % Losses reduction | |
|---|---|---|---|---|---|---|---|---|---|---|---|---|
| | MW | MVAR | | MW | MVAR | | MW | MVAR | kW | kVAR | kW | kVAR |
| **10** | 0.74 | 0.09 | **17** | 0.65 | 0.01 | **32** | 0.25 | 0.09 | 50.43 | 29.05 | 76 | 71 |
| **10** | 0.60 | 0.08 | **24** | 0.72 | 0.05 | **29** | 0.80 | 0.02 | 52.90 | 30.42 | 75 | 69 |
| **8** | 0.80 | 0.01 | **29** | 0.59 | 0.10 | **33** | 0.60 | 0.09 | 55.02 | 30.09 | 73 | 69 |
| **10** | 0.50 | 0.04 | **25** | 0.60 | 0.02 | **32** | 0.71 | 0.04 | 56.02 | 33.04 | 73 | 67 |
| **12** | 0.45 | 0.01 | **25** | 0.77 | 0.41 | **32** | 0.21 | 0.05 | 56.94 | 34.06 | 73 | 66 |
| **7** | 0.64 | 0.07 | **25** | 0.60 | 0.02 | **32** | 0.50 | 0.03 | 61.04 | 40.71 | 71 | 60 |
| **9** | 0.35 | 0.06 | **24** | 0.52 | 0.03 | **30** | 0.66 | 0.01 | 62.90 | 41.90 | 70 | 59 |
| **9** | 0.50 | 0.04 | **20** | 0.70 | 0.02 | **30** | 0.80 | 0.05 | 64.05 | 44.80 | 69 | 56 |
| **9** | 0.59 | 0.09 | **25** | 0.41 | 0.04 | **33** | 0.50 | 0.04 | 94.90 | 46.00 | 55 | 58 |
| **8** | 0.60 | 0.03 | **21** | 0.65 | 0.05 | **30** | 0.70 | 0.02 | 96.07 | 51.53 | 55 | 50 |

### 7.4.3.1 Bus Voltage Profile using Wind and PV DG (under base load) using GA

The voltage profile of case without DG, PV and wind DG was compared in Table 7.15. The lowest voltage level improves from 0.873p.u to 0.9505p.u for type one (PV) and to 0.9548p.u for type two (wind) at bus 18 as shown in Figure 7.11.

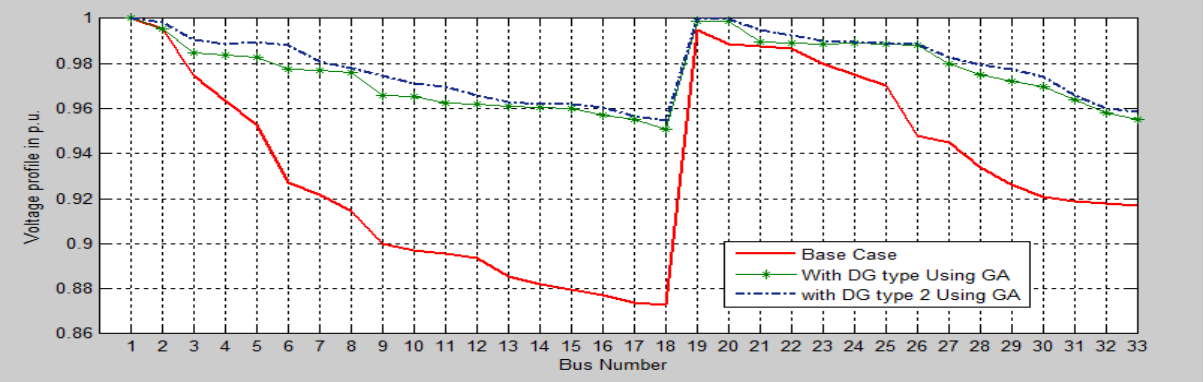


Figure 7.11: Voltage Profile for PV and Wind DG under base load, using GA.

Table 7.15: Voltage Profile for three units PV and wind DG under base load using GA

| Bus No | Base Case | Voltage Profile with DG Using GA | | Bus No | Base Case | Voltage Profile with DG Using GA | | Bus No | Base Case | Voltage Profile with DG Using GA | |
|---|---|---|---|---|---|---|---|---|---|---|---|
| | Load Flow | PV DG | Wind DG | | Load flow | PV DG | Wind DG | | Load Flow | PV DG | Wind DG |
| **1** | 1 | 1 | 1 | **12** | 0.8936 | 0.9620 | 0.9659 | **23** | 0.9800 | 0.9888 | 0.9901 |
| **2** | 0.9955 | 0.9956 | 0.9985 | **13** | 0.8852 | 0.9608 | 0.9630 | **24** | 0.9750 | 0.9889 | 0.9898 |
| **3** | 0.9744 | 0.9846 | 0.9905 | **14** | 0.8821 | 0.9605 | 0.9620 | **25** | 0.9700 | 0.9884 | 0.9889 |
| **4** | 0.9635 | 0.9840 | 0.9885 | **15** | 0.8797 | 0.9599 | 0.9618 | **26** | 0.9480 | 0.9880 | 0.9888 |
| **5** | 0.9528 | 0.9830 | 0.9897 | **16** | 0.8774 | 0.9569 | 0.9603 | **27** | 0.9450 | 0.9799 | 0.9830 |
| **6** | 0.9272 | 0.9777 | 0.9881 | **17** | 0.8740 | 0.9553 | 0.9567 | **28** | 0.9340 | 0.9750 | 0.9795 |
| **7** | 0.9217 | 0.9770 | 0.9808 | **18** | 0.8730 | 0.9509 | 0.9548 | **29** | 0.9260 | 0.9721 | 0.9775 |
| **8** | 0.9145 | 0.9760 | 0.9778 | **19** | 0.9947 | 0.9989 | 0.9998 | **30** | 0.9210 | 0.9698 | 0.9765 |
| **9** | 0.8999 | 0.9659 | 0.9744 | **20** | 0.9887 | 0.9989 | 0.9996 | **31** | 0.9190 | 0.9640 | 0.9660 |
| **10** | 0.8969 | 0.9655 | 0.9710 | **21** | 0.9878 | 0.9898 | 0.9899 | **32** | 0.9180 | 0.9580 | 0.9598 |
| **11** | 0.8957 | 0.9625 | 0.9698 | **22** | 0.9867 | 0.9893 | 0.9892 | **33** | 0.9170 | 0.9550 | 0.9586 |

### 7.4.4 Result for all Candidate Buses using GA-IPSO under base load condition

The combined sensitivity factors were analyzed for all the buses and the buses which gave a combined sensitivity factor of more than 0.8 were taken to be the candidate buses. So as to be able to choose the optimal location(s) of the DG(s) and their respective optimal sizes, results were obtained taking into consideration all the candidate buses. This was done for each of the two types of DG and the obtained results tabulated as shown in Table 7.16.

Table 7.16: Results for CSF and fitness for candidate buses under base load in 33-bus

| Candidate Bus | Sensitivity Factor | | PV DG Size | | Wind DG Size | |
|---|---|---|---|---|---|---|
| | | Fitness | MW | Fitness | MW | MVAR |
| **10** | 0.8789 | 0.9176 | 0.750 | 0.9178 | 0.510 | 0.030 |
| **13** | 0.9236 | 0.9198 | 0.800 | 0.9198 | 0.488 | 0.060 |
| **15** | 0.8352 | 0.9165 | 0.763 | 0.9157 | 0.402 | 0.015 |
| **17** | 0.8733 | 0.9173 | 0.699 | 0.9167 | 0.120 | 0.056 |
| **18** | 1.022 | 0.9004 | 0.650 | 0.9125 | 0.507 | 0.030 |
| **19** | 1.0957 | 0.9118 | 0.710 | 0.9109 | 0.787 | 0.920 |
| **20** | 1.0637 | 0.9133 | 0.588 | 0.9125 | 0.773 | 0.009 |
| **21** | 0.9973 | 0.9128 | 0.794 | 0.9119 | 0.410 | 0.081 |
| **22** | 1.0558 | 0.9169 | 0.388 | 0.9163 | 0.428 | 0.059 |
| **23** | 0.9909 | 0.9129 | 0.810 | 0.9110 | 0.301 | 0.010 |
| **24** | 1.0349 | 0.9123 | 0.501 | 0.9112 | 0.501 | 0.010 |
| **25** | 0.8743 | 0.9175 | 0.523 | 0.9154 | 0.043 | 0.020 |
| **26** | 1.0064 | 0.9221 | 0.820 | 0.9198 | 0.676 | 0.001 |
| **32** | 0.8110 | 0.9091 | 0.804 | 0.9083 | 0.707 | 0.002 |

### 7.4.5 Result of Case 3, three units of PV DG (under base load) using GA-IPSO.

In the table 7.16, the two columns for fitness and DG size under type one DG were used to facilitate the allocation of type two DG in this case. This was done by selecting those locations which had the minimum fitness values and their respective DG sizes. The three selected optimal locations and their respective optimal DG sizes were as follows in order of effectiveness:

- Bus number 18 with a DG size of 0.650 MW
- Bus number 24 with a DG size of 0.501 MW
- Bus number 32 with a DG size of 0.804 MW

With the chosen three DG sizes and locations a load flow study was done using Newton-Raphson method so as to determine the associated power losses and voltage levels. The results obtained for the power losses were compared to results from GA approach. The comparison is

given in the Table 7.17. The percentage real power loss reduction for GA-IPSO was 70.6 % compared to 67.2 % for the GA.

Table 7.17: Results comparison for PV DG using GA and GA-IPSO under base load

| Methodology | Bus Number | DG Size | Power Loss | Power loss Reduction | % Powe loss Reduction |
|---|---|---|---|---|---|
| | | MW | kW | kW | kW |
| **Base Case** | | - | 211.20 | - | - |
| **GA** | 6 | 0.80 | 69.24 | 141.96 | 67.2 |
| | 20 | 0.63 | | | |
| | 31 | 0.60 | | | |
| **GA-IPSO** | 18 | 0.650 | 62.06 | 149.14 | 70.6 |
| | 24 | 0.501 | | | |
| | 32 | 0.804 | | | |

### 7.4.5.1 Bus Voltage Profile for PV DG under base load, using GA-IPSO

The voltage profile of the IEEE 33-bus system in Table 7.18 gives the voltage comparison for the case without a DG in the system and with PV DG optimally located and sized using GA-IPSO. The lowest voltage level improves from 0.8730 p.u. at bus 18 to 0.9842 p.u. at bus 33 as shown in Table 7.18. Figure 7.12 also gives a graph for this comparison.

Table 7.18: Voltage Profile of PV DG using GA-IPSO under base load

| Bus No | Base Case | Voltage Profile with DG Type one | Bus No | Base Case | Voltage Profile with DG Type one | Bus No | Base Case | Voltage Profile with DG Type one |
|---|---|---|---|---|---|---|---|---|
| | Load flow | GA-IPSO | | Load flow | GA-IPSO | | Load flow | GA-IPSO |
| **1** | 1 | 1 | 12 | 0.8936 | 0.9954 | 23 | 0.9800 | 0.9974 |
| **2** | 0.9955 | 0.9999 | 13 | 0.8852 | 0.9900 | 24 | 0.9750 | 0.9975 |
| **3** | 0.9744 | 0.9999 | 14 | 0.8821 | 0.9890 | 25 | 0.9700 | 0.9969 |
| **4** | 0.9635 | 0.9998 | 15 | 0.8797 | 0.9870 | 26 | 0.9480 | 0.9961 |
| **5** | 0.9528 | 0.9996 | 16 | 0.8774 | 0.9843 | 27 | 0.9450 | 0.9921 |
| **6** | 0.9272 | 0.9993 | 17 | 0.8740 | 0.9962 | 28 | 0.9340 | 0.9898 |
| **7** | 0.9217 | 0.9990 | 18 | 0.8730 | 0.9998 | 29 | 0.9260 | 0.9852 |
| **8** | 0.9145 | 0.9989 | 19 | 0.9947 | 1.0009 | 30 | 0.9210 | 0.9834 |
| **9** | 0.8999 | 0.9996 | 20 | 0.9887 | 1.0006 | 31 | 0.9190 | 0.9864 |
| **10** | 0.8969 | 0.9992 | 21 | 0.9878 | 0.9998 | 32 | 0.9180 | 0.9857 |
| **11** | 0.8957 | 0.9979 | 22 | 0.9867 | 0.9989 | 33 | 0.9170 | 0.9842 |

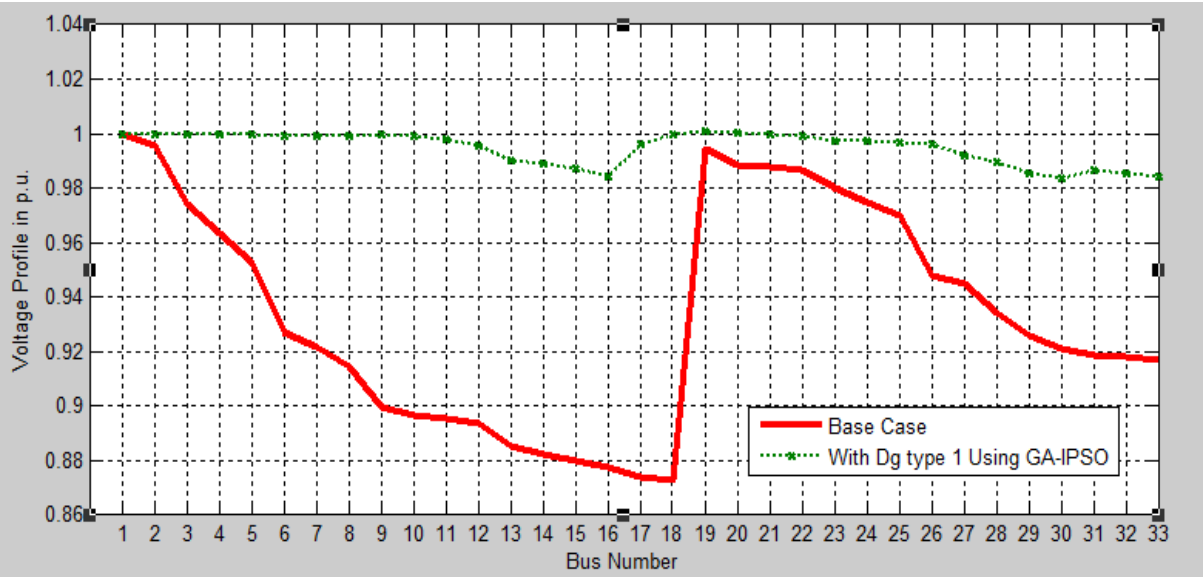

Figure 7.12: Voltage Profile for PV DG under base load, using GA-IPSO

### 7.4.6 Result of Case 4, three units of wind DG using GA-IPSO under base load

The locations which gave the minimum fitness values and their respective DG sizes were selected from Table 7.16 as follows;

1. Bus number 18 with a DG generating 0.507 MW and 0.030 MVAR
2. Bus number 23 with a DG generating 0.301 MW and 0.010 MVAR
3. Bus number 32 with a DG generating 0.707 MW and 0.002 MVAR

The chosen three DG gives a real power loss reduction of 44.60 kW and 24.62 kVAR after Newton-Raphson load flow. These result indicate a 79% real power loss reduction and 75 % reactive power loss reduction as shown in Table 7.19 below.

Table 7.19: Results comparison for wind DG using GA and GA-IPSO under base load

| Methodology | Bus No | DG Size | | Power loss | | Power loss Reduction | | % Power loss Reduction | |
|---|---|---|---|---|---|---|---|---|---|
| | | MW | MVAR | kW | kVAR | kW | kVAR | kW | kVAR |
| **Base Case** | | - | - | 211.2 | 101.1 | - | - | - | - |
| **GA** | 10 | 0.740 | 0.09 | 50.43 | 29.05 | 160.8 | 72.05 | 76 | 71 |
| | 17 | 0.650 | 0.01 | | | | | | |
| | 32 | 0.250 | 0.09 | | | | | | |
| **GA-IPSO** | 18 | 0.507 | 0.030 | 44.60 | 24.62 | 166.6 | 76.48 | 79 | 75 |
| | 23 | 0.301 | 0.010 | | | | | | |
| | 32 | 0.707 | 0.002 | | | | | | |

Table 7.20: Voltage Profile of wind DG using GA-IPSO under base load

| Bus No | Base Case | Voltage Profile with DG Using GA-PSO | | Bus No | Base Case | Voltage Profile with DG Using GA-PSO | | Bus No | Base Case | Voltage Profile with DG Using GA-PSO | |
|---|---|---|---|---|---|---|---|---|---|---|---|
| | Load Flow | DG Type 1 | DG Type 2 | | Load flow | DG Type 1 | DG Type 2 | | Load Flow | DG Type 1 | DG Type 2 |
| **1** | 1 | 1 | 1 | **12** | 0.8936 | 0.9954 | 0.9998 | **23** | 0.9800 | 0.9974 | 1.0003 |
| **2** | 0.9955 | 0.9999 | 0.9999 | **13** | 0.8852 | 0.9900 | 0.9989 | **24** | 0.9750 | 0.9975 | 1.0001 |
| **3** | 0.9744 | 0.9999 | 0.9999 | **14** | 0.8821 | 0.9890 | 0.9987 | **25** | 0.9700 | 0.9969 | 1.0000 |
| **4** | 0.9635 | 0.9998 | 1.0002 | **15** | 0.8797 | 0.9870 | 0.9986 | **26** | 0.9480 | 0.9961 | 0.9999 |
| **5** | 0.9528 | 0.9996 | 1.0003 | **16** | 0.8774 | 0.9843 | 0.9984 | **27** | 0.9450 | 0.9921 | 0.9989 |
| **6** | 0.9272 | 0.9993 | 1.0004 | **17** | 0.8740 | 0.9962 | 0.9982 | **28** | 0.9340 | 0.9898 | 0.9984 |
| **7** | 0.9217 | 0.9990 | 1.0003 | **18** | 0.8730 | 0.9998 | 0.9999 | **29** | 0.9260 | 0.9852 | 0.9979 |
| **8** | 0.9145 | 0.9989 | 1.0002 | **19** | 0.9947 | 1.0009 | 1.0001 | **30** | 0.9210 | 0.9834 | 0.9973 |
| **9** | 0.8999 | 0.9996 | 1.0001 | **20** | 0.9887 | 1.0006 | 1.0002 | **31** | 0.9190 | 0.9864 | 0.9965 |
| **10** | 0.8969 | 0.9992 | 0.9999 | **21** | 0.9878 | 0.9998 | 1.0003 | **32** | 0.9180 | 0.9857 | 0.9899 |
| **11** | 0.8957 | 0.9979 | 0.9999 | **22** | 0.9867 | 0.9989 | 1.0004 | **33** | 0.9170 | 0.9842 | 0.9856 |

### 7.4.6.1 Bus Voltage Profile for PV and wind DG using GA-IPSO under base load

Figure 7.13 was plotted to show this comparison of DG type one and type two using GA-IPSO. The lowest voltage level improves from 0.873 p.u. to 0.9834 p.u. for PV (type1) and 0.9856 p.u. for wind (type2) as shown in the Table 7.20.

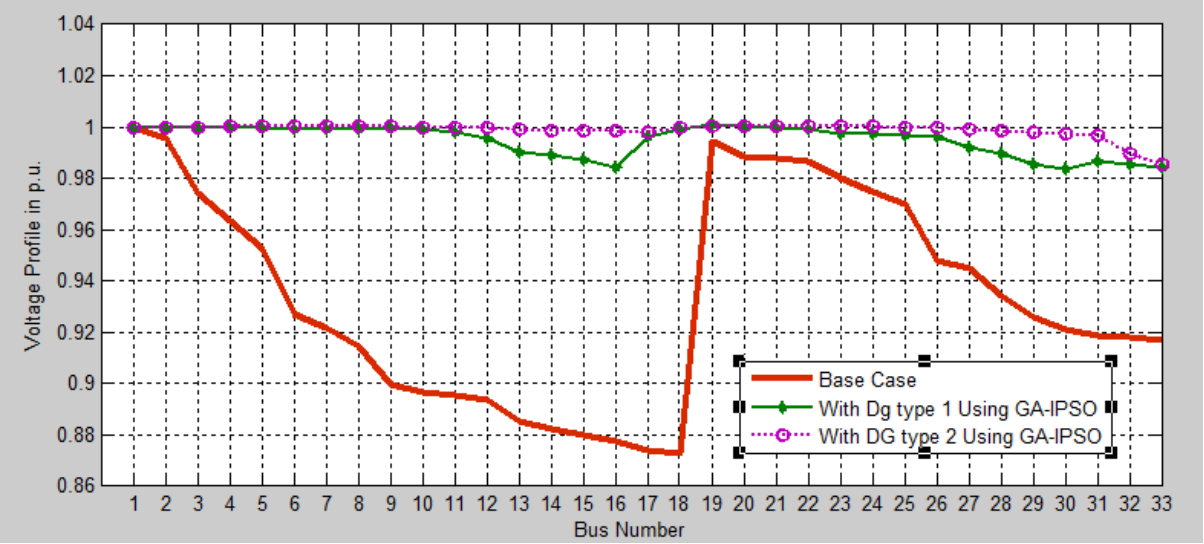


Figure 7.13: Voltage Profile for PV and Wind DG under base load, using GA-IPSO

## 7.5 Section 2: Results using Western Cape real network under peak loading

In this section, the results of optimal allocation two types of distributed generation (wind and PV) in Western Cape real network is given in this section considering the stochastic nature of their supply. The peak load within a period of 24-hours as presented in chapter 4,

Figure 4.1 were used. Also, results from GA-IPSO compared with the GA optimization method are presented. Finally, study cases are defined as:

Case 1: Two units of PV DG Using GA.

Case 2: Two units of Wind DG Using GA.

Case 3: Two units of PV DG Using GA-IPSO.

Case 4: Two units of Wind DG Using GA-IPSO.

### 7.5.1 Placement and Sizing procedure Using GA for the real network

The optimal DG sizing and placement for integrating two units DG was investigated using GA implementation in Chapter 5 as well as the network parameters in Chapter 6 to obtain the optimized solution of chromosome with the best fitness in the population. With the chosen two DG candidate bus and sizes, a load flow study was done using Newton-Raphson method so as to determine the associated power losses and voltage levels.

### 7.5.2 Result of Case 1, two units of PV (type 1) DG Using GA.

The optimal solution that minimizes the objective function was found at buses 18 and 9, with a real power output of 1.35 MW and 0.59 MW respectively. Here, total real power losses were reduced to 82 kW from 180 kW. This indicates a reduction of about 54.4 % from the base case as shown in Table 7.21 below.

Table 7.21: Best five optimal solutions for installing two units of PV DG

| S/N | DG Bus | DG Size MW | DG Bus | DG Size MW | Power loss in kW | % Losses reduction |
|---|---|---|---|---|---|---|
| **Base Case** | - | - | - | | 180 | kW |
| 1 | 18 | 1.35 | 9 | 0.59 | 82 | 54.4 |
| 2 | 12 | 0.39 | 15 | 0.46 | 87 | 51.7 |
| 3 | 16 | 0.25 | 12 | 0.75 | 89 | 50.5 |
| 4 | 18 | 0.95 | 12 | 0.35 | 91 | 49.4 |
| 5 | 16 | 0.75 | 12 | 0.65 | 94 | 47.7 |

#### 7.5.2.1 Bus Voltage Profile for two units of PV (type 1) DG using GA

The voltage level of the weakest bus improves from 0.890 p.u. voltage to 0.947 p.u. as shown in the Table 7.22. Figure 7.14 also gives a graphical representation of this and buses 6,7,8,9 and 10 are still out of limit of $\pm 5\%$.

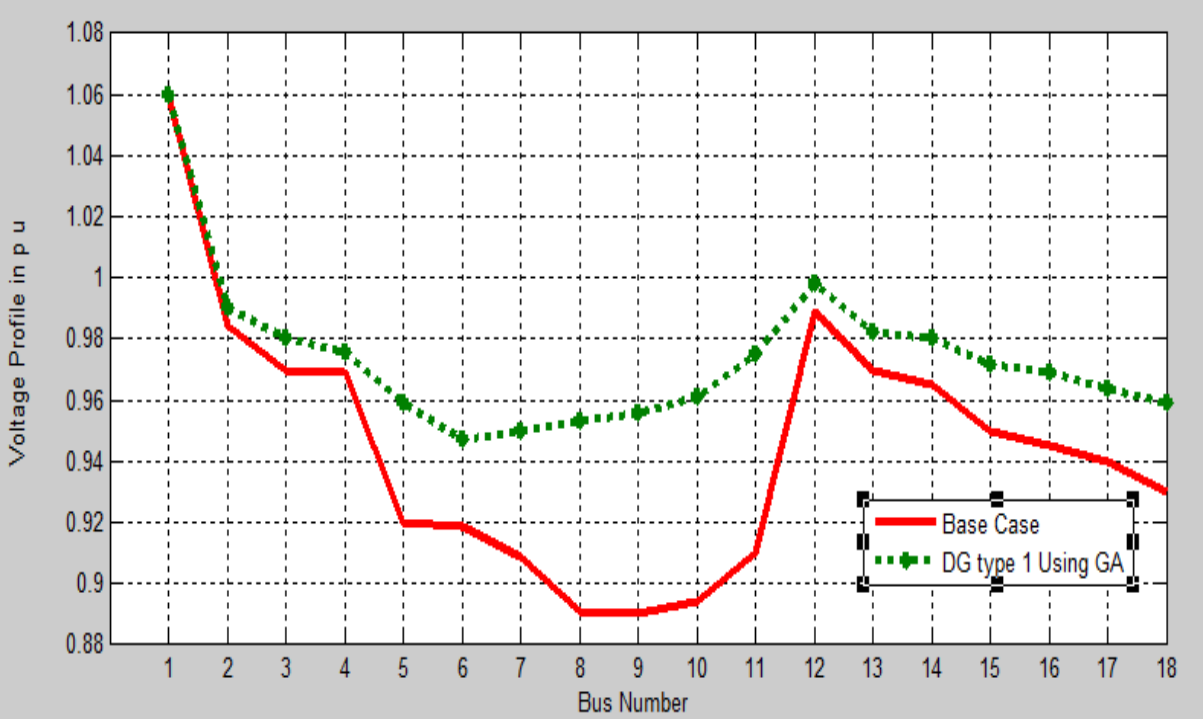


Figure 7.14: Voltage Profile of PV (type 1) DG Using G

Table 7.22: Voltage Profile for PV DG Using Genetic Algorithm

| Bus No | Base Case | Voltage Profile in p u with GA | Bus No | Base Case | Voltage Profile in p u with Using GA |
|---|---|---|---|---|---|
| | Load Flow | PV DG | | Load Flow | PV DG |
| **1** | 1.060 | 1.060 | 10 | 0.894 | 0.961 |
| **2** | 0.984 | 0.990 | 11 | 0.910 | 0.975 |
| **3** | 0.970 | 0.980 | 12 | 0.989 | 0.998 |
| **4** | 0.969 | 0.976 | 13 | 0.970 | 0.982 |
| **5** | 0.920 | 0.959 | 14 | 0.965 | 0.980 |
| **6** | 0.919 | 0.947 | 15 | 0.950 | 0.972 |
| **7** | 0.909 | 0.950 | 16 | 0.945 | 0.969 |
| **8** | 0.891 | 0.953 | 17 | 0.940 | 0.964 |
| **9** | 0.890 | 0.956 | 18 | 0.930 | 0.959 |

### 7.5.3 Result of Case 2, two units of wind (type 2) DG Using GA.

The optimal solution that minimizes the objective function was found at buses 18 and 12, with a real power output of 0.901 MW and 1.350 MW and reactive power output of 0.210 MVAR and 0.507 MVAR respectively. Here, the total active and reactive power losses were reduced to 85 kW from 180 kW and 27 kVAR from 40 kVAR. This indicates a reduction of about 52 % and 33 % from the pre-installation case as shown in the Table 7.23 below.

Table 7.23: Best five optimal solutions for installing two units of wind DG

| S/N | DG Bus | DG Size | | DG Bus | DG Size | | Power loss in | | % Losses reduction | |
|---|---|---|---|---|---|---|---|---|---|---|
| | | MW | MVAR | | MW | MVAR | kW | kVAR | kW | kVAR |
| **Base Case** | - | - | | - | - | - | 180 | 40 | - | - |
| **1** | 18 | 0.901 | 0.210 | 12 | 1.350 | 0.507 | 85 | 27 | 52 | 33 |
| **2** | 12 | 0.590 | 0.301 | 15 | 0.460 | 0.300 | 87 | 27 | 53 | 33 |
| **3** | 18 | 1.050 | 0.402 | 9 | 0.509 | 0.110 | 89 | 30 | 51 | 25 |
| **4** | 16 | 1.101 | 0.201 | 12 | 0.805 | 0.110 | 91 | 32 | 49 | 20 |
| **5** | 16 | 1.205 | 0.203 | 12 | 1.050 | 0.201 | 94 | 35 | 48 | 13 |

### 7.5.3.1 Bus Voltage Profile for two units of wind (type 2) DG using GA

The voltage profile of the system was checked for voltage deviation outside the limits. Table 7.24 gives the voltage comparison for the case without a DG in the system and then with DGs optimally located and sized using GA. The lowest voltage level increase from 0.890 p.u. lowest voltage to 0.950 p.u. as shown in the Table 7.24. Figure 7.15 also gives a graph for this comparison.

Table 7.24: Voltage Profile comparison for PV and wind DG Using GA

| Bus No | Base Case | Voltage Profile in p u with PV DG | Voltage Profile in p u with PV DG | Bus No | Base Case | Voltage Profile in p u with PV DG | Voltage Profile in p u with PV DG |
|---|---|---|---|---|---|---|---|
| | Load Flow | Using GA | Using GA | | Load Flow | Using GA | Using GA |
| **1** | 1.060 | 1.060 | 1.060 | 10 | 0.894 | 0.961 | 0.968 |
| **2** | 0.984 | 0.990 | 0.994 | 11 | 0.910 | 0.975 | 0.974 |
| **3** | 0.970 | 0.980 | 0.981 | 12 | 0.989 | 0.998 | 0.998 |
| **4** | 0.969 | 0.976 | 0.979 | 13 | 0.970 | 0.982 | 0.985 |
| **5** | 0.920 | 0.959 | 0.962 | 14 | 0.965 | 0.980 | 0.984 |
| **6** | 0.919 | 0.947 | 0.950 | 15 | 0.950 | 0.972 | 0.974 |
| **7** | 0.909 | 0.950 | 0.954 | 16 | 0.945 | 0.969 | 0.970 |
| **8** | 0.891 | 0.953 | 0.956 | 17 | 0.940 | 0.964 | 0.968 |
| **9** | 0.890 | 0.956 | 0.959 | 18 | 0.930 | 0.959 | 0.960 |

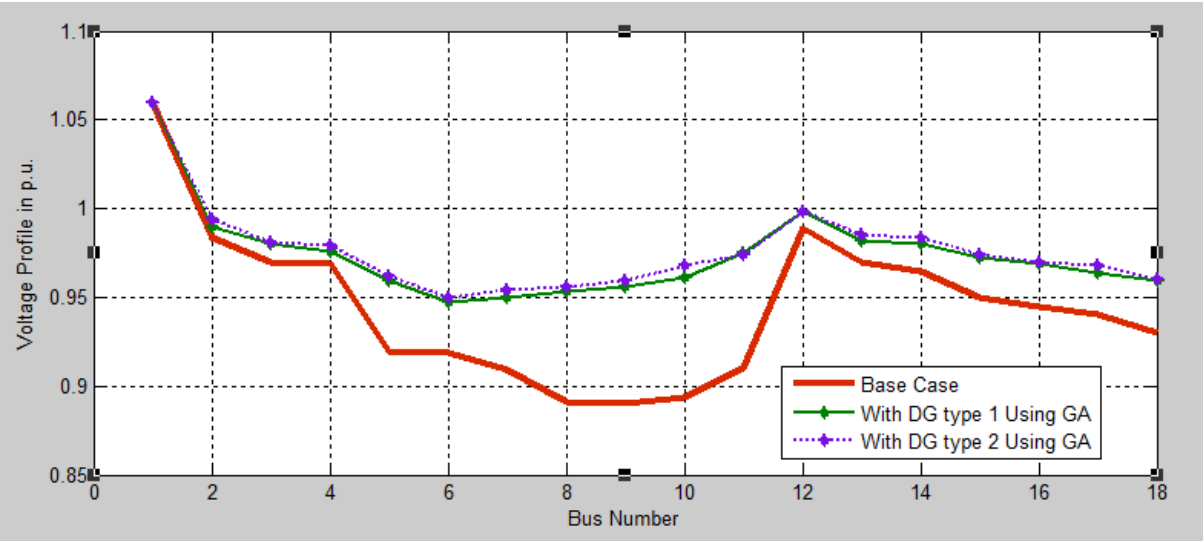


Figure 7.15: Voltage Profile for PV (type1) and Wind (type2) DG Using GA

### 7.5.4 Result for all Candidate Buses Using GA-IPSO

System power flow and power loss sensitivity analysis was carried out for the base case. GA works on result from sensitivity analysis before giving its results to IPSO. IPSO takes GA results and optimizes them to get the solution of chromosome with the best fitness in the population as shown in Chapter 6 (Figure 6.1). The combined sensitivity factors were analyzed for all the buses and the buses which gave a combined sensitivity factor of more than 0.8 and with the best fitness in the population were taken to be the candidate buses. Newton-Raphson load flow program was used to determine the power losses and voltage levels.

#### 7.5.4.1 Results of CSF for PV and wind DG Using

This was done for each of the two types of DG and the obtained results are shown in Table 7.25.

Table 7.25: Results for CSF and fitness for candidate buses under peak load in real network

| Candidate Bus | Sensitivity Factor | PV DG | | Wind DG | | |
|---|---|---|---|---|---|---|
| | | Fitness | DG Size MW | Fitness | DG Size | |
| | | | | | MW | MVAR |
| 3 | 0.8491 | 0.9199 | 1.050 | 0.9198 | 1.030 | 0.420 |
| 9 | 0.8789 | 0.9176 | 1.500 | 0.9178 | 1.010 | 0.190 |
| 12 | 0.9236 | 0.9198 | 0.988 | 0.9198 | 0.988 | 0.160 |
| 15 | 0.8352 | 0.9165 | 0.863 | 0.9157 | 0.502 | 0.115 |
| 16 | 0.8733 | 0.9173 | 1.099 | 0.9167 | 1.120 | 0.456 |
| 18 | 1.022 | 0.9134 | 1.250 | 0.9125 | 1.087 | 0.183 |

### 7.5.5 Result of Case 3, for two units of PV (type 1) DG Using GA-IPSO

The choice of the two optimal locations for the DGs of type one and their respective optimal sizes was done using Tables 7.25 above. In Table 7.25 the two columns for fitness and DG size under type 1 DG were used to facilitate this. This was done by selecting those locations which had the minimum fitness values. The two selected optimal locations and their respective optimal DG sizes were as follows in order of effectiveness;

Bus number 9 with a DG size of 0.710 MW

Bus number 16 with a DG size of 1.099 MW

Load flow study was done using Newton-Raphson method so as to determine the associated power losses and voltage levels. The results obtained for the power losses were compared to the results from GA approach. The comparison of the results in this case and GA approach is given in table 7.26.

Table 7.26: A comparison of results obtained using PV DG

| Methodology | Bus Number | DG Size | Power Loss | Power loss reduction | % loss Reduction |
|---|---|---|---|---|---|
| | | MW | kW | kW | kW |
| **Base Case** | | - | 180 | 180 | - |
| **GA** | 9<br>18 | 0.590<br>1.350 | 82 | 98 | 54.4 |
| **GA-IPSO** | 9<br>16 | 0.710<br>1.099 | 79 | 101 | 56.1 |

#### 7.5.5.1 Bus Voltage Profile PV DG Using GA-IPSO

The lowest voltage level improves from 0.890 p.u to 0.959 p.u as shown in the Table 7.27. Figure 7.16 also gives a graph for this comparison with the base case.

Table 7.27: Voltage Profile for PV DG Using GA-IPSO

| Bus No | Base Case | Voltage Profile in p u with PV DG | Base Case | Voltage Profile in p u with PV DG |
|---|---|---|---|---|
| | Load Flow | Using GA-IPSO | Load Flow | Using GA-IPSO |
| **1** | 1.060 | 1.060 | 0.894 | 0.970 |
| **2** | 0.984 | 1.005 | 0.910 | 0.979 |
| **3** | 0.970 | 0.999 | 0.989 | 0.999 |
| **4** | 0.969 | 0.998 | 0.970 | 0.989 |
| **5** | 0.920 | 0.979 | 0.965 | 0.987 |
| **6** | 0.919 | 0.968 | 0.950 | 0.979 |
| **7** | 0.909 | 0.961 | 0.945 | 0.972 |
| **8** | 0.891 | 0.959 | 0.940 | 0.968 |
| **9** | 0.890 | 0.962 | 0.930 | 0.961 |

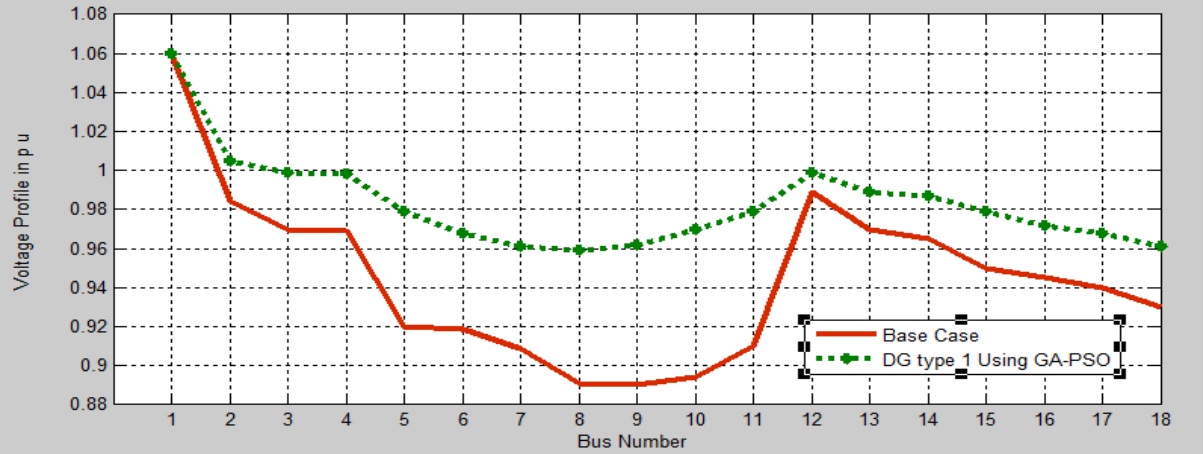


Figure 7.16: Voltage Profile for PV (type1) DG Using GA-IPSO

### 7.5.6 Results of Case 4, for two units of wind DG Using GA-IPSO

The two selected optimal locations and their respective optimal DG sizes from Table 7.25 were as follows in order of effectiveness.

Bus number 9 with a DG size of 1.010 MW and 0.190 MVAR

Bus number 18 with a DG size of 0.988 MW and 0.160 MVAR

The load flow study was carried out, using Newton-Raphson method so as to determine the associated power losses and voltage levels. The results obtained for the power losses were compared to results from the other method. The comparison is given in table 7.28.

Table 7.28: A comparison of results for Wind DG using GA and GA-IPSO

| Methodology | Bus No | DG Size | | Power loss | | Power loss Reduction | | % Power loss Reduction | |
|---|---|---|---|---|---|---|---|---|---|
| | | MW | MVAR | kW | kVAR | kW | kVAR | kW | kVAR |
| **Base Case** | | - | - | 180 | 40 | - | - | - | - |
| **GA** | 12 | 1.350 | 0.507 | 85 | 27 | 95 | 13 | 52 | 33 |
| | 18 | 0.901 | 0.210 | | | | | | |
| **GA-IPSO** | 9 | 1.010 | 0.190 | 78 | 20 | 102 | 20 | 57 | 50 |
| | 12 | 0.988 | 0.160 | | | | | | |

#### 7.5.6.1 Bus Voltage Profile for two units of PV and two wind DG using GA-IPSO

Table 7.29 also gives a comparison of voltage profile of two units of wind DG placed and sized with GA-PSO with PV using the same approach. A graph was plotted to facilitate this comparison purpose as shown in Figure 7.17. The lowest voltage level improves from 0.890 p.u to 0.980p.u as shown in the Table 7.29.

Table 7.29: Voltage Profile Comparison for PV and wind DG using GA-PSO

| Bus No | Base Case | Voltage Profile in p u with PV DG | Voltage Profile in p u with Wind DG | Bus No | Base Case | Voltage Profile in p u with PV DG | Voltage Profile in p u with Wind DG |
|---|---|---|---|---|---|---|---|
| | Load Flow | Using GA-IPSO | Using GA-IPSO | | Load Flow | Using GA-IPSO | Using GA-IPSO |
| **1** | 1.060 | 1.060 | 1.0600 | 10 | 0.894 | 0.970 | 0.9840 |
| **2** | 0.984 | 1.005 | 1.0310 | 11 | 0.910 | 0.979 | 0.9820 |
| **3** | 0.970 | 0.999 | 1.0090 | 12 | 0.989 | 0.999 | 0.9990 |
| **4** | 0.969 | 0.998 | 1.0070 | 13 | 0.970 | 0.989 | 0.9890 |
| **5** | 0.920 | 0.979 | 0.9950 | 14 | 0.965 | 0.987 | 0.9900 |
| **6** | 0.919 | 0.968 | 0.9880 | 15 | 0.950 | 0.979 | 0.9890 |
| **7** | 0.909 | 0.961 | 0.9860 | 16 | 0.945 | 0.972 | 0.9800 |
| **8** | 0.891 | 0.959 | 0.9880 | 17 | 0.940 | 0.968 | 0.9680 |
| **9** | 0.890 | 0.962 | 0.9800 | 18 | 0.930 | 0.961 | 0.9631 |

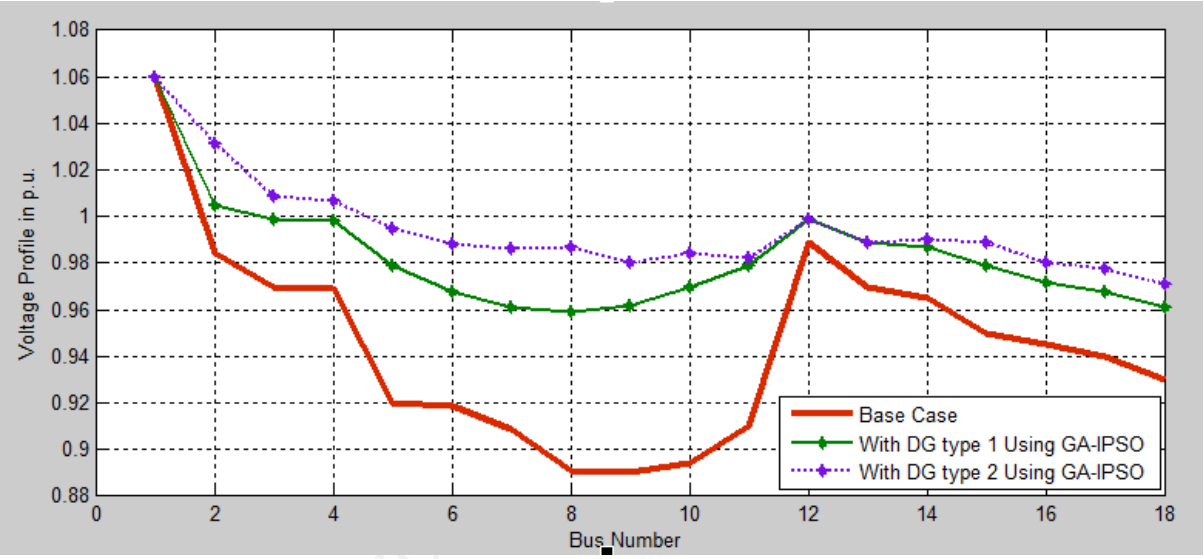


Figure 7.17: Voltage Profile for PV (type1) and Wind (type2) DG Using GA-IPSO

## 7.6 Results of Western Cape Network under base loading condition

The system details remain the same as described in the first scenario but in this case, the base load profile in chapter 4 is applied using the corresponding variable DG output during the same period. Finally, study cases are defined as:

Case 1: Two units of PV DG using GA.

Case 2: Two units of Wind DG using GA.

Case 3: Two units of PV DG using GA-IPSO.

Case 4: Two units of Wind DG using GA-IPSO.

### 7.6.1 Placement and Sizing procedure using Genetic Algorithm

Allocation of two units of DG was investigated using GA steps highlighted in Chapter 5 as well as the network parameters in Chapter 6 to obtain the optimized solution of chromosome with the best fitness in the population. With the chosen DG candidate buses and sizes, a load flow study was done using Newton-Raphson method so as to determine the associated power losses and voltage levels.

### 7.6.2 Result of Case 1, two units of PV DG under base load, using GA

The optimal solution that minimizes the objective function was found to be buses 18 and 9, with a real power output of 0.135 MW and 0.09 MW respectively. Here, total real power losses were reduced to 77 kW. This indicates a reduction of about 57 % out of ten best combinations compared to base case as shown in Table 7.30 below.

Table 7.30: Best five optimal solutions for installing two DGs units during base load

| S/N | Bus No | DG Size MW | DG Bus | DG Size MW | Power loss in kW | % Losses reduction |
|---|---|---|---|---|---|---|
| **Base Case** | - | - | - | | 180 | - |
| | 18 | 0.135 | 9 | 0.09 | 77 | 57 |
| | 18 | 0.085 | 12 | 0.15 | 80 | 55 |
| | 16 | 0.105 | 12 | 0.16 | 85 | 52 |
| | 16 | 0.205 | 12 | 0.05 | 87 | 51 |
| | 12 | 0.039 | 15 | 0.16 | 89 | 50 |

Table 7.31: Voltage Profile for PV DG under base load, using GA

| Bus No | Base Case | Voltage Profile in p u with type one DG Using GA | Bus No | Base Case | Voltage Profile in p u with type one DG Using GA |
|---|---|---|---|---|---|
| | Load Flow | PV DG | | Load Flow | PV DG |
| **1** | 1.060 | 1.061 | 10 | 0.894 | 0.964 |
| **2** | 0.984 | 0.991 | 11 | 0.910 | 0.977 |
| **3** | 0.970 | 0.985 | 12 | 0.989 | 0.999 |
| **4** | 0.969 | 0.980 | 13 | 0.970 | 0.989 |
| **5** | 0.920 | 0.972 | 14 | 0.965 | 0.985 |
| **6** | 0.919 | 0.965 | 15 | 0.950 | 0.977 |
| **7** | 0.909 | 0.955 | 16 | 0.945 | 0.970 |
| **8** | 0.891 | 0.954 | 17 | 0.940 | 0.969 |
| **9** | 0.890 | 0.956 | 18 | 0.930 | 0.961 |

### 7.6.2.1 Bus Voltage Profile for PV DG under base load, using GA

Voltage profile on Table 7.31 gives the voltage comparison for the case without DG in the system and with DG on real network using GA. The lowest voltage level improves from 0.890p.u. to 0.954p.u. as shown in the Table 7.31. Figure 7.18 gives a graph for this comparison.

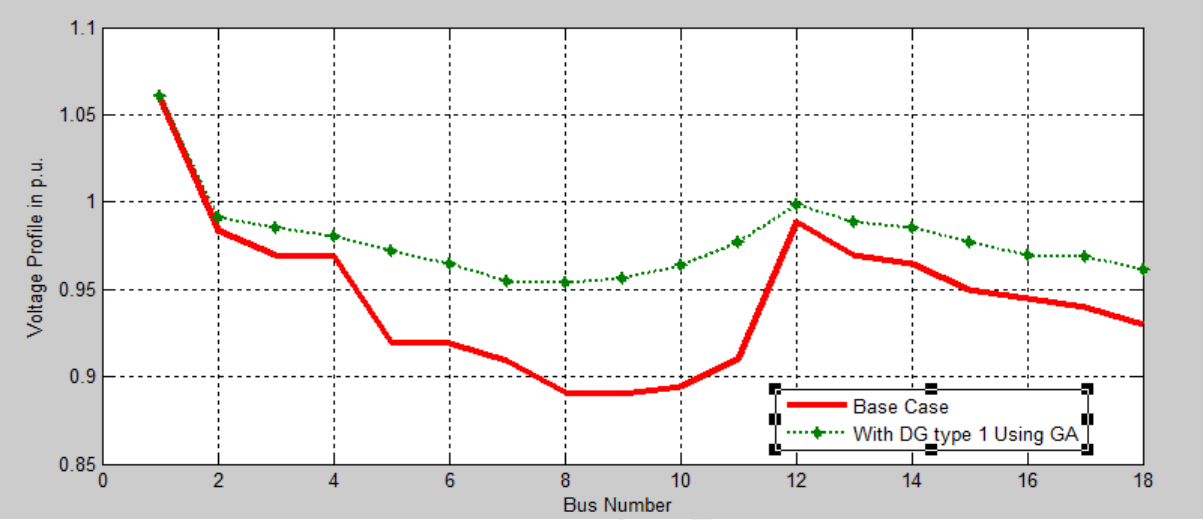


Figure 7.18: Voltage Profile for PV DG under base load, using GA

### 7.6.3 Result of Case 2, two units of wind DG under base load, using GA

The optimal solution that minimizes the objective function was found to be buses 18 and 9, with a real power output of 0.200 MW and 0.109 MW and reactive power output of 0.002 MVAR and 0.010 MVAR respectively. Here, the total active and reactive power losses were reduced to 72 kW and 25 kVAR. This indicates a reduction of about 60 % and 38 % from the pre-installation case as shown in the Table 7.32 below.

Table 7.32: Best five optimal solutions for installing wind DGs units under base load

| S/N | DG Bus | DG Size | | DG Bus | DG Size | | Power loss in | | % Losses Reduction | |
|---|---|---|---|---|---|---|---|---|---|---|
| | | MW | MVAR | | MW | MVAR | kW | kVAR | kW | kVAR |
| **Base Case** | - | - | | - | - | - | 180 | 40 | - | - |
| | **18** | 0.200 | 0.002 | **9** | 0.109 | 0.010 | 72 | 25 | 60 | 38 |
| | **18** | 0.201 | 0.010 | **12** | 0.150 | 0.107 | 75 | 27 | 58 | 33 |
| | **16** | 0.101 | 0.001 | **12** | 0.105 | 0.010 | 79 | 33 | 56 | 17 |
| | **16** | 0.205 | 0.203 | **12** | 0.050 | 0.201 | 84 | 34 | 53 | 15 |
| | **12** | 0.190 | 0.101 | **15** | 0.206 | 0.007 | 89 | 37 | 51 | 8 |

Table 7.33: Voltage Profile for wind DG under base load, using GA

| Bus No | Base Case | Voltage Profile in p u with DG Type One | Voltage Profile in p u with DG Type Two | Bus No | Base Case | Voltage Profile in p u with DG Type one | Voltage Profile in p u with DG Type Two |
|---|---|---|---|---|---|---|---|
| | Load Flow | Using GA | Using GA | | Load Flow | Using GA | Using GA |
| **1** | 1.060 | 1.061 | 1.064 | **10** | 0.894 | 0.964 | 0.968 |
| **2** | 0.984 | 0.991 | 0.998 | **11** | 0.910 | 0.977 | 0.979 |
| **3** | 0.970 | 0.985 | 0.991 | **12** | 0.989 | 0.999 | 0.999 |
| **4** | 0.969 | 0.980 | 0.986 | **13** | 0.970 | 0.989 | 0.991 |
| **5** | 0.920 | 0.972 | 0.982 | **14** | 0.965 | 0.985 | 0.989 |
| **6** | 0.919 | 0.965 | 0.975 | **15** | 0.950 | 0.977 | 0.982 |
| **7** | 0.909 | 0.955 | 0.965 | **16** | 0.945 | 0.970 | 0.979 |
| **8** | 0.891 | 0.954 | 0.959 | **17** | 0.940 | 0.969 | 0.970 |
| **9** | 0.890 | 0.956 | 0.959 | **18** | 0.930 | 0.961 | 0.974 |

#### 7.6.3.1 Bus Voltage Profile for wind DG under base load, using GA

The voltage profile in Table 7.33 gives the voltage comparison for the case without a DG in the system, PV (type1) and wind (type2) DG using GA. The lowest voltage level improves from 0.890 p.u. to 0.959 p.u. as shown in Table 7.33 above. Figure 7.19 below also gives a graph for this comparison.

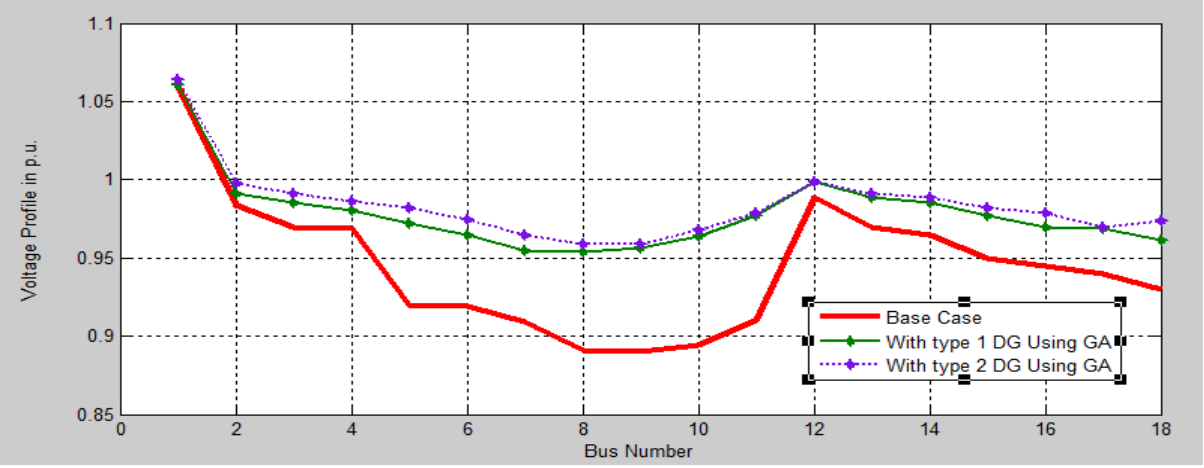


Figure 7.19: Voltage Profile for PV and Wind DG under base load, using GA

### 7.6.4 Result for all Candidate Buses using GA-IPSO under base load condition

The combined sensitivity factors were analyzed for all the buses and the buses which gave a combined sensitivity factor of more than 0.8 were taken to be the candidate buses. This was done for each of the two types of DG and the obtained results shown in Table 7.34 below.

It is worthy of note that the system used for this analysis got a smaller search space which in turn limit the bus combination in the search space.

Table 7.34: Results for CSF and fitness for candidate buses under base load under base load

| Candidate Bus | Sensitivity Factor | PV | | Wind | | |
|---|---|---|---|---|---|---|
| | | Fitness | DG Size MW | Fitness | DG Size | |
| | | | | | MW | MVAR |
| 3 | 0.8891 | 0.9199 | 0.050 | 0.9198 | 0.030 | 0.020 |
| 9 | 0.8789 | 0.9176 | 0.200 | 0.9178 | 0.101 | 0.003 |
| 12 | 0.9236 | 0.9198 | 0.1.90 | 0.9198 | 0.088 | 0.060 |
| 15 | 0.8852 | 0.9165 | 0.201 | 0.9157 | 0.202 | 0.005 |
| 16 | 0.8733 | 0.9173 | 0.109 | 0.9167 | 0.120 | 0.056 |
| 18 | 0.8022 | 0.9184 | 0.200 | 0.9125 | 0.187 | 0.103 |

### 7.6.5 Result of case 3, two units of PV DG under base load, using GA-IPSO

Table 7.34 above was use for selecting those locations which had the minimum fitness values and their respective DG sizes. The two selected optimal locations and their respective optimal DG sizes were as follows in order of effectiveness;

- Bus number 9 with a DG size of 0.200 MW
- Bus number 16 with a DG size of 0.109 MW

Load flow was done using Newton-Raphson method so as to determine the associated power losses and voltage levels. The results obtained for the power losses were compared to results from the other method. The comparison is given in Table 7.35.

Table 7.35: Results comparison for PV DG under base load using GA and GA-IPSO

| Methodology | Bus Number | DG Size | Power Loss | Power loss Reduction | % loss Reduction |
|---|---|---|---|---|---|
| | | MW | kW | kW | kW |
| **Base Case** | | - | 180 | - | - |
| **GA** | 9 | 0.090 | | | |
| | 18 | 0.350 | 77 | 103 | 57 |
| **GA-IPSO** | 9 | 0.200 | | | |
| | 16 | 0.109 | 75 | 105 | 58 |

#### 7.6.5.1 Bus Voltage Profile for PV DG under base load, using GA-IPSO

The voltage profile of the system in Table 7.36 gives the voltage comparison between base case and the case with DG using GA-IPSO. The lowest voltage level improves from 0.890 to 0.966 at bus 9. The graph is also shown in Figure 7.20.

Table 7.36: Voltage Profile for PV DG under base load, using GA-PSO

| Bus No | Base Case | Voltage Profile in p u with PV DG | Bus No | Base Case | Voltage Profile in p u with PV DG |
|---|---|---|---|---|---|
| | Load Flow | Using GA-IPSO | | Load Flow | Using GA-IPSO |
| **1** | 1.060 | 1.062 | **10** | 0.894 | 0.974 |
| **2** | 0.984 | 1.007 | **11** | 0.910 | 0.980 |
| **3** | 0.970 | 1.009 | **12** | 0.989 | 0.999 |
| **4** | 0.969 | 0.999 | **13** | 0.970 | 0.989 |
| **5** | 0.920 | 0.989 | **14** | 0.965 | 0.987 |
| **6** | 0.919 | 0.979 | **15** | 0.950 | 0.981 |
| **7** | 0.909 | 0.968 | **16** | 0.945 | 0.979 |
| **8** | 0.891 | 0.967 | **17** | 0.940 | 0.969 |
| **9** | 0.890 | 0.966 | **18** | 0.930 | 0.967 |

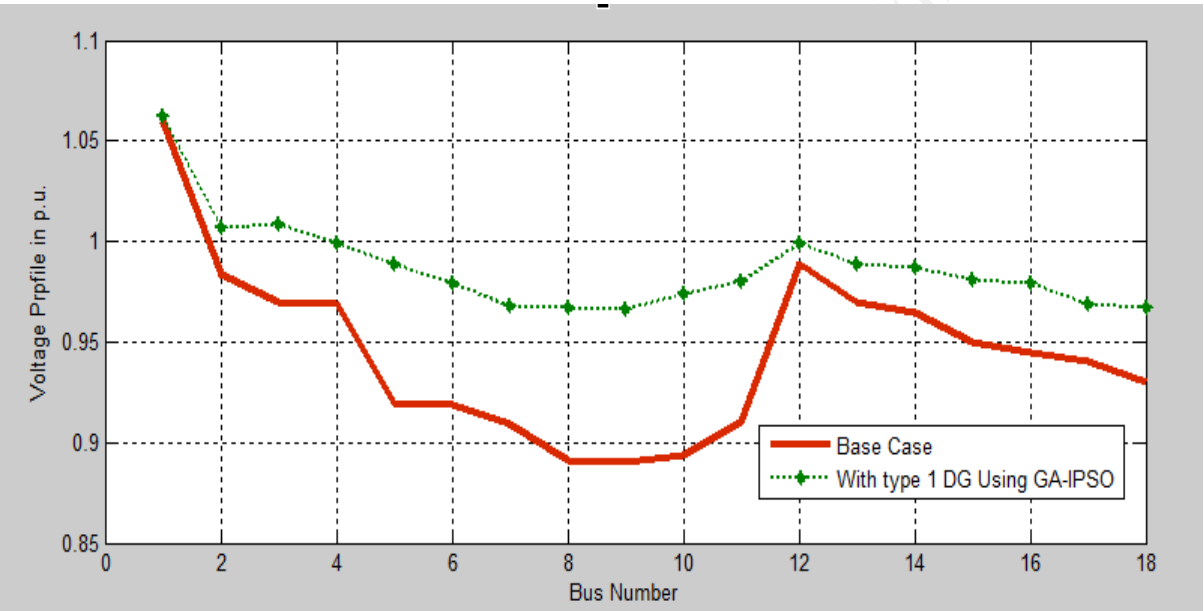


Figure 7.20: Voltage Profile for PV DG under base load of real network, using GA-IPSO

### 7.6.6 Result of case 4, two units of Wind DG under base load, using GA-IPSO

The choice of the two optimal locations for wind DG and their respective optimal sizes was done using the CSF as shown in Table 7.34 above. The two columns for fitness and DG size under wind DG were used to facilitate this by selecting those locations which had the minimum fitness values and their respective DG sizes. The two selected optimal locations and their respective optimal DG sizes were as follows in order of effectiveness.

- Bus number 9 with a DG size of 0.101 MW and 0.003 MVAR
- Bus number 15 with a DG size of 0.202 MW and 0.005 MVAR

Load flow was done using Newton-Raphson method so as to determine the associated power losses and voltage levels. The results obtained for the power losses were compared to result from the other method. The comparison is given in the Table 7.37.

Table 7.37: A comparison of results obtained using GA and GA-IPSO for wind DG

| Methodology | Bus No | DG Size | | Power loss | | Power loss Reduction | | % Power loss Reduction | |
|---|---|---|---|---|---|---|---|---|---|
| | | MW | MVAR | kW | kVAR | kW | kVAR | kW | kVAR |
| **Base Case** | | - | - | 180 | 40 | - | - | - | - |
| **GA** | **9** | 0.200 | 0.002 | 72 | 25 | 108 | 15 | 60 | 38 |
| | **18** | 0.109 | 0.010 | | | | | | |
| **GA-IPSO** | **9** | 0.101 | 0.003 | 60 | 15 | 120 | 25 | 67 | 63 |
| | **15** | 0.202 | 0.005 | | | | | | |

### 7.6.6.1 Bus Voltage Profile for Wind DG under base load, using GA-IPSO

The voltage profile comparison between case without DG, PV (type1) DG and wind (type2) DG using GA-IPSO show a reasonable improvement. The lowest voltage level improves from 0.890 p.u to 0.9880 p.u at bus 8 as shown in Table 7.38. Figure 7.21 below also gives a graph for this comparison.

Table 7.38: Voltage Profile for PV and wind DG under base load, using GA-PSO

| Bus No | Base Case | Voltage Profile in p u with PV DG | Voltage Profile in p u with Wind DG | Bus No | Base Case | Voltage Profile in p u with PV DG | Voltage Profile in p u with PV DG |
|---|---|---|---|---|---|---|---|
| | Load Flow | Using GA-IPSO | Using GA-IPSO | | Load Flow | Using GA-IPSO | Using GA-IPSO |
| **1** | 1.060 | 1.062 | 1.0600 | **10** | 0.894 | 0.970 | 0.9962 |
| **2** | 0.984 | 1.007 | 1.0350 | **11** | 0.910 | 0.979 | 0.9970 |
| **3** | 0.970 | 1.009 | 1.0210 | **12** | 0.989 | 0.999 | 1.0030 |
| **4** | 0.969 | 0.999 | 1.0100 | **13** | 0.970 | 0.989 | 0.9990 |
| **5** | 0.920 | 0.989 | 0.9950 | **14** | 0.965 | 0.987 | 0.9980 |
| **6** | 0.919 | 0.979 | 0.9890 | **15** | 0.950 | 0.979 | 0.9904 |
| **7** | 0.909 | 0.968 | 0.9889 | **16** | 0.945 | 0.972 | 0.9900 |
| **8** | 0.891 | 0.967 | 0.9880 | **17** | 0.940 | 0.968 | 0.9880 |
| **9** | 0.890 | 0.966 | 0.9960 | **18** | 0.930 | 0.961 | 1.9803 |

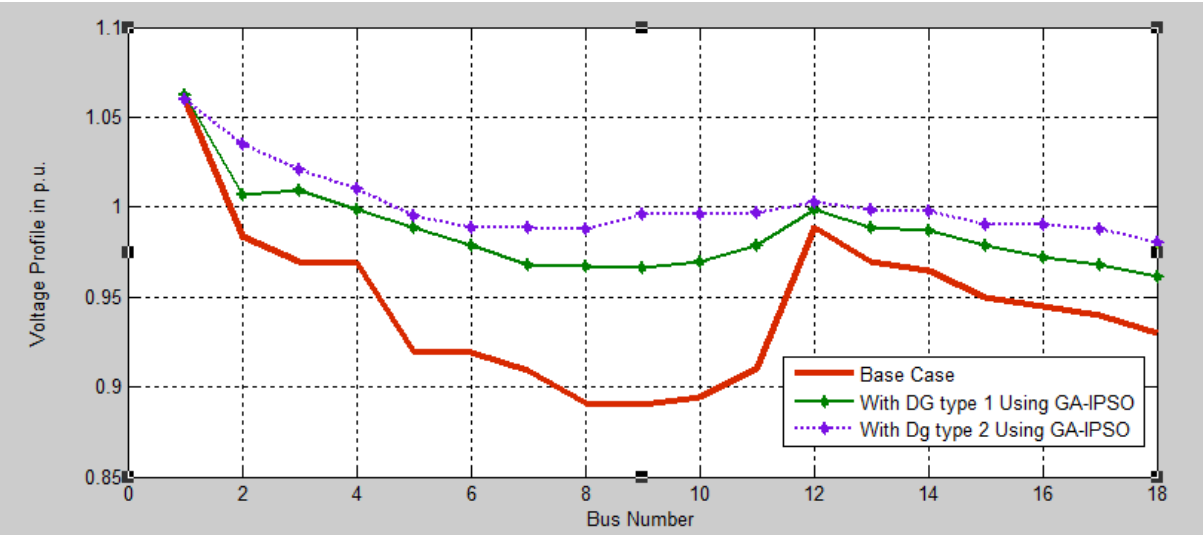


Figure 7.21: Voltage Profile for PV and Wind under base load, using GA-IPSO

## 7.7 Summary

This chapter presents the results of two major scenarios within a period of 24 hours considering the stochastic nature of DG under two load conditions using GA-IPSO and GA for optimal DG allocation in both the 33-bus system and the Western Cape Network. The next chapter will show the results comparison, discussion on the approaches used, power loss in each scenario and improvement in voltage profiles.

# Chapter 8

# RESULTS COMPARISON AND DISCUSSIONS

## 8. Introduction

This chapter presents the comparison of results obtained in the previous chapter and discussion of DG allocation as it affects losses and voltage profile in the two section while considering the approach used in each case. It also shows the effectiveness of GA-IPSO over the classical GA method.

## 8.1 Effects of allocation at peak loading with stochastic wind and PV

The multi-objective function used in the location and sizing of the DGs include minimizing the power losses and improving the voltage profile within the period under consideration. The results of section one, i.e. both GA-IPSO and GA are considered, observing the reduction in losses at the peak load period under the stochastic nature of the DGs and voltage profile.

### 8.1.1 Effects of PV penetration on IEEE 33-bus test system.

Since the PV source provides active power at unity PF, location and sizing of the DGs in the IEEE 33-bus reduces the power losses as it can be seen from Table 8.1. It can also be seen from Figure 8.1 that GA-IPSO reduces the losses better than GA under peak load condition. GA give loss percentage reduction of 58.6 % but GA-IPSO give higher value of 60 % which indicates that GA-IPSO reduces losses better than classical GA.

Also, it can be seen that during the peak load condition, the total installed DG capacity using GA-IPSO is 3.224 MW compared to 3.413 MW for GA. Also, the lowest voltage level while using the PV DG is 0.96 p.u. for GA-IPSO compared to 0.95 p.u for GA.

Table 8.1: Effect of PV DG penetration on power losses using IEEE 33-bus Network

| Methods | Bus No | DG Size | $P_{losses}$ | $\%P_{losses}$ Reduction |
|---|---|---|---|---|
| | | MW | kW | %kW |
| GA | 10 | 1.500 | 87.43 | 58.6 |
| | 25 | 0.863 | | |
| | 32 | 1.050 | | |
| GA-PSO | 19 | 0.710 | 84.51 | 60.0 |
| | 24 | 1.010 | | |
| | 32 | 1.504 | | |

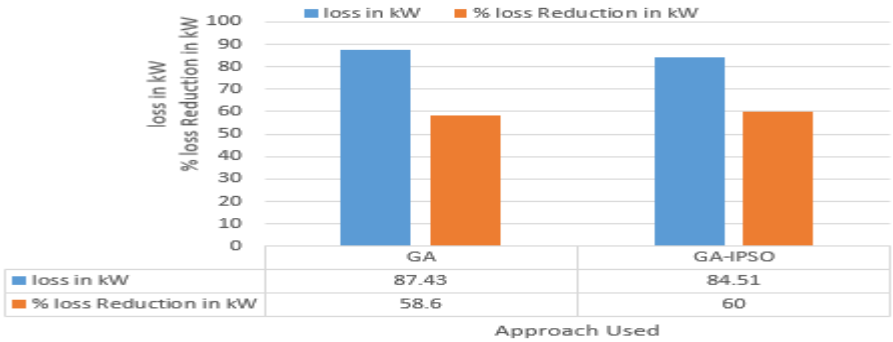


Figure 8.1: Effects of PV DG on power losses comparing GA and GA-IPSO

### 8.1.2 Effects of wind DG penetration in IEEE 33-bus test system

The results of location and sizing of wind DGs on IEEE 33-bus system shows that active and reactive power losses were reduced as shown in Table 8.2. Also, Figure 8.2 shows that GA-IPSO reduces the losses better than GA.

Table 8.2: Effects of wind DG penetration on power losses using IEEE 33-bus Network

| Method | Bus No | DG Size | | Power loss | | % loss Reduction | |
|---|---|---|---|---|---|---|---|
| | | MW | MVAR | kW | kVAR | %kW | % kVAR |
| GA | 10 | 1.040 | 0.79 | 85.41 | 39.06 | 59 | 61 |
| | 18 | 1.950 | 0.10 | | | | |
| | 32 | 1.210 | 0.92 | | | | |
| GA-PSO | 19 | 1.087 | 0.320 | 83.00 | 36.72 | 61 | 64 |
| | 24 | 1.301 | 1.010 | | | | |
| | 32 | 1.080 | 0.052 | | | | |

The total penetration level of wind DG using GA-IPSO is 3.468 MW compared to 4.110 MW for GA. And reactive power injected into the system using GA-IPSO is 1.382 MVAR compared to 1.81 MVAR for GA as shown in Table 8.2 above. The lowest voltage profile of the peak load condition while using type two DG shows that GA-IPSO is 0.9689 p.u. compared to GA of 0.9505 p.u.

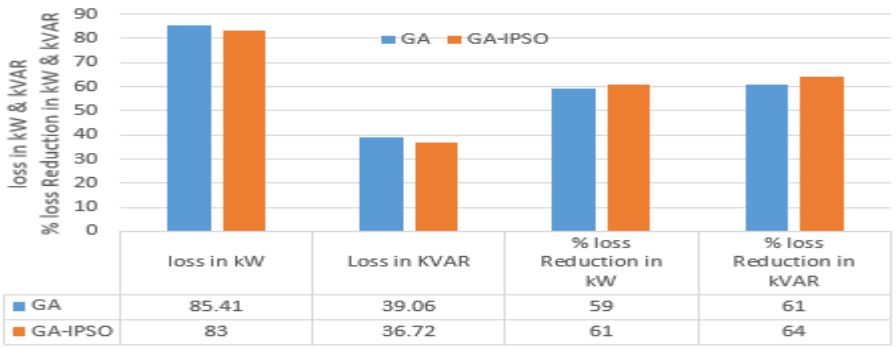


Figure 8.2: Effects of wind DG on power losses comparing GA and GA-IPSO

### 8.1.3 Effects of PV DG penetration on real network.

The optimal location and sizing of two units of PV DG in a modified real network, reduce the power losses from 180 kW to 82 kW while using GA and it was reduce to 79 kW as can be seen from Table 8.3. Figure 8.3 shows that GA-PSO reduces the losses better, with loss reduction percentage of 56.1 % than GA with of 54.4 %.

Table 8.3: Effects of PV DG penetration on power losses using real network

| Method | Bus No | DG Size | $P_{losses}$ | $\%P_{losses}$ Reduction |
|---|---|---|---|---|
| | | MW | kW | %kW |
| GA | 9 | 1.350 | 82 | 54.4 |
| | 18 | 0.950 | | |
| GA-PSO | 9 | 0.710 | 79 | 56.1 |
| | 16 | 1.099 | | |

At peak load condition, while using PV DG, GA gives the lowest voltage profile of 0.947 p.u. compared to 0.959 p.u. for GA-IPSO which is within the standard limit of ±5 p.u. The penetration level using GA-IPSO is a total of 1.809MW compared to 2.30 MW for GA, which shows that at lower penetration of GA-IPSO compared GA, GA-IPSO give better voltage profile and reduce losses.

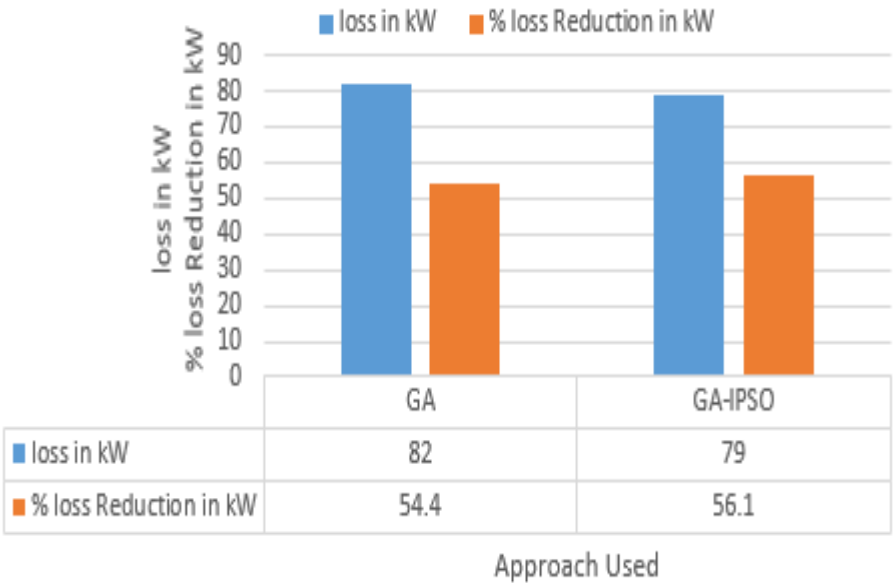


Figure 8.3: Effects of PV DG power losses comparing GA and GA-IPSO

### 8.1.4 Effects of wind DG penetration on real network.

It can be seen from Table 8.4 and Figure 8.4 that GA-PSO reduce the losses better than GA, with GA-IPSO having a loss reduction of 50 % compared to 33 % for GA.

Table 8.4: Effects of wind DG penetration on power losses using real network

| Methodology | Bus No | DG Size | | Power loss | | % Power loss Reduction | |
|---|---|---|---|---|---|---|---|
| | | MW | MVAR | kW | kVAR | kW | kVAR |
| GA | 12 | 1.350 | 0.507 | 85 | 27 | 52 | 33 |
| | 18 | 0.901 | 0.210 | | | | |
| GA-IPSO | 9 | 1.010 | 0.190 | 78 | 20 | 57 | 50 |
| | 12 | 0.988 | 0.160 | | | | |

Voltage profile of the peak load condition while using type two DG is 0.950p.u. for GA, compared to GA-IPSO which gives a better results of 0.9689 p.u. The penetration level using GA-IPSO is a total of 1.998 MW compared to 2.338 MW for GA and reactive power injected into the system using GA-IPSO is 0.350 MVAR and 0.717 MVAR for GA, this shows that at lower penetration GA-IPSO perform better.

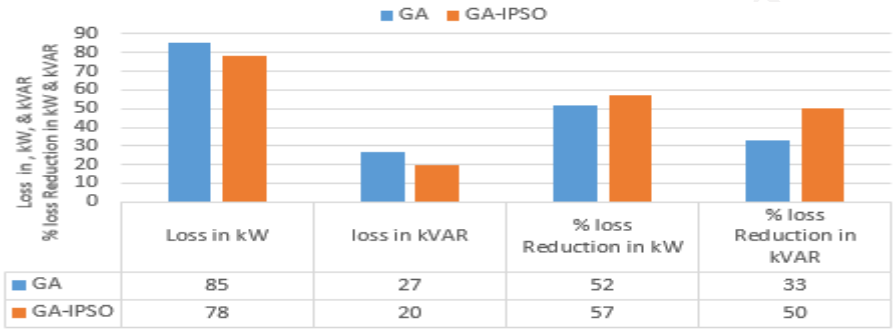


Figure 8.4: Effects of wind DG on power losses comparing GA and GA-IPSO

## 8.2 Effects of allocation at base loading with wind and PV

The objective function used in the location and sizing of the DGs including minimizing the power losses and improving the voltage profile using both types of DG was done under base load condition. The result for the second scenario for both GA-IPSO and GA are considered while observing the reduction in losses at the base load period under the stochastic nature of the DGs and voltage profile.

### 8.2.1 Effects of PV DG penetration on IEEE 33-bus test system.

Optimal allocation of three units of PV DG in IEEE 33-bus, reduce the power losses from 211.2 kW to 62.06 kW using GA-IPSO compared to 69.24 kW for GA. It can be seen from Table 8.5 and Figure 8.5 below that GA-IPSO shows higher percentage loss reduction GA The lowest voltage of the base load condition while using PV (type1) DG shows that GA-IPSO is 0.9843 p.u. compared with GA of 0.9509 p.u. and the total DG installed using GA-IPSO is 3.224 MW compared to 1.955 MW for GA as shown in Table 8.5.

Table 8.5: Effects of PV DG penetration on system power losses

| Methodology | Bus Number | DG Size | Power Loss | Power loss Reduction | % loss Reduction |
|---|---|---|---|---|---|
| | | MW | kW | kW | kW |
| Base Case | | - | 211.20 | - | - |
| GA | 6 | 0.800 | 69.24 | 141.96 | 67.2 |
| | 20 | 0.630 | | | |
| | 31 | 0.600 | | | |
| GA-IPSO | 18 | 0.650 | 62.06 | 149.14 | 70.6 |
| | 24 | 0.501 | | | |
| | 32 | 0.804 | | | |

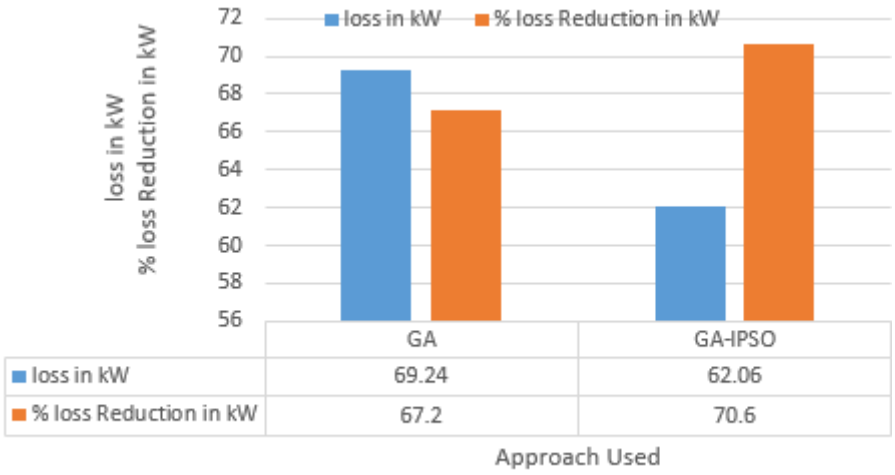


Figure 8.5: Effects of PV DG on power losses comparing GA and GA-IPSO

### 8.2.2 Effects of Wind DG penetration on IEEE 33-bus test system

Optimal allocation of three units of wind DG reduce loss while using GA-IPSO than classical GA as in Table 8.6. It can be seen from Table 8.6 and Figure 8.6 below that GA-PSO reduces the losses by 79 % compares to 76 % for GA while its reactive power losses reduce by 75 % for GA-IPSO and 71 % for GA.

Table 8.6: Effects of wind DG penetration on system power losses

| Methodology | Bus No | DG Size | | Power loss | | Power loss Reduction | | % Power loss Reduction | |
|---|---|---|---|---|---|---|---|---|---|
| | | MW | MVAR | kW | kVAR | kW | kVAR | kW | kVAR |
| Base Case | | - | - | 211.2 | 101.1 | - | - | - | - |
| GA | 10 | 0.740 | 0.090 | 50.43 | 29.05 | 160.8 | 72.05 | 76 | 71 |
| | 17 | 0.650 | 0.010 | | | | | | |
| | 32 | 0.250 | 0.090 | | | | | | |
| GA-IPSO | 18 | 0.507 | 0.030 | 44.60 | 24.62 | 166.6 | 76.48 | 79 | 75 |
| | 23 | 0.301 | 0.010 | | | | | | |
| | 32 | 0.707 | 0.002 | | | | | | |

The penetration level using GA-IPSO total of 1.515 MW compared to GA of 1.640 MW and reactive power injected into the system is 1.382 MVAR for GA-IPSO and 1.81 MVAR for GA as shown in Table 8.6 above after optimal allocation. The lowest voltage level while using wind DG is 0.9548p.u for GA compared to improve value of 0.9981p.u. for GA-IPSO.

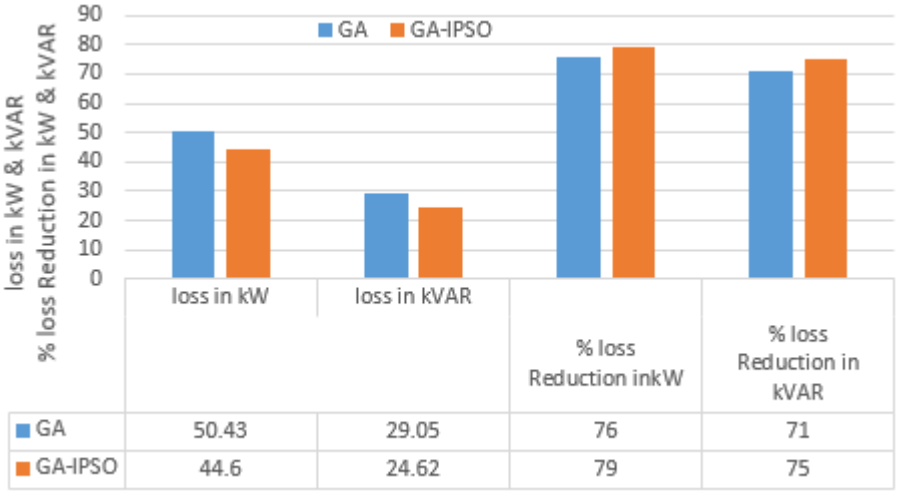


Figure 8.6: Effects of wind DG on power losses comparing GA and GA-IPSO

### 8.2.3 Effects of PV DG penetration on real network

After location and sizing of PV DG on a real network, the active power losses reduce to 75 kW from 180 kW. It can be seen from Table 8.7 and Figure 8.7 that GA-PSO reduces the losses better than GA with 58 % loss reduction compared with 57 % for GA.

Table 8.7: Effects of PV DG penetration on system power losses

| Methodology | Bus Number | DG Size | Power Loss | Power loss Reduction | % loss reduction |
|---|---|---|---|---|---|
| | | MW | kW | kW | kW |
| Base Case | | - | 180 | - | - |
| GA | 9 | 0.090 | | | |
| | 18 | 0.350 | 77 | 103 | 57 |
| GA-IPSO | 9 | 0.200 | | | |
| | 16 | 0.109 | 75 | 105 | 58 |

Voltage profile of the base load condition while using PV DG shows that GA-IPSO gives an improve value of 0.966p.u. compared to GA of 0.954p.u. under the same load condition. The penetration level using GA is 0.44 MW compared to GA-IPSO total of 0.309 MW which gives higher percentage losses reduction shown in Table 8.7 above.

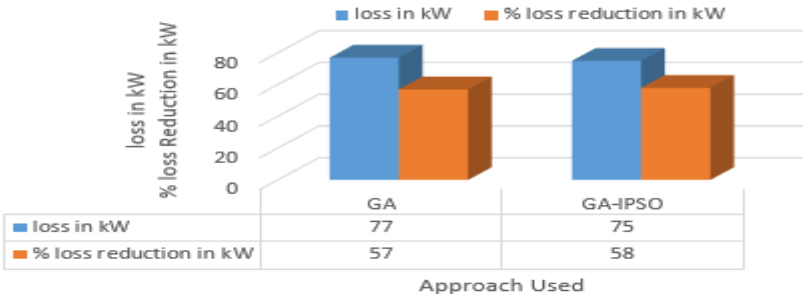


Figure 8.7: Effects of PV DG on power losses comparing GA and GA-IPSO

### 8.2.4 Effects of wind DG penetration on real network

Optimal placement and sizing of wind DGs on a real network reduce power losses as it can be seen from Table 8.8 and Figure 8.8 that GA-IPSO reduce the losses better than GA and give an improve voltage profile.

Table 8.8: Effects of wind DG penetration on system power losses

| Methodology | Bus No | DG Size | | Power loss | | Power loss Reduction | | % Power loss Reduction | |
|---|---|---|---|---|---|---|---|---|---|
| | | MW | MVAR | kW | kVAR | kW | kVAR | kW | kVAR |
| Base Case | | - | - | 180 | 40 | - | - | - | - |
| GA | 9 | 0.200 | 0.002 | 72 | 25 | 108 | 15 | 60 | 38 |
| | 18 | 0.109 | 0.010 | | | | | | |
| GA-IPSO | 9 | 0.101 | 0.003 | 60 | 15 | 120 | 25 | 67 | 62 |
| | 15 | 0.202 | 0.005 | | | | | | |

The voltage profile of the base load condition while using type two DG shows GA-IPSO is 0.988p.u. compared to 0.959p.u. for GA, in a real network. The penetration level using GA-IPSO is a total of 0.309 MW compared to GA of 0.309 MW and reactive power injected into the system is 0.012 MVAR for GA-IPSO and 0.008 MVAR for GA that gives the percentage losses reduction shown in Table 8.8 above. The higher loss reduction recoded in case of GA-IPSO shows that the approach is more suitable for optimal allocation.

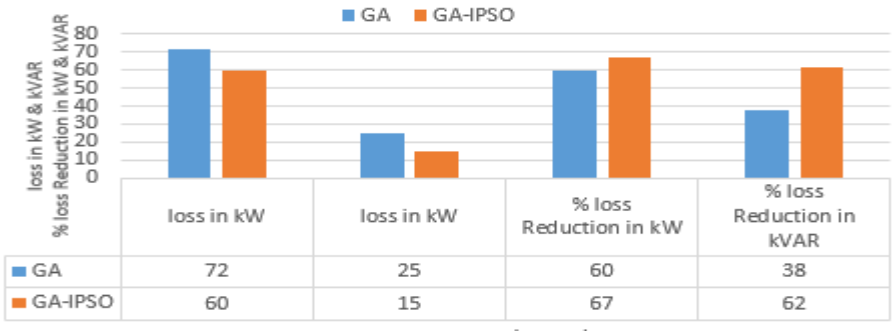


Figure 8.8: Effects of wind DG on power losses comparing GA and GA-IPSO

## 8.3 Discussion.

The factors considered in optimal allocation which include DG technology, capacity of DG unit, location of DG connection and network connection type, therefore optimal allocation of PV and wind DG was done on IEEE 33-bus system and Western Cape real network. The results of optimal allocation in this research show a reduced loss and improved voltage profile. The results comparison under two different load condition shows that GA-IPSO perform better than classical GA. In lieu of these, it proper coordination like the above in a network will reduce the power loss and improve the voltage profile using optimization method. Also GA-IPSO gives a better solution than GA in terms of allocation which can be seen from the results. The result from above provides solution to the research question in chapter one of this dissertation and the following answers were provided

- It shows clearly that GA-IPSO serve better in optimal allocation of DGs.
- It is also confirmed that wind DG has the capability to reduce losses and improve the voltage better as shown in results in chapter 7 and discussion in chapter 8.
- After coordination, it is observed that better voltage profile is obtained and the power loss reduces considerably.
- The number one advantage of GA-IPSO is that it converges faster than ordinary GA and is not trapped at local minimal unlike PSO as show in appendix x.

## 8.4 Summary

The results above from GA and GA-IPSO considering two types of DGs were obtained using both the IEEE 33-bus test and Western Cape Network. The issue of penetration was analyzed with respect to DG size and location while monitoring the losses and voltage profile improvement.

# Chapter 9

# CONCLUSIONS AND RECOMMENDATIONS FOR FUTURE WORK

## 9. Conclusion

Therefore, computational, artificial intelligence and analytical approaches have been used for DG placement and sizing, and each approach has its strengths and weakness. GA and IPSO however perform better than all other approaches. This research work showed the formulation and implementation of a hybridized GA-IPSO algorithm to help in reducing system power losses and improving the voltage profile by optimizing the location and size of multi-type DGs. The combined sensitivity factors were formulated and used effectively in reducing the search space for the algorithm. For the IEEE 33-bus test system 14 candidate buses were chosen and for the Western Cape Network 18-bus system, 6 candidate buses were chosen as possible DG locations. As seen from the results that combination GA-IPSO method gave the highest loss reduction when compared to GA.

The results obtained from section one for PV DG shows that, percentage reduction in the real power loss was 60% using GA-IPSO as well as 58.6 % using GA under peak load condition. Also, PV shows 70.6 % percentage loss reduction when GA-IPSO approach were used and 67.2 % for GA approach. The results obtained for wind using IEEE 33-bus shows that, percentage real loss reduction is 61 % using GA-IPSO as well as 59 % using GA while percentage reactive power loss reduction is 64 % for GA-IPSO approach and 61 % using GA respectively.

Similarly, under base loading condition in IEEE 33-bus, PV DG active reduce loss by 70 % using GA-IPSO approach and 67 % for classical GA. Also, wind DG reduce active power loss by 79 % using GA-IPSO and 76 % using GA approach. Consequently, wind DG reduce reactive power loss by 75 % with GA-IPSO approach and 71 % for GA methods. The voltage profile under peak loading condition was generally improved with lowest bus voltages 0.9600 p.u. for PV and 0.9689 p.u. for wind and 0.9843 p.u for PV as well as 0.9981 for wind. It is clearly seen here that optimal allocation of DG using GA-IPSO produce the best results going by loss reduction and the fact it gives the best voltage profile for two types of DGs.

Also, from our results comparison in chapter 8, for peak load condition in the Western Cape real network, GA-IPSO gives the highest power loss reduction of 56.1 % for PV DG as

well as 57 % real power reduction and 50 % reactive power reduction for wind DG. Likewise, under base load condition GA-IPSO give the highest power loss reduction of 58 % for PV as well as 67 % for active power loss reduction and 62 % reactive power loss reduction for wind DG. The approach also produce the best voltage profile under peak loading condition in Western Cape real network 0.959 p.u. was recorded for PV and 0.9689 p.u. for wind DG using GA-IPSO. Also, under base loading better voltage profile were obtained, 0.966 p. u for PV and 0.988 p.u for wind which is good improvement above standard limit of $\pm$ 5 p.u. . It is aslo shown here that optimal allocation reduces loss and improves the voltage profile in Western Cape real network in section two.

The GA-IPSO method also performed well in reducing the losses and improving the voltage profile of the IEEE 33-bus test system as it was also confirmed by real network using base and peak load.

Thus the objectives of the research work were achieved successfully and the implementation of GA-IPSO method was proved to be a better method for optimizing the location and size of multi-type DGs in different power networks with the aim of reducing both real and reactive power losses and improving voltage profiles simultaneously.

### 9.1 Beneficiaries of this work

This research work is beneficial to different parties, both directly and indirectly. The direct beneficiaries of this research work are the distribution companies. Some of the direct benefits from this work to the DISCOs include;

- This research work will help the distribution companies in reducing both real and reactive power losses in their networks. This reduction in loses will enable them to avoid some of the penalties and compensations they incur and hence result to an improvement in their profit margins.
- The work will help the power companies incorporate small-sized green energy sources to their networks easily and more reliably. This is of much importance due to the changing attention in power production with the shift to green energy.
- The research work will also ensure that they improve the voltage levels at the consumers to the required limits. This will enable the distribution companies to avoid the costs incurred during compensation of spoilt customer equipment due to voltage

deviations outside the acceptable limits. As a result this makes the companies more economical and reliable in operation.

Other parties will also benefit substantially from this research work. An example of this is the end customers who will feel secure knowing that they are operating their machines with stable voltage profiles. All these benefits relate back to the country's economy as a whole, and thus the whole community.

## 9.2 Recommendations for Future Work

- Negative impacts of DG which can be eliminated with optimal allocation of DG should be look into by planning Engineers.
- Long iteration time was noted in simulating in GA-IPSO and thus more work can be done in trying to reduce this time.
- Also, more future work can be done to make AI optimization technique accommodate more variability of renewable energy source.
- The Multi-objective function can be improved by taking into consideration other power system parameters like stability issues.
- Since the loading of the Network is not fixed, the DISCO need to apply this approach anytime the need arises to integrate DG.

# Reference


[1] A.Y. Abdelaziz, Y.G. Hegazy, W. El-Khattam and M.M. Othman, "Optimal allocation of stochastically dependent renewable energy based distributed generators in unbalanced distribution networks," *Electric Power Systems Research 119 ,* pp. 34-44, 2014 Elsevier.

[2] J. B. Gupta, A Course In Power Systems, S. K. Kataria & Sons, 2009, p. 1600 pages.

[3] R. E. Brown, Electric Power Distribution Reliability, CRC Press, Sep 2008.

[4] M. M. A. Salama and A. Y. Chikhani, "Classification of capacitor allocation techniques," *IEEE Transactions on power delivery,* vol. 15, no. 1, pp. 387-392, 2000.

[5] P. Renuga, S. M. Priya and D. Kavitha, "Optimal placement and location of distributed generators in distorted distribution system," in *International Conference on Circuit, Power and Computing Technologies (ICCPCT),* , Nagercoil , 2014.

[6] E. I.Administration, "http://tonto.eia.doe.gov/energy_in_brief/renewable_energy.cfm," 10 May 2013. [Online]. [Accessed 2015 06 03].

[7] P.S. Georgilakis and N. D. Hatziargyriou, "Optimal Distributed Generation Placement in Power Distribution Networks: Models, Methods, and Future Research," *IEEE Transactions on Power Systems,* vol. 28 , no. 3, pp. 3420 - 3428, 2013.

[8] T. Ackermanna, G. Andersson, and l. Soder, "Distributed generation: a definition," *Electric Power Systems Research,* vol. 57, no. 3, pp. 195-204, 2001.

[9] Y.A. Katsigiannis and P.S. Georgilakis, "Effect of customer worth of interrupted supply on the optimal design of small isolated power systems with increased renewable energy penetration," *IET Gener. Transm. Distrib,* vol. 7, no. 3, p. 265–275, 2013.

[10] J. A. Pecas Lopes, N. Hatziargyriou, J. Mutale, P. Djapic and N. Jenkins , "Integrating distributed generation into electric power systems: a review of drivers, challenges and opportunities," *Electric Power Systems Research,* vol. 77, no. 9, pp. 1189-1203, 2007.

[11] A. Keane, F. L. Ochoa, and C.L.T. Borges, "State-of-the-Art Techniques and Challenges Ahead for Distributed Generation Planning and Optimization," *IEEE Transaction on Power Systems,* vol. 28, no. 20, pp. 1493-1502, 2013.

[12] A. Alarcon-Rodriguez, G. Ault and S. Galloway, "Multi-objective planning of distributed energy resources," *Renewable and Sustainable Energy Review,* vol. 14, no. 6, pp. 1353-1366, 2010.

[13] D. Q. Hung, N. Mithulananthan, and R. C. Bansal, "Analytical expressions for DG allocation in primary distribution networks," *IEEE Transactions on Energy Conversion,* vol. 25, no. 3, pp. 814-820, 2010.

[14] B. A. De-Souza and J. M. C. De-Albuquerque, "Optimal Placement of Distributed Generators Networks Using Evolutionary Programming," in *Transmission & Distribution Conference and Exposition* , Latin America, 2006.

[15] M. Z. C. Wanik, I. Erlich, and A. Mohamed, "Intelligent Management of Distributed Generators Reactive Power for Loss Minimization and Voltage Control," in *15th IEEE Mediterranean Electrotechnical Conference*, MELECON 2010, 2010.

[16] A.M. El-Zonkoly, "Optimal placement of multi-distributed generation units including different load models using particle swarm optimisation," *IET Gener. Trans. Distrib,* vol. 1, no. 1, pp. 760-771, 2011.

[17] C. L. T. Borges and D.M. Falcao, "Optimal distributed generation allocation for reliability, losses and voltage improvement," *International journal of power and energy systems,* vol. 28, no. 6, pp. 413-420, 2006.

[18] M. Bollen, Y. Yang, and F. Hassan, "Integration of distributed generation in the power system - a power quality approach," in *13th International Conference on Harmonics and Quality of Power*, Wollongong, Australia, 2008.

[19] T. N. Shukla, S.P. Singh, K. B. Naik, "Allocation of optimal distributed generation using GA for minimum system losses in radial distribution networks," *International Journal of Engineering, Science and Technology,* vol. 2, no. 3, pp. 94-106, 2010.

[20] M. Wang and J. Zhong, "A Novel Method for Distributed Generation and Capacitor Optimal Placement considering Voltage Profiles," in *IEEE Power and Energy Society General Meeting*, San Diego, CA, 2011.

[21] T. Kim, "A method for determining the introduction limit of distributed generation system in distribution system," *IEEE Transaction on Power Delivery,* vol. 4, no. 2, pp. 100-117, 2001.

[22] R.C. Dugan, T.E. McDermott and G.J. Ball, "Planning for distributed generation," *IEEE Industrial Application Magazine,* vol. 7, no. 2, pp. 80-88, 2001.

[23] S. Chandrashekhar Reddy, P. V. N. Prasad and A. Jaya Laxmi, "Power Quality Improvement of Distribution System by Optimal Placement and Power Generation of DGs using GA and NN," *European Journal of Scientific Research ISSN 1450-216X,* vol. 69, no. 3, pp. 326-336, 2012.

[24] J. D. Vu and V. Thong, "Interconnection of Distributed Generators and Their Influences on Power System," Katholieke Univeristeit , Leuven, Belgium, 2004 MSc.

[25] 21st IEEE Standards Coordinating Committee, "IEEE Standard for Interconnecting Distributed Resources with Electric power system," The Institute of Electrical and Electronics Engineers, Inc., 3 Park Avenue, New York, NY 10016-5997, USA, 2003.

[26] A.Borbely and J. F. Kreider, "A New Paradigm for the Distributed Generation," in *Green Technologies Conference (IEEE-Green), 2011 IEEE*, Baton Rouge, LA, 2011.

[27] P. Dondi, D. Bayoumi, C. Haederli, D. Julian and M. Suter, "Network integration of distributed power generation," *Journal of Power Source,* vol. 106, no. 1, pp. 1-9, 2002.

[28] H. Anders, "Voltage Control in Distribution Network with local Generation," Norwegian University of Sicence and Technology, Norwey, 2014 MSc.

[29] C. Fortoul, "Review of Distributed Generation Concept," in *Proceedings of International Conference on Renewable Energies and Power Quality*, Espana, 2005.

[30] "www.altenergy.org/renewables/renewables.html," 30 05 2012. [Online]. [Accessed 05 2016].

[31] A. Konstantinos, "Integration of Distributed Generation in Low Voltage Network," University of Strathclyde, Glasgow, 2004 PhD.

[32] Century, Laboratories for the 21st, "www.femp.energy.gov," U.S. Environmental Protection Agency Office of Administration and Resources Management, september 2011. [Online]. [Accessed 02 march 2015].

[33] Popular Mechanics, "www.jcbpowerproducts.com," January 1953. [Online]. [Accessed 31 03 2015].

[34] Inc., Energy OR Technologies, "www.alternativeenergy.org," 15 February 2011. [Online]. [Accessed 25 03 2015].

[35] Century, Alternative Energy Solution for 21st, "www.alternativeenergy.org," Alternative Energy Solution. [Online]. [Accessed 03 03 2015].

[36] S. Rahman, "Green Power: What is and where we Can Find It," *IEEE Power and Energy Magazine,* vol. 11, no. 2, pp. 30-37, January - February 2003.

[37] Electric, Corporation Yokogawa, " Yokogawa www.yokogawa.com," Yokogawa Electric Corporation, 4 April 2015. [Online]. [Accessed 09 04 2015].

[38] IEA International, Distributed Generation in Liberalised Electricity Markets, France: International Energy Agency, 2002.

[39] M. Suter, "Active filter for a microturbine," in *Proceedings of the Telecommunications Energy Conference*, Edinburgh, UK, 2001.

[40] J. D. Monaco, "The role of distributed generation in the critical electric power infrastructure," in *Power Engineering Society Winter Meeting, 2001*, Columbus, OH, 2001.

[41] B. Lasseter, "Microgrids [distributed power generation," in *Proceedings of the Power Engineering Society Winter Meeting IEEE*, Columbus, OH, 2001.

[42] IEA, "Renewables for Power Generation: Status and Prospects," International Energy Agency France, 2003.

[43] E. S. H. Association, "http://www.esha.be/," European Small Hydropower Association, 22 09 2007. [Online]. [Accessed 05 03 2015].

[44] D. Gielen, "Renewable Energy Technologies: Cost Analysis Series: Wind Power," *International Renewable Energy Agency,* 11 03 2015.

[45] V. Fthenakis and H. C. Kim, "Land use and electricity generation: A life-cycle analysis," *Renewable and Sustainable Energy Reviews,* vol. 13, pp. 6-7, 2009.

[46] M. R. Patel, Wind and Solar Power Systems, in Design, analysis and Operation, CRC Press, July 15, 2005, p. p. 303..

[47] A. Kulmala, "Active Voltage Control in Distribution Networks Including Distributed Energy Resources," Tampere University of Technology, Tampere, 2014 MSc.

[48] R. M. Swanson, "Photovoltaics Power Up," in *Science 324*, 2009.

[49] K. Branker, M. Pathak and J. Pearce, "A Review of Solar Photovoltaic Levelized Cost of Electricity," in *Renewable and Sustainable Energy Reviews 15*, 2011.

[50] F. A. Viawan, "Voltage Control and Voltage Stability of Power Distribution Systems in the Presence of Distributed Generation," Chalmers University of Technology, Göteborg, Sweden 2008, 2008 MSc.

[51] P. Gipe, "Renewable Energy World," 02 06 2010. [Online]. Available: http://www.renewableenergyworld.com. [Accessed 13 06 2015].

[52] D. Green, "Green Energy Saving 'Pros and Cons of Photovoltaic (PV) panels'," 13 june 2012. [Online]. Available: http://www.greenenergysavingtips.com. [Accessed 03 04 2015].

[53] G. C. Stocks, "Clean Energy in China," 22 03 2015. [Online]. Available: http://www.greenchipstocks.com. [Accessed 04 04 2015].

[54] W. El-Khattam and M.M.A. Salama, "Distributed generation technologies, definitions and benefits," in *Electric Power Systems Research 119–128*, Waterloo, Ont, Canada, 2004.

[55] P. Smart Dinning, A. Maloyd, A. A. Causebrook and S. Cowdroy, "Accommodating Distributed Generation," *Econnect Project,* vol. 2, no. 1, pp. 91-100, 2006.

[56] P. Philip, and R. W. Barker, "Determining the Impact of Distributed Generation on Power Systems: Part 1 Radial Distribution Systems," in *IEEE Power Engineering Society Summer Meeting*, Seattle, WA, 2011.

[57] P. P. Barker and R. W. de Mello,, "Determining the impact of distributed generation on power systems l radial distribution systems," in *Power Engineering Society Summer Meeting, 2000. IEEE* , Seattle, WA, 2000.

[58] A. Fernández, "Impact of distributed generation on distribution system," Aalborg University, Aalborg, Denmark, 2011 MSc.

[59] T. F. Chan, "Synchronous Machines," Encyclopedia of Life Support Systems, Polythecnic University, Hong kong, 2003.

[60] C. T L. Borges and D. M. Falcao, "Optimal distributed generation allocation for reliability,losses and voltage improvement," *International journal of power and energy systems,* vol. 28, no. 6, pp. 413-420, 2006.

[61] F. Bastiao; P. Cruz; R. Fiteiro, "Impact of Distributed Generation on Distributed Network," in *EEM 2009. 6th International Conference on the European* , Leuven , 2009.

[62] P. Philip and R. W. Barker, "Determining the Impact of Distributed Generation on Power Systems Radial Distribution Systems," in *IEEE. Retrieved 02 16*, 2011.

[63] J. A. Martin-Arnedo, "Impacts of Distributed Generation on Protection and Power Quality," in *IEEE Power & Energy Society General Meeting*, Calgary, AB, 2009.

[64] R. E. Brown and L. A. Freeman, "Analyzing the reliability impact of distributed generation," in *Power Engineering Society Summer Meeting*, Vancouver, BC, Canada, 2001.

[65] A. C. Neto, M. G. da Silva and A. B. Rodrigues, "Impact of Distributed Generation on Reliability Evaluation of Radial Distribution Systems Under Network Constraints," in *9th International Conference on Probabilistic Methods Applied to Power Systems*, KTH, Stockholm, Sweden, 2006.

[66] M. J. H. Bollen and F. Hassan., "Integration of distributed generation in the power system - a power quality approach," in *13th International Conference on Harmonics and Quality of Power*, Wollongong, NSW, 2008.

[67] H. L. Z. Chen, "Overview of different wind generator sysytems and their comparison," *IET renew power generation ,* vol. 2, no. 2, pp. 123-138, 2008.

[68] M. Chinchilla, S. Arnaltes and J. C. Burgo, "Control of Permanent-Magnet Generators Applied to Variable- Speed Wind-Energy Systems Connected to the Grid," *IEEE Trans. on Energy Conversion,* vol. 21, no. 1, pp. 130-135, 2006.

[69] J. M. S. Pinherio, C. R. R. Dornellas, M. T. Schilling, A. C. G. Melo and J. C. O. Mello, "Probing the new IEEE reliability test system (RTS-96): HL-II assessment," *IEEE Trans. Power Syst,* vol. 13, no. 1, pp. 171-176, Feb 1998.

[70] C. Wang and M. H. Nehrir, "Analytical approaches for optimal placement of distributed generation sources in systems," *IEEE Trans. Power Syst,* vol. 16, no. 4, pp. 2068-2076, Nov 2006.

[71] Z. Chen, J. M. Guerrero and F. Blaabjerg, "A review of the state of the art of power electronics for wind turbines," *IEEE Trans. on Power Electronics,* vol. 24, no. 8, pp. 1859-1875, 2008.

[72] Y. Lei, A. Mullane and G. Lightbody, "Modeling of the wind turbine with a doubly fed induction generator for grid integration studies," *IEEE Trans. on Energy Conversion,* vol. 21, no. 1, pp. 257-264, 2006.

[73] T. Jen-Hao, L. Shang-Wen, L. Dong-Jing and H. Yong-Qing, "Optimal Charging/ Discharging Scheduling of Battrey Storage Systems for Distribution Systems Interconnected With Sizeable PV Generation Systems," *IEEE Transactions on power systems,* vol. 28, no. 2, pp. 1425-1433, 2013.

[74] E. K. Faruk Ugranli, "Multiple Distributed Generation planning under load uncertainty and different penetrationlevels," *Electrical power and energy systems,* vol. 46, pp. 132-144, 2013.

[75] C. J. Kilonzi and N. A. Odero, "A ga/ipso based approach for system loss reduction and voltage profile improvement employing arithmetic crossover and mutation," *International Journal of Engineering Science and Technology (IJEST),* vol. 5, no. 7, pp. 1501- 1510, 2004.

[76] H. Saadat, Power System Analysis, Boston: McGraw-Hill, 2004.

[77] "Grid connection code for Renewable Power Plant (RPP) connected to the electricity Transmission system (TS) or Distribution system (DS) in South Africa," 2012.

[78] A. S. Akinyemi and K. Awodele, "Voltage profiles improvement with wind energy converter connected to a distribution network," in *Southern Africa University Power Engineering Conference SAUPEC*, Johannesburg, 2015.

[79] J. Carpentier, "Contribution a.'l'etude du Dispatching Economique," *Bulletin de la Societe Francaise des Electriciens,* vol. 3, pp. 431-447, 1962.

[80] A. M. Sasson, "Combined Use of the Parallel and Fletcher-Powell Non-Linear Programming Methods for Optimal Load Flows," *IEEE Transactions on Power Apparatus and Systems,* vol. 10, no. 4, pp. 1530-1537, 1969.

[81] R. R. shoult and D. T. Sun, "Optimal Power Flow Based Upon P-Q Decomposition," *IEEE Transactions on Power Apparatus and Systems,* vol. 101, no. 2, pp. 397-405, 1982.

[82] B. F. Wollenberg and W. O. Stadlin, "A Real Time Optimizer for Security Dispatch," *IEEE Transactions on Power Apparatus and Systems,* vol. 96, no. 4, pp. 1640-1649, 1974.

[83] G. F. Raid and L. Hasdorff, "Economic Dispatch Using Quadratic Programming," *IEEE Transactions on Power Apparatus and Systems,* vol. 92, no. 6, pp. 2015- 2023, 1973.

[84] G.F. Reid and L. Hasdorf, "Economic Dispatch Using Quadratic Programming," *IEEE Transactions on Power Apparatus and Systems,* vol. 92, no. 6, pp. 2015-2023, 1973.

[85] S. N. Talukdar, "A Fast and Robust Variable Metric Method for Optimum Power Flows," *IEEE Transactions on Power Apparatus and Systems,* vol. 101, no. 2, pp. 415 - 420, 1982.

[86] G. W. Ault and J.R. McDonald, "Planning for distribution generation within distribution networks in restructuted electricity markets," *IEEE Power Eng. Rev,* vol. 20, no. 2, pp. 52-54, 2000.

[87] W. Graham, A. James and R. Mc-Donald, "Optimal placement of distributed generation sources in power systems," *IEEE Transaction Power System,* vol. 19, no. 5, pp. 127-145, 2000.

[88] A. Kumar and G. Wenzhong, "Voltage Profile Improvement and Line Loss Reduction with Distributed Generation in Deregulated Electricity Markets," in *TENCON IEEE Region 10 Conference*, Hyderabad, 2008.

[89] C. L. Su, "Comparative Analysis of Voltage Control Strategies in Distribution Networks with Distributed Generation," in *IEEE Power & Energy Society General Meeting, PES '09.* , Calgary, AB, 2009.

[90] W. Huang, D. Gan, X. Xia, N. Kobayashi and X. Xu, "Distributed Generation on Distribution System Voltage Regulation: An Optimization-based Approach," in *IEEE Power and Energy Society General Meeting*, Minneapolis, MN, 2010.

[91] D. Issicaba, A. L. Bettiol, J. Coelho and M. V. P. Alcantara, "A New Approach for Optimal Capacitor Placement in Distribution Systems," in *Proceedings of the 6th WSEAS International Conference on Power Systems*, Lisbon, Portugal, 2006.

[92] T. S. Sirish, G. V. Srihara Rao and K. V. S. Ramachandra Murthy, "Optimal Capacitor and DG Placement for Loss Less Distribution on 69- Bus System using KVS – Direct Search Algorithm," *International Journal of Engineering Trends in Electrical and Electronics,* vol. 3, no. 1, pp. 2320-9569, 2013.

[93] M. Karayat, G. V. Srihara Rao, R. K. Kenguva and K. V. S. Ramachandra Murthy, "Optimal Capacitor and Type -2 DG Placement using Modified KVS – Direct Search Algorithm for Loss Less Distribution," *International Journal of Engineering Trends in Electrical and Electronics,* vol. 3, no. 1, pp. 2320-9569, 2013.

[94] D.T. Le and M.A. Kashem, "Maximising Voltage Support in Distribution Systems by Distributed Generation," in *Australian Research Council and Aurora Energy*, Tasmania, 2007.

[95] A. Volkanovski, M. Cepin and M. Borut , "Optimization of reactive power compensation in distribution network," *Elektrotehniški vestnik,* vol. 76, no. 2, pp. 57-62, 2009.

[96] A. Keane, L. F. Nando. O. E. Vittal, J.Chris and G. P. Harrison, "Enhanced Utilization of Voltage Control Resources With Distributed Generation," in *IEEE Power and Energy Society General Meeting*, San Diego, CA, 2011.

[97] J. Kennedy and R. Eberhart, "A modified particle swarm optimizer," in *Evolutionary Computation Proceedings IEEE World Congress on Computational Intelligence The 1998 IEEE International Conference on ,*, Anchorage, AK, 1998.

[98] D. Sedighizadeh and E. Masehian, "Particle Swarm Optimization Methods, Taxonomy and Applications," *International Journal of Computer Theory and Engineering,* vol. 1, no. 5, pp. 486-502, 2009.

[99] Y. Alinejad-Beromi, M. Sedighizadeh, M. Sadighi, "A particle swarm optimization for sitting and sizing of Distributed Generation in distribution network to improve voltage profile and reduce THD and losses," in *43rd International Universities Power Engineering Conference, UPEC* , Padova, 2008.

[100] M. Sedighi, A. Igderi and A. Parastar, "Sitting and sizing of distributed generation in distribution network to improve of several parameters by PSO algorithm," in *IPEC, Conference Proceedings*, Singapore, 2010.

[101] O. Amanifar, "Optimal distribution generation placement and sizing for loss and THD reduction and voltage profile improvement in distribution systems using PSO and sensitivity analysis," in *16th Conference on Electrical Power Distribution Networks, EPDC*, Bandar Abbas, 2011.

[102] A. P. Kai Zou, K. M. Agalgaonkar, K. M. Muttaqi and S. Perera, "Voltage Support by Distributed Generation Units and Shunt Capacitors in Distribution Systems," in *IEEE Power & Energy Society General Meeting, PES* , Calgary, AB, 2009.

[103] I. Ziari, G. Ledwich, A. Ghosh and G. Platt, "A New Method for Improving Reliability and Line Loss in Distribution Networks," in *20th Australasian Universities Power Engineering Conference AUPEC*, Christchurch, December 2010.

[104] N. Jain, S.N. Singh and S.C. Srivastava, "Particle Swarm Optimization Based Optimal Siting and Sizing of Multiple Distributed Generators," in *IEEE Power and Energy Society General Meeting*, San Diego, CA, 2011.

[105] K. Varesi, "Optimal Allocation of DG Units for Power Loss Reduction and Voltage Profile Improvement of Distribution Networks using PSO Algorithm," *World Academy of Science, Engineering and Technology,* vol. 5, pp. 12-26, 2011.

[106] M. Mohammad and M. A. Nasab,, "PSO Based Multiobjective Approach for Optimal Sizing and Placement of Distributed Generation," *Research Journal of Applied Sciences,Engineering and Technology,* vol. 2, no. 8, pp. 832-837, 2011.

[107] J. J. Jamian, M.W. Mustafa, H. Mokhlis and M. A. Baharudin, "Implementation of Evolutionary Particle Swarm Optimization in Distributed Generation Sizing," *International Journal of Electrical and Computer Engineering,* vol. 2, no. 1, pp. 137-146, February 2012.

[108] A. Afraz, F. Malekinezhad, S. J. S. Shenava and A. Jlili, "Optimal Sizing and Sitting in Radial Standard System using PSO," *American Journal of Scientific Research,* vol. 4, no. 67, pp. 50-58, 2012.

[109] N. A. Khan, S. Ghosh and S. P. Ghoshal, "Optimal siting and sizing of shunt capacitors in radial distribution systems using Novel BPSO algorithm," *International Journal of Emerging Technology and Advanced Engineering,* vol. 3, no. 2, pp. 220-225, 2013.

[110] M. Heydari, S.M. Hosseini, and S.A. Gholamian, "Optimal Placement and Sizing of Capacitor and Distributed Generation with Harmonic and Resonance Considerations Using Discrete Particle Swarm Optimization," *International Journal of Intelligent Systems and Applications,* vol. 5, no. 7, pp. 42-49, 2013.

[111] D. C. Hong and D. Wenliang, "Multi-objective optimal allocation of distributed generation in smart grid," in *2011 International Conference on Electrical and Control Engineering (ICECE)*, Yichang, 2011.

[112] S. F. Abu-Mouti, E. Mohamed and El-Hawary, "Overview of Artificial Bee Colony (ABC) Algorithm and Its Applications," in *International Systems Conference (SysCon), 2012* , Vancouver, BC, 2012.

[113] D. Karaboga, "An Idea based on Honey Bee Swarm for Numerical Optimization," Erciyes University, Engineering Faculty, Kayseri/Türkiye, 2005.

[114] D. Karaboga and B. Basturk,, "A Powerful and Efficient Algorithm for Numerical Function Optimization:Artificial Bee Colony (ABC) Algorithm," *Artificial Bee Colony (ABC) Algorithm,* vol. 39, no. 3, pp. 459-471, 2007.

[115] D. Karaboga and B. Basturk, "Artificial Bee Colony (ABC) Optimization Algorithm for Solving Constrained Optimization Problems," *Foundations of Fuzzy Logic and Soft Computing,* vol. 24, no. 6, pp. 789-798, 2007.

[116] M. F. Mustafar, I. Musirin, M. R. Kalil, and M. K. Idris, "Ant colony optimization (ABC) based technique for voltage control and loss minimization using transformer tap setting," in *5th Student Conference on Research and Development*, Selangor, Malaysia, 2007.

[117] F. S. El-Hawary and M. E. Abu-Mouti, "Heuristic curve-fitted technique for distributed generation optimisation in radial distribution feeder systems," *Generation, Transmission & Distribution, IET.,* vol. 5, no. 2, pp. 172-180, 2011.

[118] K. Rayudu, A. Jayalaxmi, G. Yesuratnam, and Y.D. Kumar., "Multi objective comparison of GA and IPSO techniques for generator reactive power optimization," in *IEEE Fifth Power India Conference*, India, 2012.

[119] N. Nimpitiwan and C. Chaiyabut, "Centralized control of system voltage/reactive power using genetic algorithm," in *International Conference on Intelligent Systems Applications to Power Systems*, Toki Messe, Niigata , 2007.

[120] R. Hooshmand and M. Ataei, "Real-Coded Genetic Algorithm Applied to Optimal Placement of Capacitor Banks for Unbalanced Distribution Systems with Meshed/Radial Configurations," *International Energy Journal,* vol. 8, no. 1, pp. 51-62, 2007.

[121] H. Rahmat-Allah and M. Ataei, "Optimal capacitor placement in actual configuration and operational conditions of distribution systems using RCGA," *Journal of Electrical Engineering,* vol. 58, no. 4, pp. 187-199, 2007.

[122] S.Jalilzadeh, S. Galvani, H. Hosseinian, and F.Razavi, "Voltage Profile Modification using Genetic Algorithm in Distribution Systems," in *Proceedings of the World Congress on Engineering and Computer Science (WCECS) 2007*, San Francisco, USA, 2007.

[123] Y. Alinejad-Beromi, M. Sedighizadeh, M. R. Bayat and M. E. Kohadaya, "Using genetic algorithm for distribution generation allocation to reduce losses and improve voltage profile," in *42nd International Universities Power Engineering Conference (UPEC)* , Brighton, 2007.

[124] D. Lawrence, Handbook of genetic Algorithm, United State of America: International Thomson Computer Press, 1996.

[125] M. Gandomkar, M. Vakilian, and M. Ehsan, "A combination of genetic algorithm and simulated annealing for optimal DG allocation in distribution networks," in *Canadian Conference on Electrical and Computer Engineering*, Saskatoon, Sask, 2005.

[126] Y. M. Ashari and A. Soeprijanto, "Optimal Distributed Generation (DG) Allocation for Losses Reduction Using Improved Particle Swarm Optimization (IPSO) Method," *Journal of Basic. Applied Scientific Research,* vol. 2, no. 7, pp. 7016-7023, 2012.

[127] T. N. Shukla, S.P. Singh, K. B. Naik, "Allocation of optimal distributed generation using GA for minimum system losses in radial distribution networks," *International Journal of Engineering, Science and Technology,* vol. 2, no. 3, pp. 94-106, 2010.

[128] S. Boyerahmadi, M. P. Movahed , "Evaluation of Power Loss Reduction with the place of Shunt Capacitors and Distributed Generation Power Plant in the Radial Distribution Systems using Genetic Algorithms," *American Journal Of Advanced Scientific Research,* vol. 1, no. 6, pp. 278-283, 2013.

[129] K. Deb, Optimization for Engineering Design: Algorithm and Examples, New Delhi: Prentice Hall of India Ltd., 1995.

[130] D. E. Goldenberg, Genetic Algorithm in Search, Optimization and Machine Learning, Wesley Publishing Co. Inc, 1989.

[131] H. Zareipour, K. Bhattacharya and C.A. Canizares, "Distributed generation: Current status and challenges," in *IEEE Proceedings of NAPS*, 2004 .

[132] Mathworks, "http://www.mathworks.com/help/toolbox/gads/f6174dfi10.html.," [Online].

[133] T. Hsien-Yu, "A genetic algorithm for assessing flatness in automated manufacturing Systems," © *Springer Science+Business Media, LLC 2006,* pp. 301-306, 2006.

[134] V. M.Jegadeesan, "Optimal Sizing and Placement of Distributed Generation in Radial Distribution Feeder Using Analytical Approach," *2014 International Conference on Innovations in Engineering and Technology ,* vol. 3, no. 3, pp. 358-364, 2014.

[135] W. El-Khattam and M. M. A. Salama, "Distributed generation technologies, definitions and benefits," *Electr. Power Syst. Res,* vol. 71, no. 2, pp. 119-128, 2004.

[136] A. Azmy, "Simulation and management of distributed generating units using," Fachbereich Ingenieurwissenschaften, Universitat, Duisburg-Essen, Duisburg., 2005 Phd.

[137] El-Khattam W. and Salama, M. M. A., "Distributed generation technologies,definitions and benefits," *Electric power systems research,,* vol. 71, no. 2, p. 119–128, 2004.

# Appendices

## Appendix I

Line diagram of 33-bus distribution System

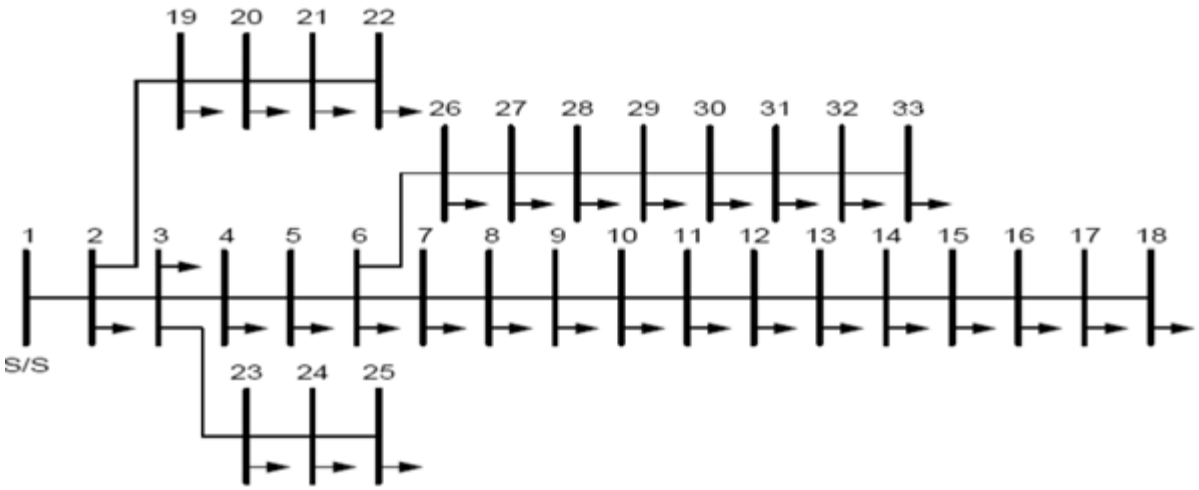


## Appendix II

Table. AI Load data for 33-bus distribution system

| Bus No | $P_L$(kW) | $Q_L$(kVAR) | Bus No | $P_L$(kW) | $Q_L$(kVAR) |
|---|---|---|---|---|---|
| **2** | 100 | 60 | 18 | 90 | 40 |
| **3** | 90 | 40 | 19 | 90 | 40 |
| **4** | 120 | 80 | 20 | 90 | 40 |
| **5** | 60 | 30 | 21 | 90 | 40 |
| **6** | 60 | 20 | 22 | 90 | 40 |
| **7** | 200 | 100 | 23 | 90 | 40 |
| **8** | 200 | 100 | 24 | 420 | 200 |
| **9** | 60 | 20 | 25 | 420 | 200 |
| **10** | 60 | 20 | 26 | 60 | 25 |
| **11** | 45 | 30 | 27 | 60 | 25 |
| **12** | 60 | 35 | 28 | 60 | 20 |
| **13** | 60 | 35 | 29 | 120 | 70 |
| **14** | 120 | 80 | 30 | 200 | 100 |
| **15** | 60 | 10 | 31 | 150 | 70 |

| | | | | | |
|---|---|---|---|---|---|
| **16** | 60 | 20 | 32 | 210 | 100 |
| **17** | 60 | 20 | 33 | 60 | 40 |

## Appendix III

Table I Branch data for 33-bus distribution system

| Branch Number | Sending end bus | Receiving end bus | R (Ω) | X (Ω) |
|---|---|---|---|---|
| **1** | 1 | 2 | 0.0922 | 0.0470 |
| **2** | 2 | 3 | 0.4930 | 0.2512 |
| **3** | 3 | 4 | 0.3661 | 0.1864 |
| **4** | 4 | 5 | 0.3811 | 0.1941 |
| **5** | 5 | 6 | 0.8190 | 0.7070 |
| **6** | 6 | 7 | 0.1872 | 0.6188 |
| **7** | 7 | 8 | 0.7115 | 0.2351 |
| **8** | 8 | 9 | 1.0299 | 0.7400 |
| **9** | 9 | 10 | 1.0440 | 0.7400 |
| **10** | 10 | 11 | 0.1967 | 0.0651 |
| **11** | 11 | 12 | 0.3744 | 0.1298 |
| **12** | 12 | 13 | 1.4680 | 1.1549 |
| **13** | 13 | 14 | 0.5416 | 0.7129 |
| **14** | 14 | 15 | 0.5909 | 0.5260 |
| **15** | 15 | 16 | 0.7462 | 0.5449 |
| **16** | 16 | 17 | 1.2889 | 1,7210 |
| **17** | 17 | 18 | 0.7320 | 0.5739 |
| **18** | 2 | 19 | 0.1640 | 0.1565 |
| **19** | 19 | 20 | 1.5042 | 1.3555 |
| **20** | 20 | 21 | 0.4095 | 0.4784 |
| **21** | 21 | 22 | 0.7089 | 0.9373 |
| **22** | 3 | 23 | 0.4512 | 0.3084 |
| **23** | 23 | 24 | 0.8980 | 0.7091 |
| **24** | 24 | 25 | 0.8959 | 0.7071 |
| **25** | 6 | 26 | 0.2031 | 0.1034 |
| **26** | 26 | 27 | 0.2842 | 0.1447 |
| **27** | 27 | 28 | 1.0589 | 0.9338 |
| **28** | 28 | 29 | 0.8043 | 0.7006 |
| **29** | 29 | 30 | 0.5074 | 0.2585 |
| **30** | 30 | 31 | 0.9745 | 0.9629 |
| **31** | 31 | 32 | 0.3105 | 0.3619 |
| **32** | 32 | 33 | 0.3411 | 0.5302 |
| **34** | 8 | 21 | 2.0000 | 2.0000 |
| **35** | 9 | 15 | 2.0000 | 2.0000 |
| **36** | 12 | 22 | 2.0000 | 2.0000 |
| **37** | 18 | 33 | 0.5000 | 0.5000 |
| **33** | 25 | 29 | 0.5000 | 0.5000 |

## Appendix IV

Table IV Branch data for Western Cape Network

| Branch Number | Sending end bus | Receiving end bus | R (**Ω**) | X (**Ω**) |
|---|---|---|---|---|
| **1** | 11 | 12 | 0.00231 | 0.00240 |
| **2** | 12 | 13 | 0.00272 | 0.03063 |
| **3** | 13 | 14 | 0.00421 | 0.00255 |
| **4** | 14 | 20 | 0.00229 | 0.02566 |
| **5** | 20 | 21 | 0.00519 | 0.05710 |
| **6** | 20 | 22 | 0.00240 | 0.02526 |
| **7** | 20 | 24 | 0.00240 | 0.02546 |
| **8** | 20 | 26 | 0.00332 | 0.03726 |
| **9** | 25 | 30 | 0.00220 | 0.02341 |
| **10** | 30 | 31 | 0.00304 | 0.03241 |
| **11** | 31 | 32 | 0.00357 | 0.03888 |
| **12** | 32 | 33 | 0.00147 | 0.01594 |
| **13** | 32 | 37 | 0.00353 | 0.04285 |
| **14** | 32 | 40 | 0.00185 | 0.02083 |
| **15** | 40 | 41 | 0.00079 | 0.00905 |
| **16** | 40 | 50 | 0.00069 | 0.00785 |
| **17** | 50 | 51 | 0.00170 | 0.01690 |
| **18** | 51 | 52 | 0.00299 | 0.03139 |

## Appendix V

Table. AV Load data for Western Cape Network

| **Bus No** | $P_L$ **(kW)** | $Q_L$ **(kVAR)** | **Bus No** | $P_L$ **(kW)** | $Q_L$(kVAR) |
|---|---|---|---|---|---|
| **1** | 10 | 15 | 10 | 30 | 20 |
| **2** | 20 | 10 | 11 | 15 | 15 |
| **3** | 30 | 10 | 12 | 20 | 12 |
| **4** | 25 | 12 | 13 | 40 | 19 |
| **5** | 20 | 17 | 14 | 40 | 26 |
| **6** | 20 | 12 | 15 | 20 | 10 |
| **7** | 16 | 14 | 16 | 24 | 16 |
| **8** | 12 | 8 | 17 | 20 | 12 |
| **9** | 20 | 15 | 18 | 18 | 10 |

## Appendix VI

Modified Western Cape Network

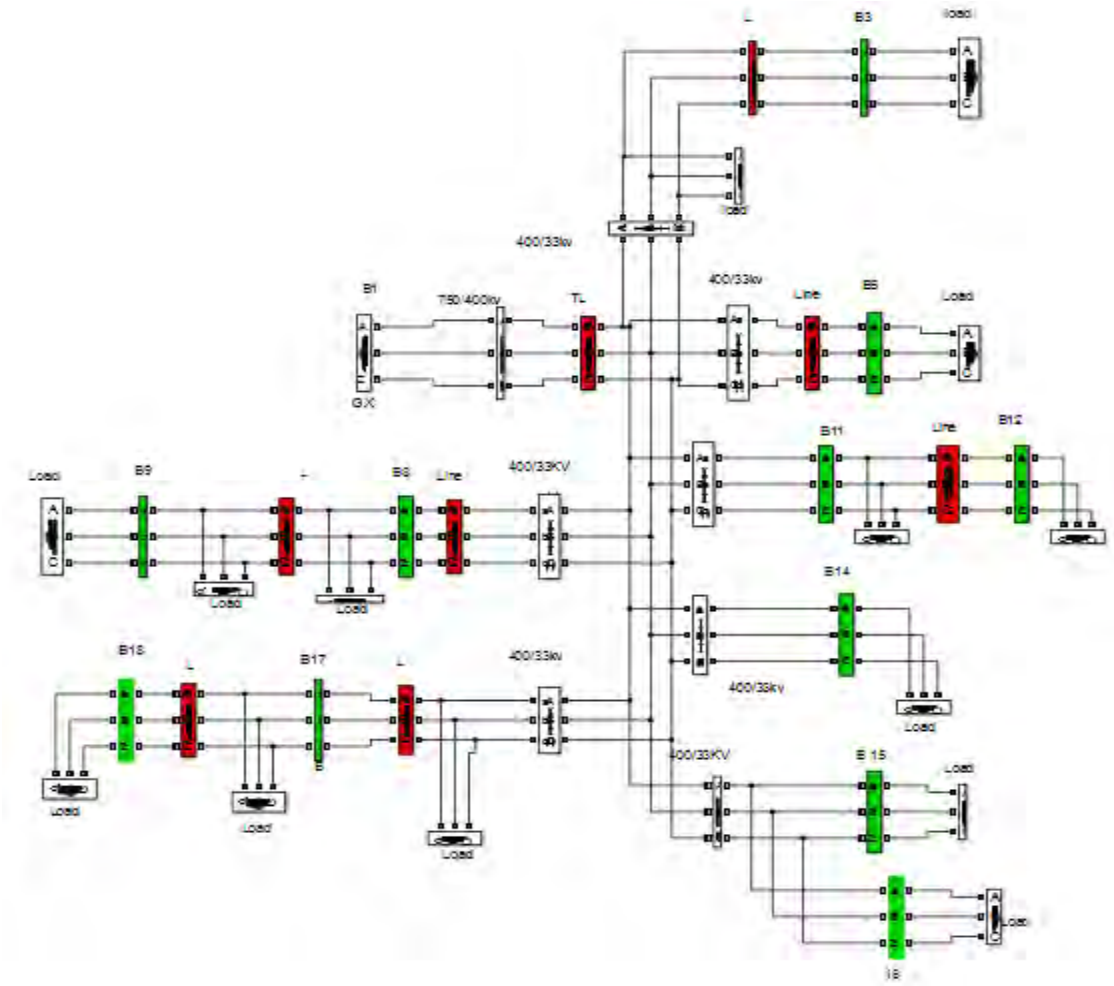

**Details of Western Cape Network Model Investigated**

It is an 18-bus system containing a source voltage which is modelled as an infinite bus and local loads. The transformers are used to step down the voltage to local load voltage values such as 33 KV. After load flow, total real power loss is 180 kW, while the total reactive power loss is 40 kVAR. The following are the fact about the system**:**

- Bus 10 contains the source voltage and is modelled as an infinite bus since most of the power supplied to the network is from an external source
- Local loads are connected by step down transformers at the load bus bars
- The voltage at the distribution level in the network is constant. i.e. 33 kV
- The loads were modelled as constant power loads.

The external grid was assumed to represent the rest of the Eskom grid to which the 400 kV network is connected. The base case voltage profile is shown below in Figure 7.10.

**Appendix VII**

**Power Flow Sensitivity Factor Formulation**

The equation below gives the change in real and reactive power flow.

$$\begin{bmatrix}\Delta P_{ij}\\ \Delta Q_{ij}\end{bmatrix}=\begin{bmatrix}\frac{\partial P_{ij}}{\partial \delta} & \frac{\partial P_{ij}}{\partial V}\\ \frac{\partial Q_{ij}}{\partial \delta} & \frac{\partial Q_{ij}}{\partial V}\end{bmatrix}[J]^{-1}\begin{bmatrix}\Delta P\\ \Delta Q\end{bmatrix}$$

Using this equation the real and reactive power flow sensitivity factors can be determined

$$\begin{bmatrix}\Delta P_{ij}\\ \Delta Q_{ij}\end{bmatrix}=\begin{bmatrix}\frac{\partial P_{ij}}{\partial \delta} & \frac{\partial P_{ij}}{\partial V}\\ \frac{\partial Q_{ij}}{\partial \delta} & \frac{\partial Q_{ij}}{\partial V}\end{bmatrix}\begin{bmatrix}J_{11}^{*} & J_{12}^{*}\\ J_{21}^{*} & J_{22}^{*}\end{bmatrix}\begin{bmatrix}\Delta P\\ \Delta Q\end{bmatrix}$$

$$=\begin{bmatrix}\frac{\partial P_{ij}}{\partial \delta} & \frac{\partial P_{ij}}{\partial V}\\ \frac{\partial Q_{ij}}{\partial \delta} & \frac{\partial Q_{ij}}{\partial V}\end{bmatrix}\begin{bmatrix}J_{11}^{*}\Delta P_n + J_{12}^{*}\Delta Q_n\\ J_{21}^{*}\Delta P_n + J_{22}^{*}\Delta Q_n\end{bmatrix}$$

$$=\begin{bmatrix}\frac{\partial P_{ij}}{\partial \delta}(J_{11}^{*}\Delta P_n + J_{12}^{*}\Delta Q_n) + \frac{\partial P_{ij}}{\partial V}(J_{21}^{*}\Delta P_n + J_{22}^{*}\Delta Q_n)\\ \frac{\partial Q_{ij}}{\partial \delta}(J_{11}^{*}\Delta P_n + J_{12}^{*}\Delta Q_n) + \frac{\partial Q_{ij}}{\partial V}(J_{21}^{*}\Delta P_n + J_{22}^{*}\Delta Q_n)\end{bmatrix}$$

From the above matrix the changes in real and reactive power losses can now be expressed as;

$$\Delta P_{ij} = J_{11}^{*}\Delta P_n \frac{\partial P_{ij}}{\partial \delta} + J_{12}^{*}\Delta Q_n \frac{\partial P_{ij}}{\partial \delta} + J_{21}^{*}\Delta P_n \frac{\partial P_{ij}}{\partial V} + J_{22}^{*}\Delta Q_n \frac{\partial P_{ij}}{\partial V}$$

$$\Delta Q_{ij} = J_{11}^{*}\Delta P_n \frac{\partial Q_{ij}}{\partial \delta} + J_{12}^{*}\Delta Q_n \frac{\partial Q_{ij}}{\partial \delta} + J_{21}^{*}\Delta P_n \frac{\partial Q_{ij}}{\partial V} + J_{22}^{*}\Delta Q_n \frac{\partial Q_{ij}}{\partial V}$$

From the above two equations we deduce that;

$$\frac{\Delta P_{ij}}{\Delta P_n} \cong \frac{\partial P_{ij}}{\partial P_n} = J_{11}^{*}\frac{\partial P_{ij}}{\partial \delta} + J_{21}^{*}\frac{\partial P_{ij}}{\partial V}$$

$$\frac{\Delta P_{ij}}{\Delta Q_n} \cong \frac{\partial P_{ij}}{\partial Q_n} = J_{12}^{*}\frac{\partial P_{ij}}{\partial \delta} + J_{22}^{*}\frac{\partial P_{ij}}{\partial V}$$

$$\frac{\Delta Q_{ij}}{\Delta Q_n} \cong \frac{\partial Q_{ij}}{\partial Q_n} = J_{12}^{*}\frac{\partial Q_{ij}}{\partial \delta} + J_{22}^{*}\frac{\partial Q_{ij}}{\partial V}$$

$$\frac{\Delta Q_{ij}}{\Delta P_n} \cong \frac{\partial Q_{ij}}{\partial P_n} = J_{11}^{*}\frac{\partial Q_{ij}}{\partial \delta} + J_{21}^{*}\frac{\partial Q_{ij}}{\partial V}$$

These equations can be re-arranged as shown below

$$\begin{bmatrix} \frac{\partial P_{ij}}{\partial P_n} \\ \frac{\partial P_{ij}}{\partial Q_n} \end{bmatrix} = \begin{bmatrix} F_{P-P} \\ F_{P-Q} \end{bmatrix} = \begin{bmatrix} J_{11}^* J_{12}^* \\ J_{21}^* J_{22}^* \end{bmatrix}^{-1} \begin{bmatrix} \frac{\partial P_{ij}}{\partial \delta} \\ \frac{\partial P_{ij}}{\partial V} \end{bmatrix} = [J^T]^{-1} \begin{bmatrix} \frac{\partial P_{ij}}{\partial \delta} \\ \frac{\partial P_{ij}}{\partial V} \end{bmatrix}$$

$$\begin{bmatrix} \frac{\partial Q_{ij}}{\partial P_n} \\ \frac{\partial Q_{ij}}{\partial Q_n} \end{bmatrix} = \begin{bmatrix} F_{Q-P} \\ F_{Q-Q} \end{bmatrix} = \begin{bmatrix} J_{11}^* J_{12}^* \\ J_{21}^* J_{22}^* \end{bmatrix}^{-1} \begin{bmatrix} \frac{\partial Q_{ij}}{\partial \delta} \\ \frac{\partial Q_{ij}}{\partial V} \end{bmatrix} = [J^T]^{-1} \begin{bmatrix} \frac{\partial Q_{ij}}{\partial \delta} \\ \frac{\partial Q_{ij}}{\partial V} \end{bmatrix}$$

where,

$F_{P-P}$ is the real power flow sensitivity related to the real power injection.

$F_{P-Q}$ is the active flow sensitivity related to the reactive power injection.

$F_{Q-P}$ is the reactive power flow sensitivity related to the active power injection.

$F_{Q-Q}$ is the reactive power flow sensitivity related to the reactive power injection.

$J$ is the Jacobian matrix of power flow, and the superscript $T$ indicates the transpose

**Appendix VIII.**

**The equation below gives the change in real and reactive power losses.**

$$\begin{bmatrix}\Delta P_{L(ij)}\\ \Delta Q_{L(ij)}\end{bmatrix} = \begin{bmatrix}\frac{\partial P_{L(ij)}}{\partial \delta} & \frac{\partial P_{L(ij)}}{\partial V}\\ \frac{\partial Q_{L(ij)}}{\partial \delta} & \frac{\partial Q_{L(ij)}}{\partial V}\end{bmatrix} [J]^{-1} \begin{bmatrix}\Delta P\\ \Delta Q\end{bmatrix}$$

Using this equation the real and reactive power loss sensitivity factors can be determined. We have;

$$\begin{bmatrix}\Delta P_{L(ij)}\\ \Delta Q_{L(ij)}\end{bmatrix} = \begin{bmatrix}\frac{\partial P_{L(ij)}}{\partial \delta} & \frac{\partial P_{L(ij)}}{\partial V}\\ \frac{\partial Q_{L(ij)}}{\partial \delta} & \frac{\partial Q_{L(ij)}}{\partial V}\end{bmatrix} \begin{bmatrix}J_{11}^{*} & J_{12}^{*}\\ J_{21}^{*} & J_{22}^{*}\end{bmatrix} \begin{bmatrix}\Delta P\\ \Delta Q\end{bmatrix}$$

$$= \begin{bmatrix}\frac{\partial P_{L(ij)}}{\partial \delta} & \frac{\partial P_{L(ij)}}{\partial V}\\ \frac{\partial Q_{L(ij)}}{\partial \delta} & \frac{\partial Q_{L(ij)}}{\partial V}\end{bmatrix} \begin{bmatrix}J_{11}^{*}\Delta P_n + J_{12}^{*}\Delta Q_n\\ J_{21}^{*}\Delta P_n + J_{22}^{*}\Delta Q_n\end{bmatrix}$$

$$= \begin{bmatrix}\frac{\partial P_{L(ij)}}{\partial \delta}\left(J_{11}^{*}\Delta P_n + J_{12}^{*}\Delta Q_n\right) + \frac{\partial P_{L(ij)}}{\partial V}\left(J_{21}^{*}\Delta P_n + J_{22}^{*}\Delta Q_n\right)\\ \frac{\partial Q_{L(ij)}}{\partial \delta}\left(J_{11}^{*}\Delta P_n + J_{12}^{*}\Delta Q_n\right) + \frac{\partial Q_{L(ij)}}{\partial V}\left(J_{21}^{*}\Delta P_n + J_{22}^{*}\Delta Q_n\right)\end{bmatrix}$$

From the above matrix the changes in real and reactive power losses can now be expressed as;

$$\Delta P_{L(ij)} = J_{11}^{*}\Delta P_n \frac{\partial P_{L(ij)}}{\partial \delta} + J_{22}^{*}\Delta Q_n \frac{\partial P_{L(ij)}}{\partial \delta} + J_{21}^{*}\Delta P_n \frac{\partial P_{L(ij)}}{\partial V} + J_{22}^{*}\Delta Q_n \frac{\partial P_{L(ij)}}{\partial V}$$

$$\Delta Q_{L(ij)} = J_{11}^{*}\Delta P_n \frac{\partial Q_{L(ij)}}{\partial \delta} + J_{22}^{*}\Delta Q_n \frac{\partial Q_{L(ij)}}{\partial \delta} + J_{21}^{*}\Delta P_n \frac{\partial Q_{L(ij)}}{\partial V} + J_{22}^{*}\Delta Q_n \frac{\partial Q_{L(ij)}}{\partial V}$$

From the above two equations we deduce that

$$\frac{\Delta P_{L(ij)}}{\Delta P_n} \cong \frac{\partial P_{L(ij)}}{\partial P_n} = J_{11}^{*}\frac{\partial P_{L(ij)}}{\partial \delta} + J_{21}^{*}\frac{\partial P_{L(ij)}}{\partial V}$$

$$\frac{\Delta P_{L(ij)}}{\Delta Q_n} \cong \frac{\partial P_{L(ij)}}{\partial Q_n} = J_{12}^{*}\frac{\partial P_{L(ij)}}{\partial \delta} + J_{22}^{*}\frac{\partial P_{L(ij)}}{\partial V}$$

$$\frac{\Delta Q_{L(ij)}}{\Delta Q_n} \cong \frac{\partial Q_{L(ij)}}{\partial Q_n} = J_{12}^{*}\frac{\partial Q_{L(ij)}}{\partial \delta} + J_{22}^{*}\frac{\partial Q_{L(ij)}}{\partial V}$$

$$\frac{\Delta Q_{L(ij)}}{\Delta P_n} \cong \frac{\partial Q_{L(ij)}}{\partial Q_n} = J_{11}^{*}\frac{\partial Q_{L(ij)}}{\partial \delta} + J_{21}^{*}\frac{\partial Q_{L(ij)}}{\partial V}$$

These equations can be re-arranged as shown below;

$$\begin{bmatrix} \frac{\Delta P_{L(ij)}}{\Delta P_n} \\ \frac{\Delta P_{L(ij)}}{\Delta Q_n} \end{bmatrix} = \begin{bmatrix} S_{P-P} \\ S_{P-Q} \end{bmatrix} = \begin{bmatrix} J_{11}^* & J_{12}^* \\ J_{21}^* & J_{22}^* \end{bmatrix}^{-1} \begin{bmatrix} \frac{\partial P_{L(ij)}}{\partial \delta} \\ \frac{\partial P_{L(ij)}}{\partial V} \end{bmatrix} = [J]^{-1} \begin{bmatrix} \frac{\partial P_{L(ij)}}{\partial \delta} \\ \frac{\partial P_{L(ij)}}{\partial V} \end{bmatrix}$$

$$\begin{bmatrix} \frac{\Delta Q_{L(ij)}}{\Delta P_n} \\ \frac{\Delta Q_{L(ij)}}{\Delta Q_n} \end{bmatrix} = \begin{bmatrix} S_{Q-P} \\ S_{Q-Q} \end{bmatrix} = \begin{bmatrix} J_{11}^* & J_{12}^* \\ J_{21}^* & J_{22}^* \end{bmatrix}^{-1} \begin{bmatrix} \frac{\partial Q_{L(ij)}}{\partial \delta} \\ \frac{\partial Q_{L(ij)}}{\partial V} \end{bmatrix} = [J]^{-1} \begin{bmatrix} \frac{\partial Q_{L(ij)}}{\partial \delta} \\ \frac{\partial Q_{L(ij)}}{\partial V} \end{bmatrix}$$

Where;

$S_{P-P}$ is the real power loss sensitivity related to the real power injection.

$S_{P-Q}$ is the active loss sensitivity related to the reactive power injection.

$S_{Q-P}$ is the reactive power loss sensitivity related to the active power injection.

$S_{Q-Q}$ is the reactive power loss sensitivity related to the reactive power injection.

*J* is the Jacobian matrix of power flow, and the superscript *T* indicates the transpose

## Appendix IX

**The total system power loss is formulated as follows**

$$P_{loss} + jQ_{loss} = \sum_{i=1}^{n} V_i I_i^* \quad (1)$$

where $V_i$ and $I_i$ are the voltage and current of $i$th bus, and $Q_{loss}$ is the total reactive power losses. The expression for the bus voltage in terms of the bus current can be derived simply as

$$V_i = \sum_{j=1}^{n} I_j Z_{ij} \quad \text{for} \quad i = 1,2,\ldots\ldots,n \quad (2)$$

where $Z_{ij}$ is the $ij$th element of the bus impedance matrix. The inclusion of shunt branch parameters into the mathematical model is carried out by using bus admittance matrix.

$$P_{loss} + jQ_{loss} = \sum_{i=1}^{n} \sum_{j=1}^{n} I_j Z_{ij} I_i^* \quad (3)$$

To separate the active and reactive components of the power loss, bus current and impedance should be written as complex variables.

$$P_{loss} + jQ_{loss} = \sum_{i=1}^{n} \sum_{j=1}^{n} [(I_{pj} + jI_{qj})(R_{ij} + jX_{ij})(I_{pi} - jI_{qi})] \quad (4)$$

where $I_p$ and $I_q$ are the active and reactive components of the bus current, respectively. R and X are the resistance and reactance of the bus impedance matrix. The power loss equation can be separated into its real and imaginary parts as follows:

$$P_{loss} = \sum_{i=1}^{n} \sum_{j=1}^{n} [R_{ij}(I_{pj}I_{pi} + I_{qj}I_{qi})] \quad (5)$$

$$Q_{loss} = \sum_{i=1}^{n} \sum_{j=1}^{n} [X_{ij}(I_{pj}I_{pi} + I_{qj}I_{qi})] \quad (6)$$

In (8) and (9), the bus currents should be expressed in respect of voltage and power injection by using the complex power equation which is expressed as follows:

$$P_i + jQ_i = V_i^* I_i \quad (7)$$

where Pi and Qi are real and reactive power injection in bus $i$, respectively. The bus voltage in this equation is expressed as

$$V_i = |V_i|(\cos(\delta_i) + jsin(\delta_i)) \quad (8)$$

where $\delta_i$ is angle of the bus $i$ which is the phase angle difference between bus $i$ and reference bus (slack bus). By substituting (8) into (7), the bus current expression is obtained as

$$I_i = \frac{1}{|V_i|}(P_i\cos(\delta_i) + Q_i sin(\delta_i) + jP_i sin(\delta_i) - jQ_i \cos(\delta_i)) \quad (9)$$

Finally, (9) is broken into its real and imaginary parts as follows:

$$I_{pi} = \frac{1}{|V_i|}(P_i cos(\delta_i) + Q_i sin(\delta_i)) \quad (10)$$

$$I_{qi} = \frac{1}{|V_i|}(P_i sin(\delta_i) - Q_i \cos(\delta_i)) \quad (11)$$

By substituting (10) and (11) into (5), "the exact loss formula" can be obtained simply as follows:

$$P_{loss} = \sum_{i=1}^{n} \sum_{j=1}^{n} [a_{ij}(P_i P_j + Q_i Q_j) + b_{ij}(Q_i P_j - P_i Q_j)] \quad (12)$$

where,

$$a_{ij} = \frac{R_{ij}}{V_i V_j} \cos(\delta_i - \delta_j) \quad (13)$$

$$b_{ij} = \frac{R_{ij}}{V_i V_j} \sin(\delta_i - \delta_j) \quad (14)$$

Consequently, the exact reactive power loss is given by

$$Q_{loss} = \sum_{i=1}^{n} \sum_{j=1}^{n} [c_{ij}(P_i P_j + Q_i Q_j) + d_{ij}(Q_i P_j - P_i Q_j)] \quad (15)$$

where,

$$c_{ij} = \frac{X_{ij}}{V_i V_j} * \cos(\delta_i - \delta_j) \quad (16)$$

$$d_{ij} = \frac{X_{ij}}{V_i V_j} * \sin(\delta_i - \delta_j) \quad (17)$$

$n$ is the bus number

$a_{ij}$, $b_{ij}$, $c_{ij}$ and $d_{ij}$ are function of loss coefficient between bus $i$ $and$ $j$.

$P_i$ is real power flow at bus in kW

$Q_i$ is reactive power flow at bus $i$ in kVAR

$P_j$ is real power flow at bus j in kW

$Q_j$ is reactive power flow at bus j in kVAR

$R_{ij}$ is Resistance of the line connecting bus i and j in Ohms

$X_{ij}$ is Reactance of the line connecting bus i and j in Ohms

$V_i$ $and$ $V_j$ are bus voltage magnitude at bus i and j in PU

$\delta_i$ $and$ $\delta_j$ are bus voltage angle at bus i and j [134]

## Appendix X

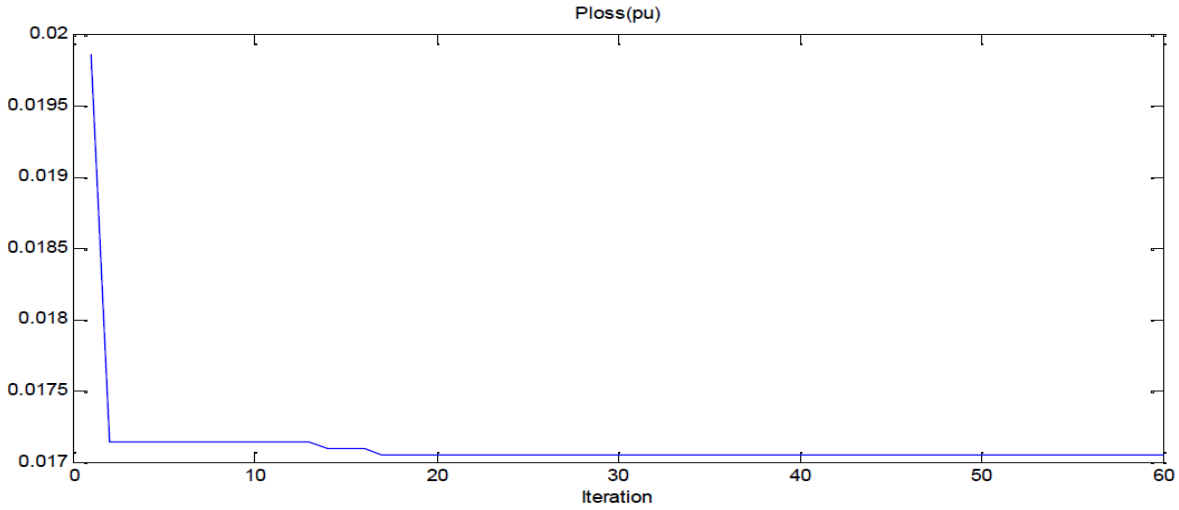


A convergence characteristic for GA-IPSO.

## EBE Faculty: Assessment of Ethics in Research Projects (Rev2)

Any person planning to undertake research in the Faculty of Engineering and the Built Environment at the University of Cape Town is required to complete this form before collecting or analysing data. When completed it should be submitted to the supervisor (where applicable) and from there to the Head of Department. If any of the questions below have been answered YES, and the applicant is NOT a fourth year student, the Head should forward this form for approval by the Faculty EIR committee: submit to Ms Zulpha Geyer (Zulpha.Geyer@uct.ac.za; Chem Eng Building, Ph 021 650 4791).
**NB: A copy of this signed form must be included with the thesis/dissertation/report when it is submitted for examination**

***This form must only be completed once the most recent revision EBE EIR Handbook has been read.***

---

**Name of Principal Researcher/Student:** OSAHONI OKUWAFUNSO O. **Department:** ELECTRICAL ENGINEERING

**If a Student:** **Degree:** MSC **Supervisor:** MRS K. O. AWODELE
Prof K. Folly

**If a Research Contract indicate source of funding/sponsorship:**

**Research Project Title:** OPTIMAL ALLOCATION OF DISTRIBUTED GENERATION FOR POWER LOSS REDUCTION AND VOLTAGE PROFILE IMPROVEMENT

**Overview of ethics issues in your research project:**

| | | |
|---|---|---|
| **Question 1: Is there a possibility that your research could cause harm to a third party (i.e. a person not involved in your project)?** | YES | NO ✓ |
| **Question 2: Is your research making use of human subjects as sources of data?** If your answer is YES, please complete Addendum 2. | YES | NO ✓ |
| **Question 3: Does your research involve the participation of or provision of services to communities?** If your answer is YES, please complete Addendum 3. | YES | NO ✓ |
| **Question 4: If your research is sponsored, is there any potential for conflicts of interest?** If your answer is YES, please complete Addendum 4. | YES | NO ✓ |

If you have answered YES to any of the above questions, please append a copy of your research proposal, as well as any interview schedules or questionnaires (Addendum 1) and please complete further addenda as appropriate. Ensure that you refer to the EIR Handbook to assist you in completing the documentation requirements for this form.

**I hereby undertake to carry out my research in such a way that**

- there is no apparent legal objection to the nature or the method of research; and
- the research will not compromise staff or students or the other responsibilities of the University;
- the stated objective will be achieved, and the findings will have a high degree of validity;
- limitations and alternative interpretations will be considered;
- the findings could be subject to peer review and publicly available; and
- I will comply with the conventions of copyright and avoid any practice that would constitute plagiarism.

**Signed by:**

| | Full name and signature | Date |
|---|---|---|
| Principal Researcher/Student: | | 23/02/2016 |

**This application is approved by:**

| | | |
|---|---|---|
| Supervisor (if applicable): | | 23/02/2016 |
| HOD (or delegated nominee):<br>*Final authority for all assessments with NO to all questions and for all undergraduate research.* | | 29/2/16 |
| Chair : Faculty EIR Committee<br>For applicants other than undergraduate students who have answered YES to any of the above questions. | | |